

This Page Is Inserted by IFW Operations
and is not a part of the Official Record

BEST AVAILABLE IMAGES

Defective images within this document are accurate representations of the original documents submitted by the applicant.

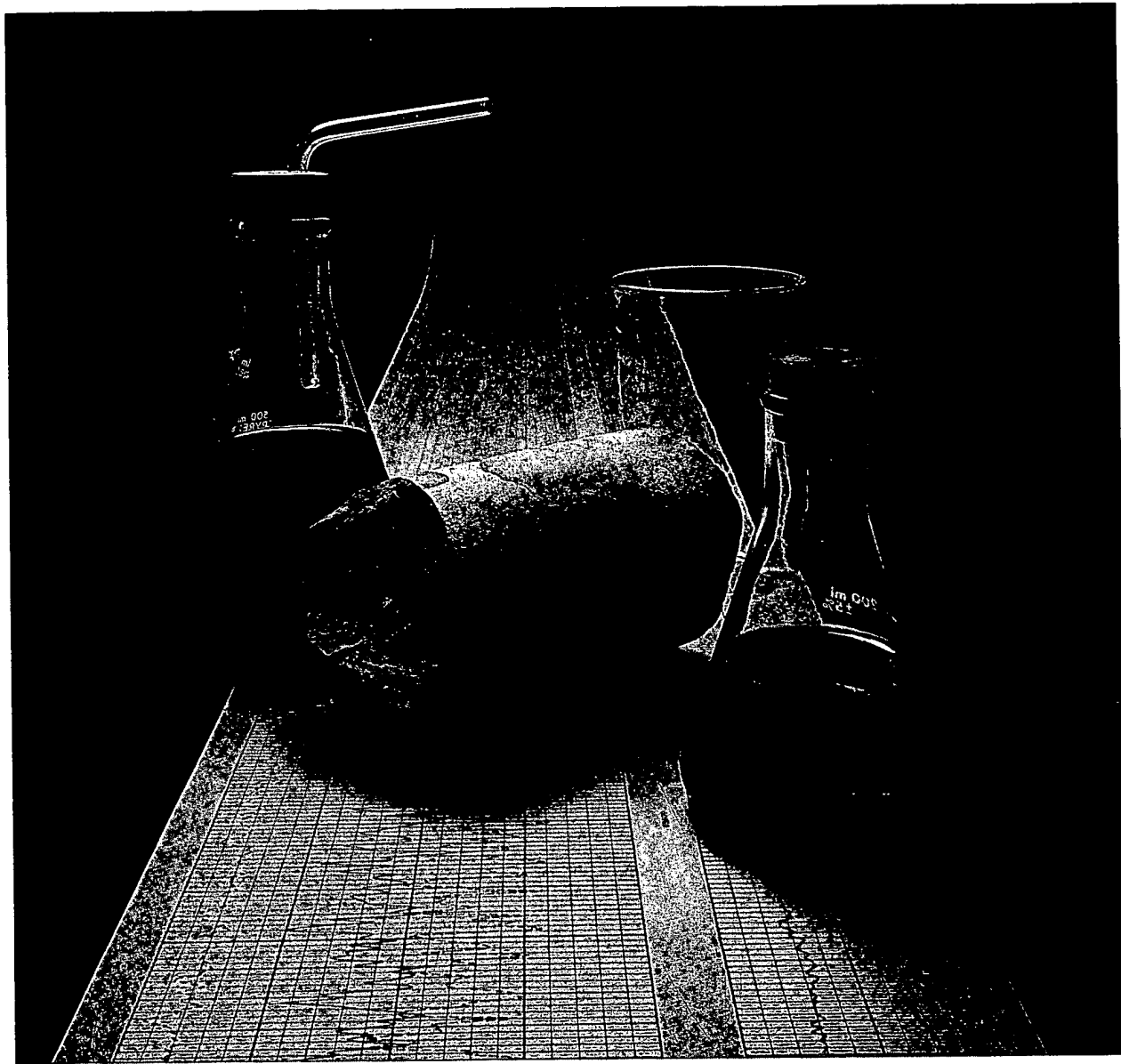
Defects in the images may include (but are not limited to):

- BLACK BORDERS
- TEXT CUT OFF AT TOP, BOTTOM OR SIDES
- FADED TEXT
- ILLEGIBLE TEXT
- SKEWED/SLANTED IMAGES
- COLORED PHOTOS
- BLACK OR VERY BLACK AND WHITE DARK PHOTOS
- GRAY SCALE DOCUMENTS

IMAGES ARE BEST AVAILABLE COPY.

**As rescanning documents *will not* correct images,
please do not report the images to the
Image Problem Mailbox.**

Victor Hugo Franco T. - 1992



Introduction to Wireline Log Analysis

Copyright © 1992 Western Atlas International, Inc.,
Houston, Texas. All rights reserved. Printed in U.S.A.
This book, or parts thereof, may not be reprinted in any
form without permission of the copyright holder.

AT91-158 9651 7/92 3M SPC

UNIVERSITY LIBRARY
UNIVERSITY OF ALBERTA

With neutron logging already being available, the first attempts to more adequately quantify porosity and estimate lithology mix occurred when acoustic logs were introduced, followed soon afterwards by the introduction of density logs. Comparing neutron data to the newer log measurements yielded better differentiation of gas from oil or water. In the early 1960s, neutron (often scaled in counts), acoustic Δt , and density data (usually in some form of counts) were all available. Petrophysicists quickly realized that different combinations of these logs could provide better estimates of porosity. Recognizing that different log responses occurred in different rock matrices also led to lithology estimations. Nevertheless, the lithology descriptions from logs did not gain reasonable acceptability until about 1970 when computer-processed log analysis reached maturity. Borehole-compensated equipment was introduced in stages (acoustic, then density, and finally neutron) during the 1960s, but adequate porosity/lithology results from log crossplot techniques were still considered suspect. Much of the groundwork for today's lithology/porosity models was developed during this time.

The rapid evolution of digital circuitry, microelectronics, and telemetry has played a major role in bringing formation evaluation to its current level. Data acquisition is at least an order of magnitude more efficient than it was 15 years ago. Today, processing routines are quick, well documented, visually appealing, and acceptable to the industry. That is the good news. The bad news is that many fundamental considerations are overlooked in the quest to reach goals of speed, eye appeal, and a distorted view of accuracy. By no accident, training has focused more and more on direct computer methods, often bypassing analytical fundamentals that provide insight into the functions of computer processing. This chapter is dedicated to re-establishing basic rules of crossplotting data to determine what additional insights the results offer and what crossplotted data do not describe. Those seriously interested in acquiring expertise in formation evaluation must develop a strong understanding of the fundamentals, including crossplot methods.

DUAL-MINERAL LITHOLOGY-POROSITY CROSSPLOTS

Assorted measurements are available from a variety of logging tools. Individual comparisons of any one of these measurements to the other measurements often define petrophysical or geological characteristics that are very important to reservoir descriptions. Crossplots also provide a mechanism to recognize log calibration problems and to correct data not in significant error. Plots can be

made on linear, logarithmic, semilogarithmic, or exponential scales, and one axis of a plot can be a different scale type from the other axis. Information that relates log responses to primary and total porosity, secondary porosity, grain-size estimates in reservoir rock, and matrix mixes of clastics, carbonates, evaporites, or other rock types can usually be inferred from the proper comparison of log data.

No crossplot method is completely accurate; every method has advantages and weaknesses. Two or more measurements can be used for plotting, and quite often, several two-way crossplots are required to obtain the "best answer." Computer-processing facilitates handling of the data, but plotting by hand still offers an effective cross-check of accuracy. Experienced log analysts consistently compare computer results to hand calculations for quality control.

It is imperative that basic log response functions and their relation to porosity and lithology be fully understood if crossplotting techniques are to be intelligently evaluated. Dual-mineral methods utilize two sets of log data to determine porosity and a mix of two defined rocks or minerals. A shale index can be inferred from the crossplot or independent shale index methods, but at most, only two types of rock can be defined with two log measurements.

Acoustic, density, and neutron log measurements are sensitive to porosity. Each of these logs can be converted to a porosity value; however, fluid and matrix values must be known or assumed in order to solve the equation converting the raw measurement to porosity. The use of two logs eliminates some of the guesswork that might be necessary when only one log is available. For example, each of the three logs is known to have the following response to sands and clays found in clastics –

$$\rho_b = \text{effective porosity} \pm \text{clay effect} + \text{light hydrocarbon (gas effect)}$$

$$\phi_N = \text{effective porosity} \pm \text{clay effect} - \text{light hydrocarbon (gas effect)} \text{ or} + \text{heavy oil effect}$$

$$\Delta t = \text{effective porosity} + \text{clay effect} + \text{compaction} + \text{light hydrocarbon (gas effect)}$$

A dual-mineral crossplot makes the assumption that only two rocks/minerals are present in the formation (or that those two rocks virtually dominate the mixture). It has never been proven that lithology response is linear between two matrix lines, and empirically derived matrix lines tend to indicate a certain degree of nonlinearity. If

the initial assessment of matrix mix is wrong, the resultant output is definitely wrong. Several log measurements are sensitive to lithology, porosity, or both, but the sensitivity to each varies considerably depending on the type measurement. Protocol requires that the analyst be well aware of the inherent traps that occupy the road from raw data to a result. Competent analytical or digital log analysis requires an awareness of the strengths and weaknesses of different crossplot methods.

Crossplots are the basis from which computed log interpretation programs evolved. Sidestepping such data prior to computing log results is a guarantee of mistakes and customer dissatisfaction.

ARBITRARY MATHEMATICAL SOLUTIONS FROM CROSSPLOT DATA

Ambiguity exists in most computerized solutions of crossplotted log data because the formulae generally assume linearity. Individual log measurements were discussed in detail previously, and it is obvious each logging device has unique responses to a number of physical, petrophysical, and geological parameters such as –

- Lithology
- Porosity
- Drilling fluid salinity, weight, and other characteristics
- Mud filtrate salinity and depth of invasion
- Depth of investigation
- Vertical resolution
- Connate water salinity
- Gas and/or oil effects on the measurements
- Temperature and pressure
- Borehole size
- Mudcake thickness

Physical, chemical, geological, mechanical, and electrical attributes are the readily identifiable roadblocks that inhibit log-evaluation methods.

FUNDAMENTALS OF CROSSPLOT CONSTRUCTION

All dual-mineral crossplot methods use a minimum of three anchor points to resolve data from two log measurements. One point is always the 100% porosity or fluid parameter. The other control points represent the predictable zero porosity value for each of the two measure-

ments and the particular matrices selected. For example, if lithology is assumed to be limestone and dolomite and the two log measurements are bulk density (ρ_b) and compensated neutron porosity ϕ_N (calculated for limestone matrix), the zero porosity values for limestone and dolomite would likely be –

ρ_b = 2.71 g/cm³ and 2.86 to 2.87 g/cm³ for each of the two rock types

ϕ_N = 0 and 0.02 limestone ϕ units, respectively

Specific neutron devices can alter parameters slightly. Fluid parameters are generally selected as 1 g/cm³ (fresh mud) or 1.1 g/cm³ (salt mud) for the density and 1 for neutron porosity (Fig. 5-1). Several log parameters for different rocks and minerals are given in Table 5-1. Generally, crossplots are enlarged to show only the porosity and lithology trends that occur below the 50% porosity values; less than one-half the entire model is shown (Fig. 5-2). If an acoustic log were used instead of the neutron log, the zero matrix points for limestone ($\Delta t = 47.6 \mu\text{sec}/\text{ft}$) and dolomite ($\Delta t = 43.5 \mu\text{sec}/\text{ft}$) would probably be selected,

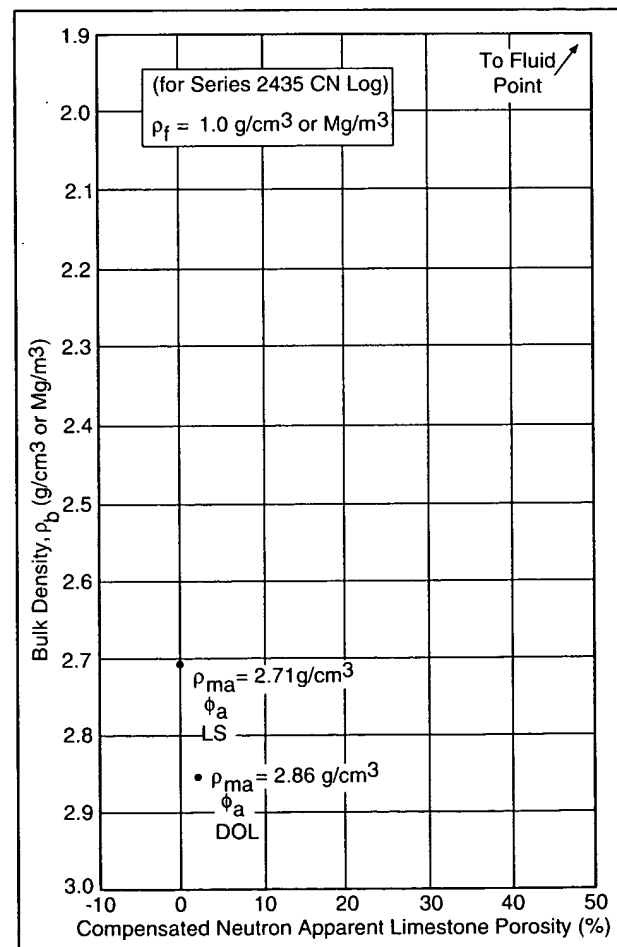


Fig. 5-1 – Zero porosity control points for two rock types plotted at their proper coordinates

TABLE 5-1 - Logging Parameters for Some Common Rocks and Minerals

		ρ_b (g/cc)	Σ (c.u.)	Δt (μ s/ft)	ϕ_{CN} (lime)	K (%)	U (ppm)	Th (ppm)
Common Sediment	Quartz	1.8	2.65	8.0 - 13.0	51.3 - 55.5	- 0.04	< 0.15	< 0.4
	Calcite	5.1	2.71	8.0 - 10.0	47.6	0.00	< 0.40	1.5 - 15.0
	Dolomite	3.1	2.87	8.0 - 12.0	43.5	0.02	0.1 - 0.3	1.5 - 10.0
	Shales		1.80 - 2.70	25.0 - 45.0	63.0 - 170.0	0.09 - 0.45		< 2.0
Common Evaporites	Halite	4.7	2.04	748.0	67.0	- 0.02 - 0.03	< 0.3	< 0.2
	Anhydrite	5.0	2.98	12.3	50.0	0.00	0.25 - 0.43	< 0.2
	Gypsum	4.0	2.35	18.8	52.5	0.50 - 0.60		
	Trona	0.7	2.10	18.5	65.0	0.42		
Coals	Lignite	0.16	1.05	12.8	140.0	0.60		
	Bituminous	0.17	1.33	16.4	120.0	0.60		
	Anthracite	0.20	1.57	10.5	105.0	0.40		
Iron Minerals	Limonite	13.0	3.59		57.0			
	Pyrite	17.0	4.99	90.0	39.0			
	Siderite	14.7	3.94	52.3	48.0			
	Hematite	21.5	5.18		44.0			
Micas	Glauconite	5.5 - 7.1	2.54	23.4		0.19	5.08 - 5.30	
	Biotite	6.2 - 6.4	2.99	30.0	51.0	0.06	6.7 - 8.3	< 0.01
	Muscovite	2.4	2.82	16.9	49.0	0.13	7.9 - 9.8	< 0.01
Clays	Kaolinite		2.61	12.8		0.37	0.42	1.5 - 3.0
	Chlorite		2.88	25.3		0.32		6.0 - 19.0
	Illite		2.63	15.5		0.09	4.50	1.0 - 5.0
	Smectite		2.02	14.5		0.17	0.16	< 2.0

and fluid transit time might be selected as 189 μ sec/ft for fresh mud and 185 μ sec/ft for salt mud. Sandstone is also a common selection for one of the minerals, but other rocks such as anhydrite, salt, or gypsum occasionally become important crossplot parameters.

Further construction of the density-neutron crossplot entails plotting of points representative of numerous values of porosity (5% limestone porosity, 10% limestone porosity, etc. and 5% dolomite porosity, 10% dolomite porosity, etc.). The numerous points for ϕ at the two different lithologies are crossplotted for both ρ_b and ϕ_N (Fig. 5-3).

The various ρ_b , ϕ_N porosity levels are connected from one level to the next, and similar porosities for each lithology are connected. The dolomite line in this illustration is not a straight line. Parameters for each of the logs and other specific minerals might then be superimposed on the crossplot. Similar methods are used to construct any lithology/porosity crossplot (Fig. 5-4).

Shale Volume Determination

The same crossplot can also be used to calculate a shale volume (V_{sh}) because neutron logs are much more affected by shale (hydrogen content) than density logs. Control points on the example just described can also be selected to describe a clean line (0% V_{sh}). For example,

the line connecting zero porosity limestone coordinates and the 100% ϕ_f -coordinates could be used as the "clean line." A point or general area representative of ρ_b and ϕ_N values selected from a nearby shale is then used to establish a "100% shale line"; a line parallel to the clean line is drawn through the 100% shale data (Fig. 5-5). The shale line is very near the dolomite matrix line, and assuming limestone is considered clean, a formation that is pure dolomite will calculate as 80% shale. In such a circumstance, density-neutron crossplot data would not be a reliable indicator of shale volume. As long as other shale indicators (gamma ray) show a lower percentage of shale, the crossplot indication does not hinder the analysis.

Gas Correction on Density-Neutron Crossplots

If the neutron log is affected by gas, the apparent neutron porosity will be undervalued. Density logs are also affected by gas on occasion, but not as severely as neutron logs. For example, if $\rho_b = 2.23 \text{ g/cm}^3$ and $\phi_{Nls} = 0.10$, the data will plot above the empirically derived sandstone line. (Salt and/or excessive hole signal cause similar responses on density and neutron logs, and caliper information therefore becomes important.) The conventional way to correct gas-effected crossplot data is to adjust the crossplotted point a 30° slope downward to the right; the corrected point will be on the clean sand line at $\approx 23.5\%$ porosity (Fig. 5-6).

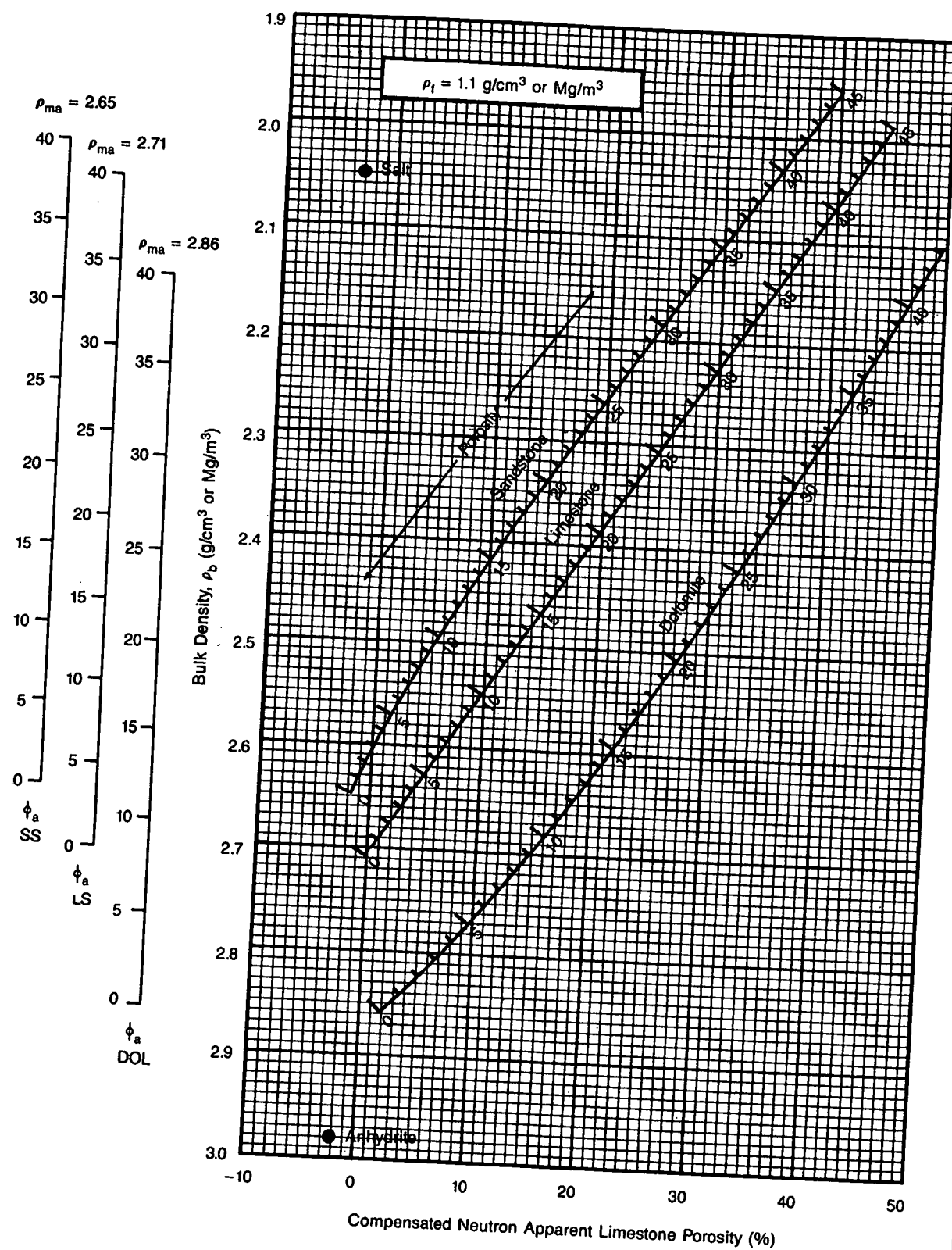


Fig. 5-2 – Typically, chart book crossplots are scaled from 0 to 50% porosity.

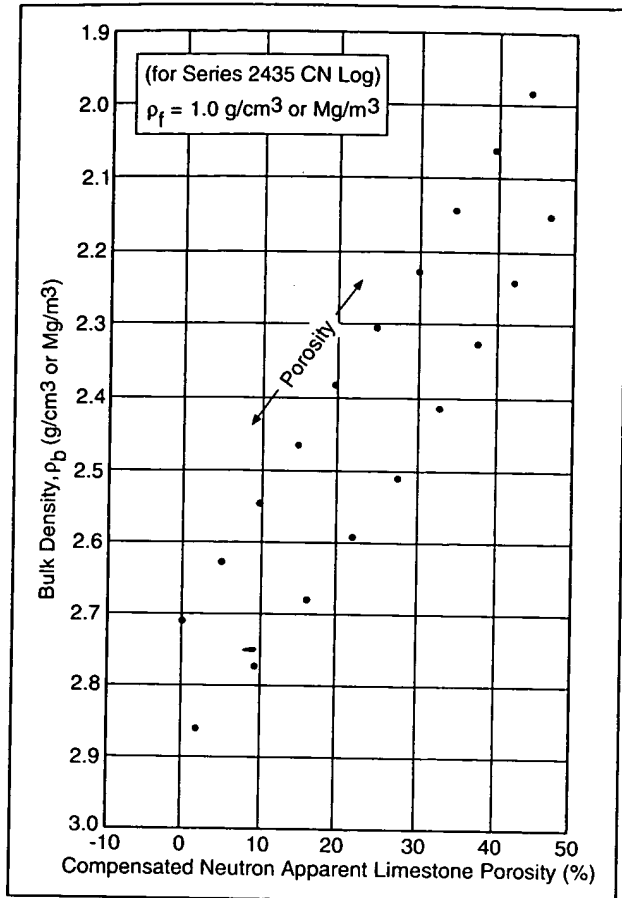


Fig. 5-3 – Crossplot construction requires that points be plotted for several different porosity values of the proposed lithologies.

In some areas, gas correction is modified to fit local empirical evidence. Gas affects neutron, density, and acoustic measurements differently and to different degrees depending on invasion. Neutron devices have slightly deeper depths of investigation and are more susceptible to gas effects. Density logs are affected by gas if invasion is very shallow, such as in the high-porosity, high-permeability formations in the Gulf of Mexico. Acoustic log measurements are made from such a shallow depth of investigation that gas seldom affects Δt measurements, but when it does, the log often cycle skips. There are no sophisticated rules, but the following "rule-of-thumb" is suggested as a guide, or functional variable, depending on locality.

Porosity Range Gas Correction

> 30%	45° slope to the clean matrix line
13-29%	30° slope to the clean matrix line
< 12%	15° slope to the clean matrix line

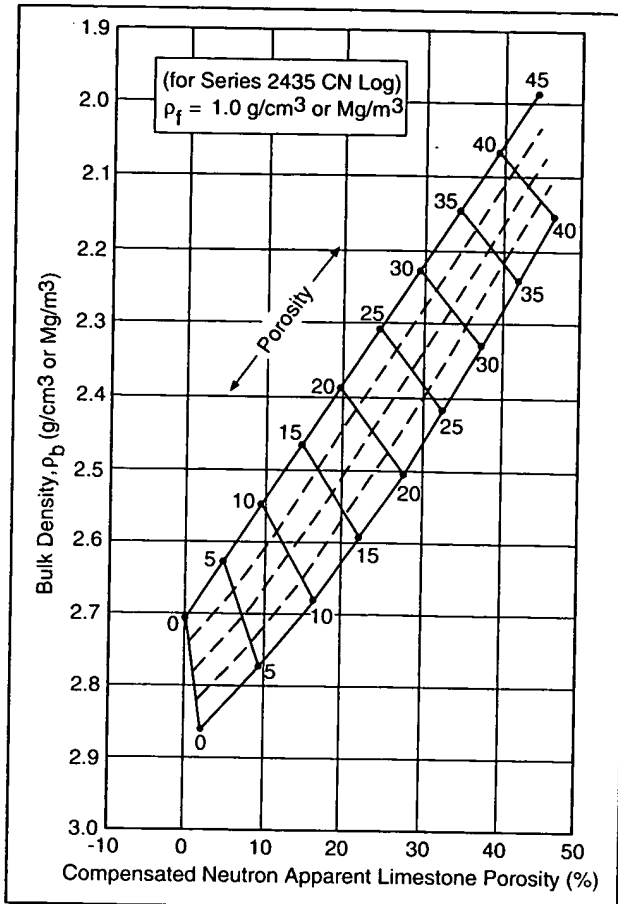


Fig. 5-4 – The lines in a crossplot are connected between the plotted points and labeled for porosity value and lithology, with interpolation used between the two lithology lines to estimate lithology mix and porosity values.

Comparing gas-effected log data to core data is often the best way to obtain estimates of total effective porosity. Correcting a data point to a clean matrix line also requires another source of lithology reference.

DENSITY-NEUTRON CROSSPLOT VERSATILITY

Virtually all formation evaluation specialists agree that the density-neutron crossplot is the most accurate log analysis method for determining porosity. Both tools are calibrated against a water-filled limestone basic calibration fixture. With respect to the limestone calibration standard, sandstone and dolomite cause opposite measurement responses. Gas effect also causes an opposite response, and although the neutron is usually more affected by gas, empirical corrections have found general acceptability. The density log measurement is more sensitive to pore space, and the neutron measurement is more sensitive to lithology changes; these tendencies also balance out in crossplotted results.

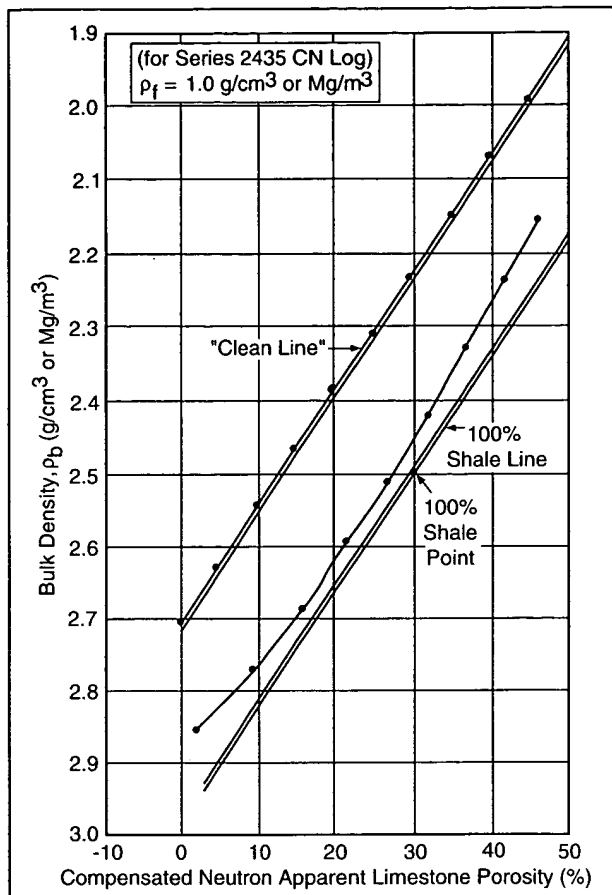


Fig. 5-5 – Average shale values can be determined and plotted on the crossplot.

Density-neutron crossplot techniques have been the preferred dual-mineral method in carbonate reservoir rocks for nearly 30 years. Despite a few drawbacks, these techniques usually provide satisfactory shale volume estimates in sand-shale sequences and are the basis for several commercial computed log analysis programs (Fig. 5-7). The major handicaps for the crossplot models in clastics are gas effects in shaly sands, admixtures of carbonate or evaporite, borehole rugosity and washouts, and resolution in low-porosity ($\phi < 12\%$) rocks.

Sand-shale models of density and neutron data are also used to determine the percentages of silt and clay (commonly considered shale in log analyst terminology). A clean sand line is typically established using the common sandstone parameters for density (2.65 g/cm^3) and neutron (ϕ_{Nls}) ≈ -0.03 to -0.04); a clay line is established from a dry colloid point ($\rho_b \approx 2.85 \text{ g/cm}^3$, $\phi_{Nls} \approx 0.1$ – 0.30) to the 100% ϕ fluid point (Fig. 5-8). The dry clay band represents clay minerals that have been baked dry in the laboratory and have average measurements of 2.85 g/cm^3 ($-0.12\% \phi_{sd}$). Different clays exhibit different neutron responses, and different neutron tools often

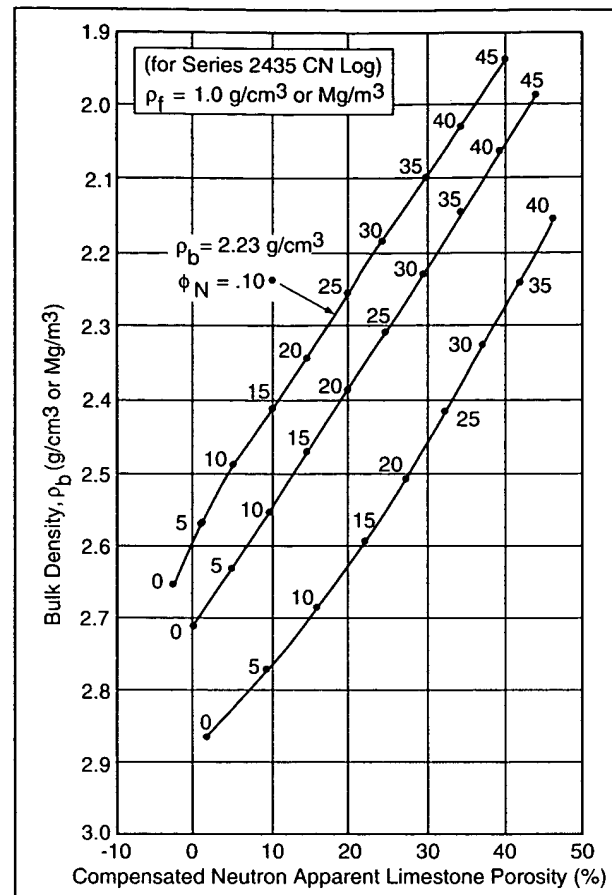


Fig. 5-6 – Correction for gas effect on a known lithology

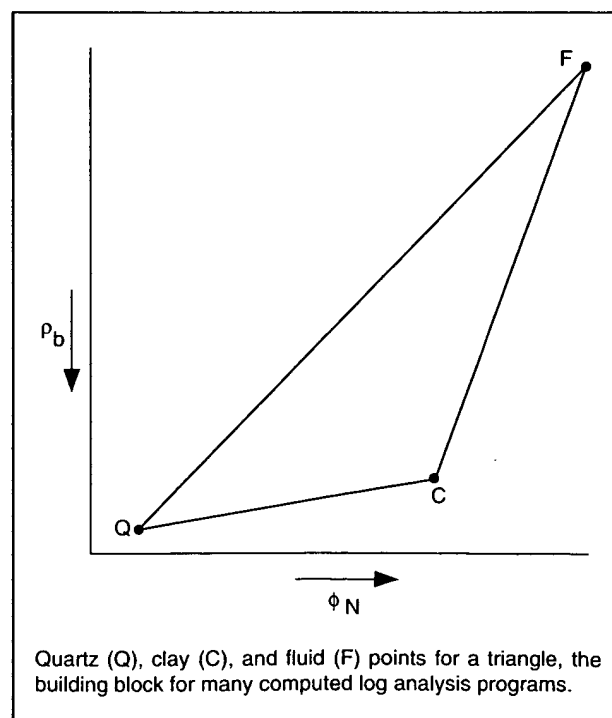


Fig. 5-7 – Three control points for a shaly sand crossplot

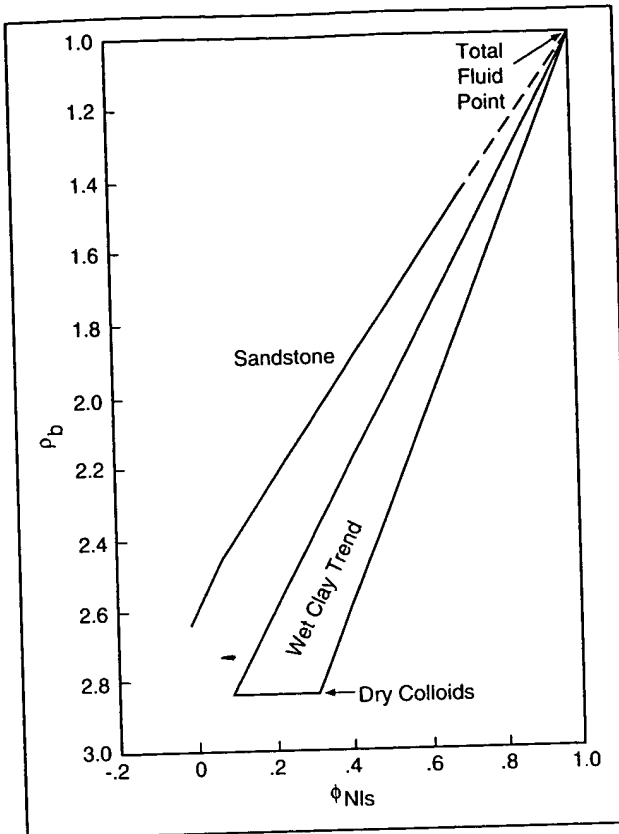


Fig. 5-8 – Sandstone-shale models utilize a statistically determined clay line that extends from the fluid point to the dry clay line.

respond differently to the same clay. A 100% silt point, or index, is selected from data points that represent a high apparent V_{sh} and lie between the zero porosity sand point and the clay line (Fig. 5-9). Data that plot similar to the indicated star (Fig. 5-10) would be construed by the computer program as having an approximate mix of 66% sand, 25% silt, and 9% clay. Total porosity, including the noneffective pore space, would be selected from the location of that data point and corrected to effective porosity (ϕ_e) using the minimum V_{sh} value calculated at that depth. V_{sh} is calculated by several methods, and the program accepts the method that calculates the least shale.

Clays occur in three forms—structural, dispersed, and laminated (Fig. 5-11). Empirical attempts to segregate the effects on density-neutron measurements are bracketed on the crossplot (Fig. 5-12). Dispersed clays generally cause a considerably lower value of effective porosity, but clay laminae do not appreciably lower total porosity because the porosity is restricted to the sand laminae. Structural clays essentially fall into the "unlikely area," the area where appreciable amounts of questionable log data and bad hole data plot.

Clay-typing with density-neutron data is arguably ambiguous and subject to question and speculation. Nevertheless, postulations have been made that some smectites are

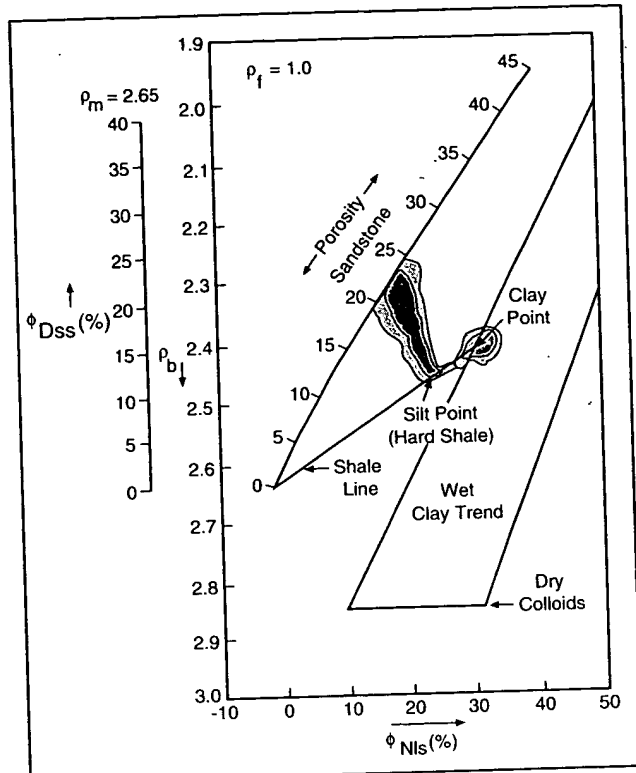


Fig. 5-9 – A silt index point is selected from a concentration of crossplotted data that occurs between the wet clay line and zero porosity.

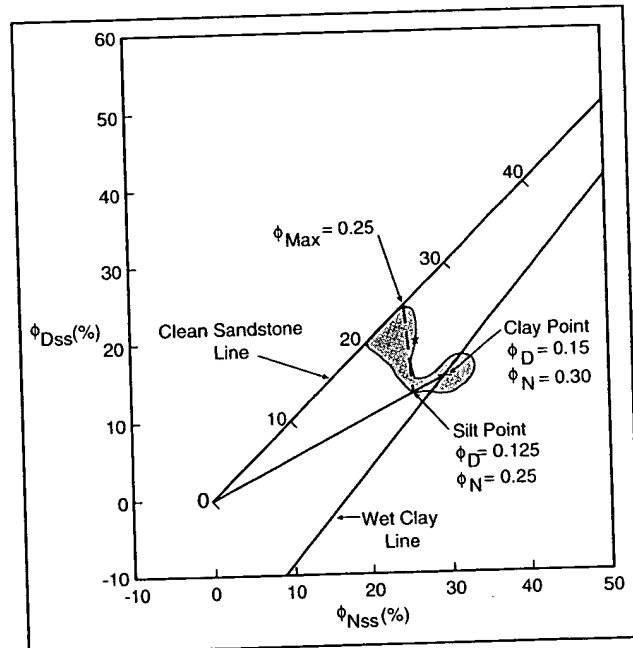


Fig. 5-10 – Silt coordinates permit a calculation of sand, silt, and clay proportions.

related to structural clays (montmorillonite) and occur more frequently within the higher porosity rocks (usually younger, less compacted shaly sand environs). Kaolinites and mixed layer clays generally occur with laminar and silty fractions of shale. High-potassium illites relate more

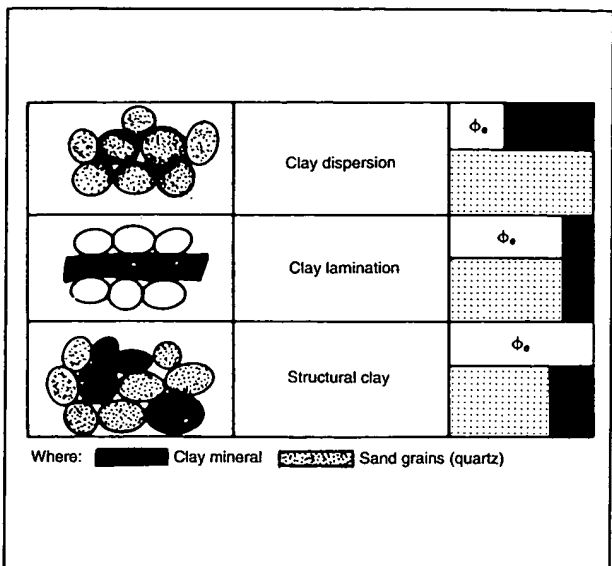


Fig. 5-11 – Effects of clay distribution

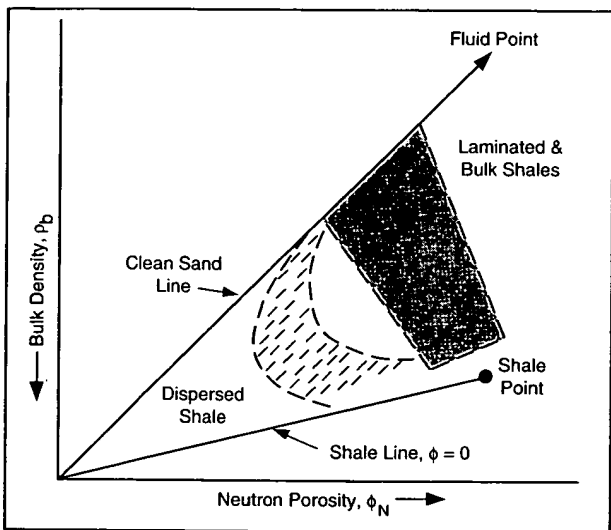


Fig. 5-12 – Clay distribution patterns on a density vs. neutron crossplot

to the dispersed clays that are detrimental to reservoir quality (Fig. 5-13).

Today, the density-neutron crossplot is the basic crossplot used in most log analysis routines. It has also been used effectively to differentiate sand from shale where "radioactive sands" occur. Natural gamma ray counts in such sands may indicate high API values indicative of shale, whereas the crossplot data indicate relatively clean sands. These "hot sands" are usually high in potassium or thorium and potassium content. Natural gamma ray spectroscopy and/or z-axis plots play an important role in identifying these phenomena and are discussed later.

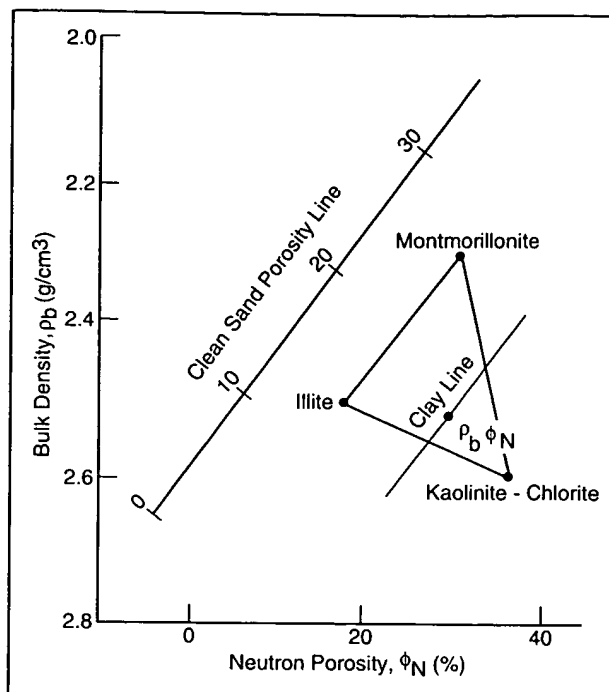


Fig. 5-13 – General locations of clay types on a density vs. neutron crossplot

SHALY SANDS AND ACOUSTIC-DENSITY CROSSPLOTS

It was discovered early that crossplots of density and acoustic log data were very helpful in clarifying sand-shale mixtures and determining more accurate water saturation in shaly sands. Shales are considered loose, earthy mixtures of clay and silt-sized particles that are dominated mostly by clay minerals. The structural lattice of clay minerals results in a highly negative electrical charge, caused mostly by the substitution of Al^{+++} ions. Electrical imbalance is compensated for by cations that attach to the surface of the clay sheets. The positive surface charge, called the cation exchange coefficient (CEC), is discussed in more detail later in the text.

The presence of shales (or clay) within a formation complicates the definition of porosity because clay's bound surface waters often provide a significant amount of pore space, albeit non-effective. Log measurements are affected differently by the amounts and properties of particular shales, and the way shale is distributed in the rock becomes significant to log analysis. Many sand reservoirs were created in conditions that cause layers of sand to be separated by layers of clay, and the sand laminae are essentially unaffected by the clay laminae that separate the layers. Shale also occurs as a structural component of the rock; the shale is part of the matrix and has minimal effect on the porosity responses of logs. Clays are also dispersed in the pore throats of some sand bodies, partially filling the interconnecting lattices, and thereby cause a large reduction in permeability. Any combination of the three clay types can occur simultaneously.

Laminar Sand-Shale Model

An acoustic-density crossplot was introduced as early as 1963.^{2, 159} The graphical solution was constructed from the two linear response functions –

$$\rho_b = (\phi_{ss}, \rho_{ss}, \rho, \rho_{sh}, V_{sh}), \text{ and}$$

$$\Delta t = (\phi_{ss}, \Delta t_{ss}, \Delta t, \Delta t_{sh}, \text{ and } V_{sh}),$$

where

ϕ_{ss} = porosity value calculated for sandstone using the linear functions for each respective device,

ρ = density values used respectively for sandstone matrix, chosen from log data in an adjacent shale and a value for fluid density,

Δt = transit time values used respectively for sandstone matrix, chosen from log data in an adjacent shale and a value for fluid transit time,

and

V_{sh} = shale volume determined from the acoustic vs. density laminated sand-shale model.

Again, the crossplot is constructed from three control points that represent the 100% porosity fluid point, the zero porosity sandstone point, and the 100% shale point (Fig. 5-14). Typically, the 0% point for sandstone or quartz (Q) is plotted at the point where ρ_b of 2.65 g/cm^3 and Δt of $55.6 \mu\text{sec/ft}$ intersect (other parameters are sometimes used for sandstone matrix). For fresh-mud drilling fluids, ρ_f of 1 g/cm^3 and Δt_f of $189 \mu\text{sec/ft}$ typically represent the 100% porosity fluid point (F). The fluid point would be slightly different ($\approx 1.1 \text{ g/cm}^3$ and $185 \mu\text{sec/ft}$) for salt muds. The shale point (S) is arbitrarily chosen from reliable ρ_b values and Δt values observed in adjacent shale beds. This technique assumes the adjacent shale is similar to those within the sand body. Lines are constructed between the points QS , QF , and SF . The line QF is linearly subdivided into percentages of clean sand porosity. The line QS is linearly subdivided into percentages of V_{sh} . The FS line is also subdivided linearly, which allows lines parallel to QF to be constructed for apparent porosity (ϕ_a). Lines are also constructed parallel to the clean sand line and segmented into linear percentages of sand/shale mixture out to the 100% V_{sh} point. Log data plotted at any point on the crossplot then lead to an estimate of sand and shale percentages and total effective porosity (ϕ_e). This plot is known as a laminated model. Dotted lines are constructed to fan out from the V_{sh} point to incremental values of porosity along the clean sand line QF . Clean sand porosity is interpreted within the dotted line bound-

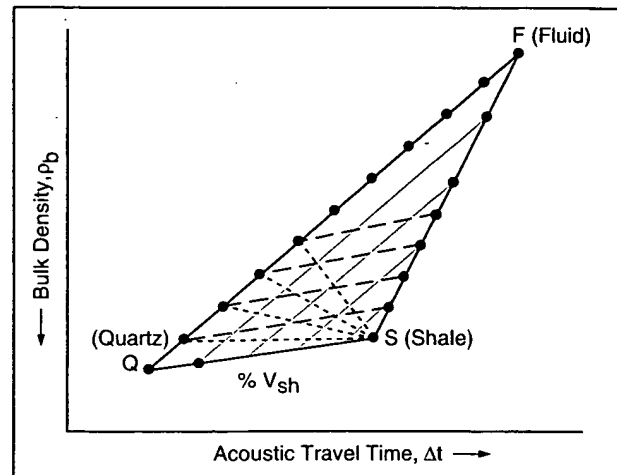


Fig. 5-14 – Crossplot concept for a laminated shaly sand

aries as the clean sand portion of the laminar model and is used for saturation determination in the laminar model. Resistivity of the clean sand laminae is calculated as follows –

$$\left(\frac{1}{R_a} \right) = \left(\frac{V_{sh}}{R_{sh}} \right) + \left(\frac{1 - V_{sh}}{R_{sd}} \right)$$

Once the clean sand resistivity is determined and porosity is converted to formation factor by the proper relationship, only connate water resistivity (R_w) is needed to calculate water saturation in the clean sand portion of the laminated reservoir rock. The apparent water saturation (S_{wa}) is then found by –

$$S_{wa} = \sqrt{\frac{F_{sd} \cdot R_w}{R_a}}$$

Similar laminated models can be constructed with density-neutron data. In laminated shaly gas sands, a comparison of both models has often been employed successfully to determine more accurate and acceptable ϕ_e and S_w values.

Dispersed Clay Model

At the outset, a crossplot for sands and dispersed clays is constructed in a fashion similar to that for other plots (control points Q, F, C are plotted). The QF line (Fig. 5-15) is again linearly subdivided into percentages of clean sand porosity. The term clay becomes very appropriate in this model, and assuming a 100% clay point (C) as illustrated, line QC is subdivided into percentages of dispersed clay. The points along the QC line are used to construct lines parallel to the QF line. The concept of using acoustic and density data to evaluate sands with dispersed shales is based on the premise that Δt values are "seeing" the clays as a slurry, and the log value is accepted as total porosity (ϕ_t). ρ_b values are essentially unaffected by the dispersed clays and see only matrix and effective pore space. This is because the

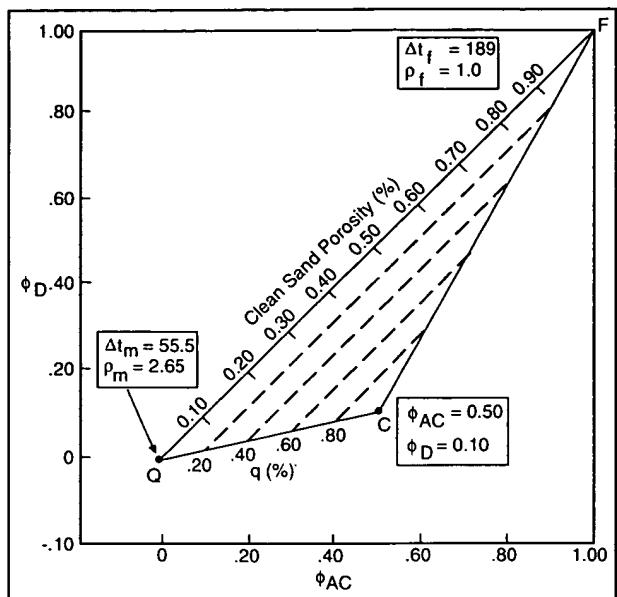


Fig. 5-15 – Dispersed clay model

difference in ρ_{cl} and ρ_b values is relatively small. Later, these concepts led to the conclusion –

$$q = \frac{\phi_a - \phi_d}{\phi_a}$$

where q is representative of the amount of dispersed clay. Earlier work³⁹⁻⁴¹ suggested water and dispersed shale conduct electrical current as a mixture of electrolytes, resulting in a complex equation illustrating S_w to be the water saturation of the true effective porosity fraction. The value q leads to acceptable estimates of the dispersed clay fraction, but values for R_{sh} were much more difficult to define. The simplified approach takes a resistivity value from the adjoining shale beds. This value is not critical if $R_{sh} \gg R_w$, which is usually the case. The simplified form of the dispersed clay saturation model became –

$$S_w = \frac{\sqrt{F_z R_w / R_t + q^2 / 4} - q/2}{1 - q}$$

where

S_w = water saturation determined,

F_z = the formation factor determined from ϕ_a and the appropriate transform,

R_w = the connate water resistivity,

R_t = the true formation resistivity,

and

q = the estimate of pore space occupied by the dispersed clays.

Conventional chartbook crossplots of density vs. acoustic data include matrix lines for limestone, dolomite, and sandstone (Fig. 5-16). Matrix resolution between any two of the three lines is poor, and density-acoustic crossplots are therefore used more for evaluating sand-shale sequences than for any porosity-lithology mix in carbonate environments. Obviously, the two clastic models discussed are accurate only for the conditions described; the laminated model yields inaccurate results for sand with dispersed clays, and the dispersed clay model provides inaccurate results if laminated sand-shales are the rock characteristics. The two-way crossplots have limitations and require known or assumed parameters to provide accurate answers.

ACOUSTIC-NEUTRON CROSSPLOT

Construction of this crossplot also requires control points. The acoustic-neutron crossplot closely resembles the density-neutron crossplot (Fig. 5-17) and is often significant in differentiating radioactive or "hot" carbonates from shales and evaluating tight shaly gas sands. It is often not a wise choice, however, for determining shale volume. For example, $\Delta t_{sh} \approx 100 \mu\text{sec}$ and $\phi_{Nsh} \approx 30\%$ are not unusual shale parameters in many geographical areas, but these values plot at or near the clean sand line on the acoustic-neutron crossplot. In other words, when using this plot for V_{sh} calculations, shale beds may appear as clean sands.

In radioactive dolomites, natural gamma rays may cause high readings (high concentrations of uranium or potassium), and the gamma ray measurement is therefore not a realistic indicator of V_{sh} . Neutron and acoustic data generally provide reliable shale estimates because the dolomite line has ample resolution compared to the probable shale point. For example, $\Delta t_{sh} \approx 80 \mu\text{sec}$ and ϕ_{Nsh} values of $\approx 20\%$ are typical shale values found near such environs (typically complex supratidal and/or intertidal), and they usually plot near the sandstone matrix line or between the sandstone and limestone line. This crossplot is often significant in the analysis of shallow, nearshore reservoirs, but it typically gives optimistic estimates of porosity in shaly sand reservoirs because both logs are influenced by shale content.

Gas Affect on Acoustic-Neutron Crossplots

Corrections for gas affects discussed for density-neutron crossplotted data also apply here. Although acoustic data are seldom affected by gas, the affects are usually extreme when it occurs and cycle skips occur. In many tight, shaly gas sands, density, neutron, and acoustic data are necessary to effectively evaluate the reservoir.

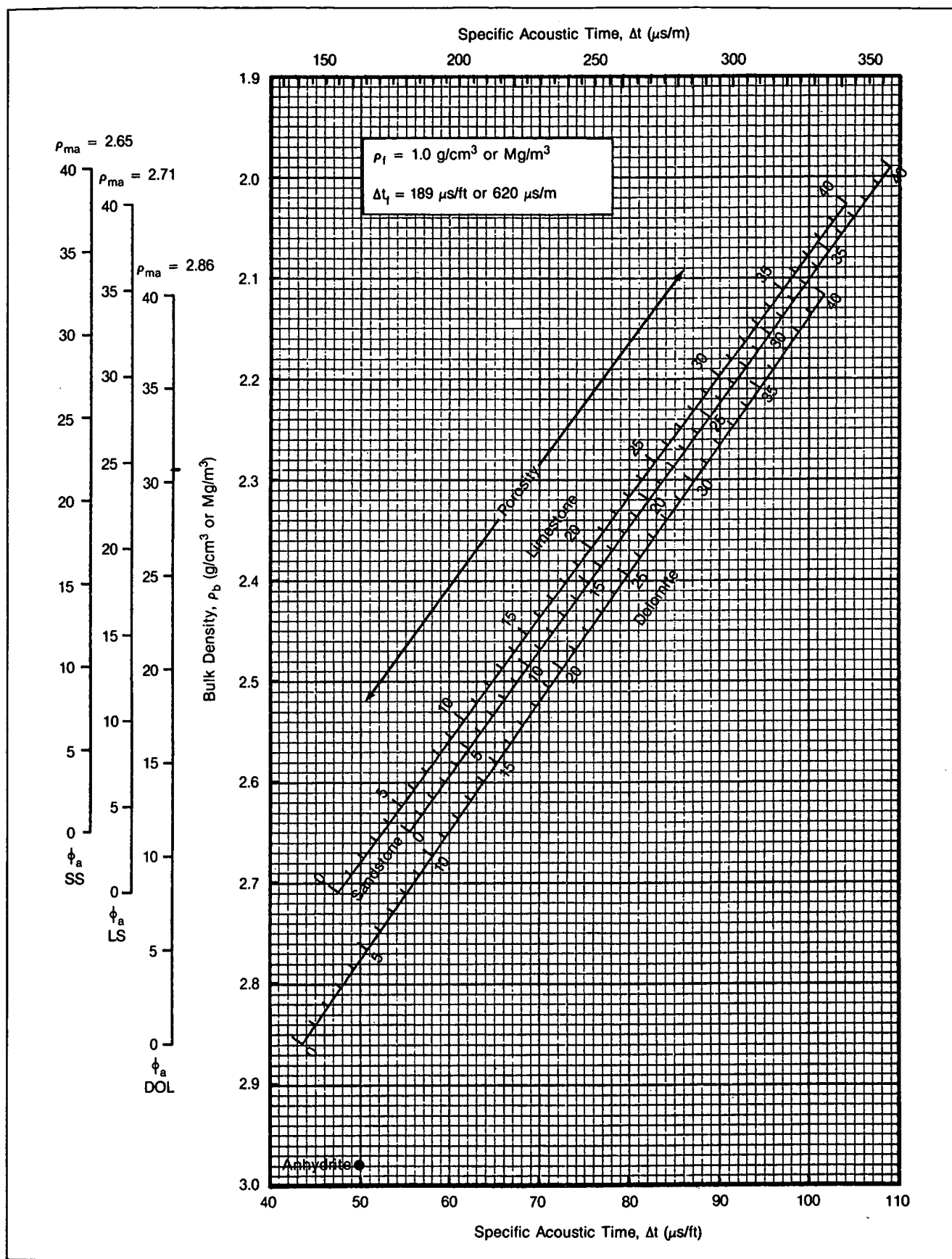


Fig. 5-16 – Porosity and lithology determination from compensated density and BHC Acoustilog

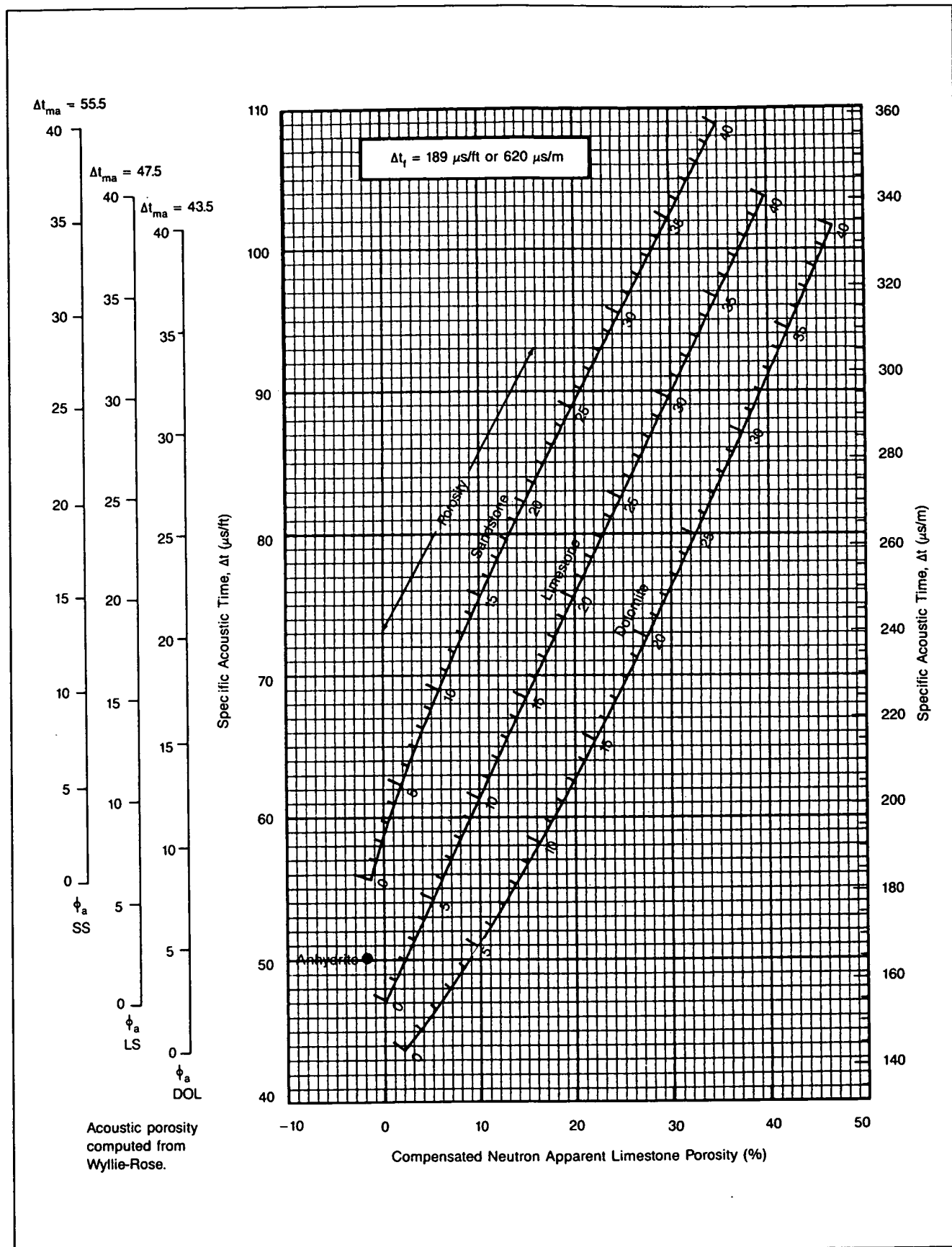


Fig. 5-17 – Porosity and lithology determination from BHC Acoustilog and Compensated Neutron Log

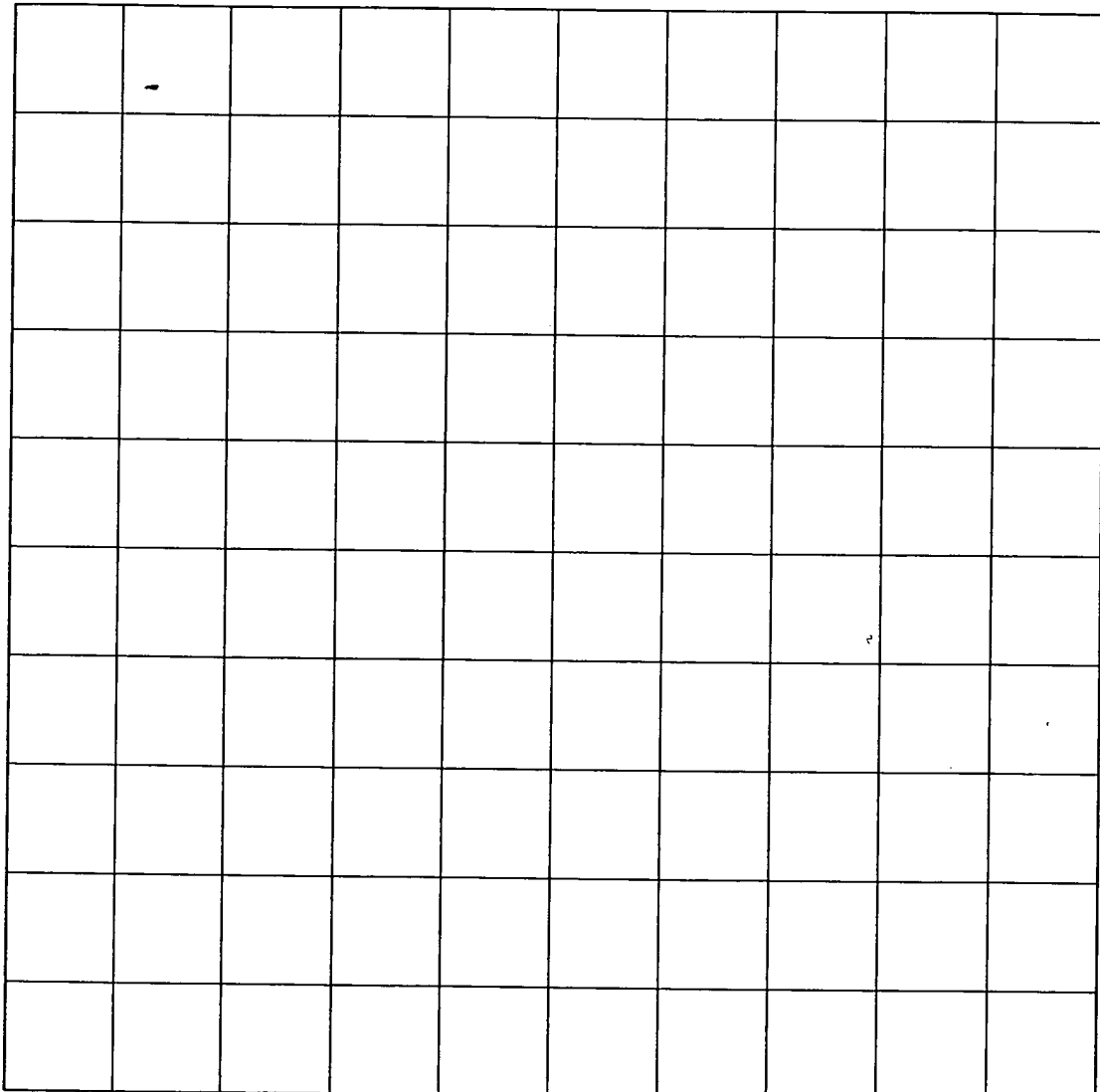
PRACTICAL WORK SESSION

Problem 1

On the linear graph, scale the y-axis to increase downward (in ρ_b increments) and the x-axis to increase to the right (in ϕ_{NL} values). The scale should extend from about 1 to 3 g/cm³ and from 0% to 100% apparent limestone porosity. The drilling fluid is fresh-mud gel – plot the 100% porosity or fluid point. The given matrix is limestone – plot the zero porosity matrix point. Adjacent beds

have shale values of approximately $\rho_{sh} \approx 2.6$ g/cm³ and $\phi_{Nsh} \approx 0.40$ – plot these points.

Connect the three points with lines to form a triangle. At this time, you have established three coordinate points for a density-neutron crossplot. Along the matrix-to-fluid line, interpolate porosity segments in increments of 10%. When this is completed, you have established a dual-mineral crossplot designed to solve for porosity and limestone vs. shale lithology mix.

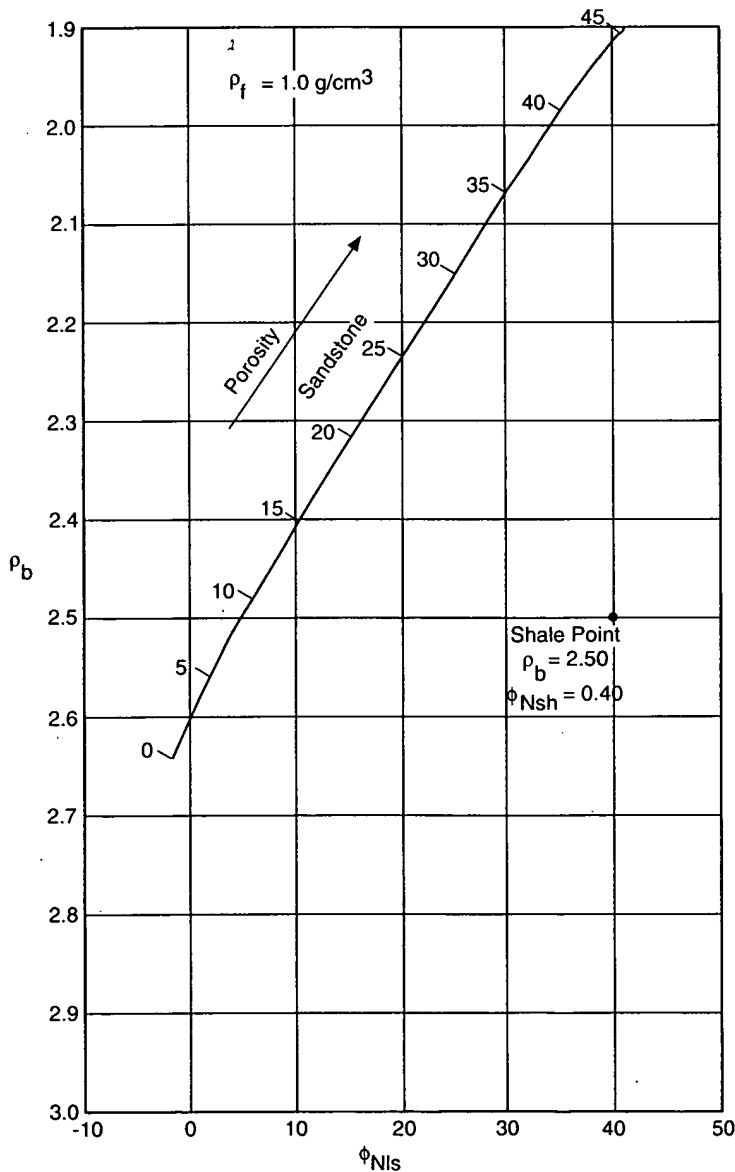


Problem 2

The working area of a crossplot is generally within 40% to 50% porosity limits (occasionally higher). That is why chart books generally show crossplots that do not extend beyond 50% porosity values. The grid and lithology lines are given for a density-neutron crossplot that is designed for sandstone, shale, and porosity estimates. You are given $\rho_{sh} \approx 2.5 \text{ g/cm}^3$ and $\phi_{Nsh} \approx 0.40$ as values from adjacent shale beds. First, construct the lines from the clean sand matrix point to the approximate 100% shale point. Then, construct eight separate but equally spaced parallel lines (parallel to the sand matrix line) between sandstone and shale.

By plotting the log data from a shaly sand with the values given below, porosity and sand-shale distribution can be estimated.

Porosity	Lithology Mixture
$\rho_b = 2.40, \phi_{Na} = 0.10$	_____
$\rho_b = 2.30, \phi_{Na} = 0.20$	_____
$\rho_b = 2.20, \phi_{Na} = 0.25$	_____
$\rho_b = 2.20, \phi_{Na} = 0.10$	_____
$\rho_b = 2.15, \phi_{Na} = 0.30$	_____

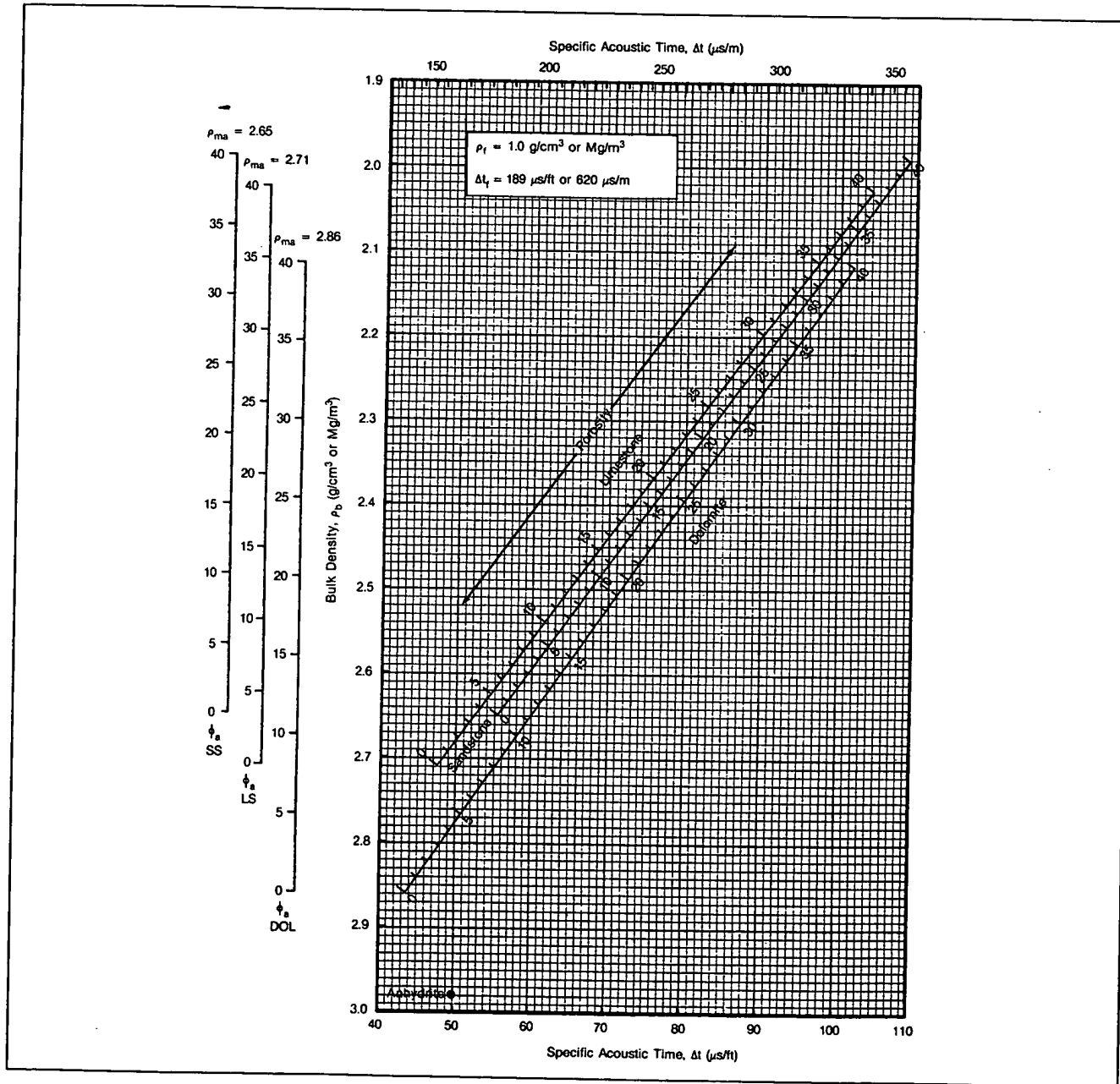


Problem 3

A density-acoustic chart book crossplot for fresh mud is given below. The lithology is sand-shale, and the sandstone line is constructed on the plot. Plot the shale values [$\rho_{sh} = 2.6 \text{ g/cm}^3$ and $\Delta t_{sh} = 100 \mu\text{sec/ft}$ (or $328 \mu\text{sec/m}$)]. Then, connect a line from the zero porosity sand matrix point to the shale point, and construct eight lines parallel to the clean sand line, between the 0% shale and 100% shale points, thus dividing V_{sh} incrementally between the two points. The next step is to construct dashed lines from the sandstone porosity values (along the sand matrix line) to the shale point. You now have a laminated shale model for the reservoir. Determine percent shale,

total effective porosity, and porosity of the sand laminae using the following input values.

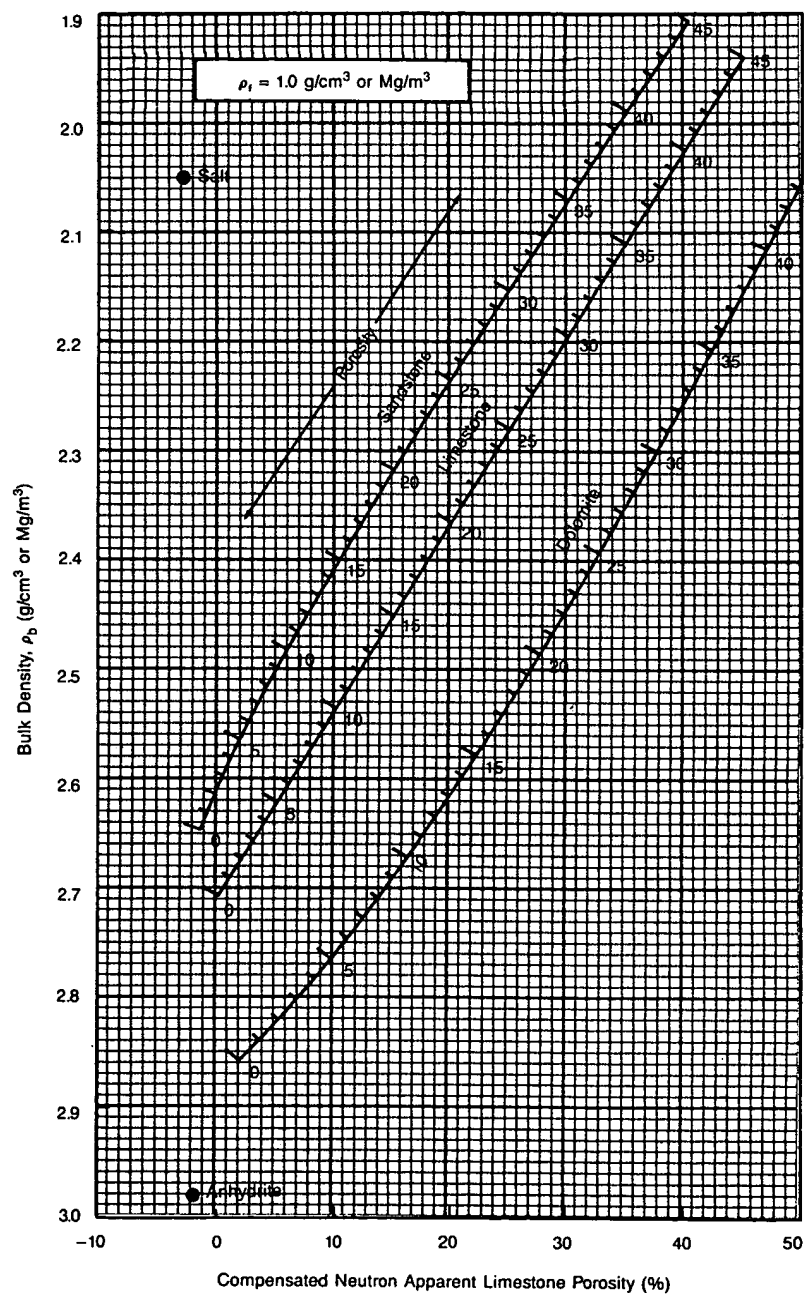
	ϕ_{eff}	V_{sh}	ϕ_{lam}
$\rho_b = 2.50, \Delta t = 73$	_____	_____	_____
$\rho_b = 2.52, \Delta t = 93$	_____	_____	_____
$\rho_b = 2.41, \Delta t = 80$	_____	_____	_____
$\rho_b = 2.54, \Delta t = 74$	_____	_____	_____
$\rho_b = 2.57, \Delta t = 72$	_____	_____	_____



Problem 4

Given a neutron-density crossplot, and assuming it is the correct chart for the log data provided, determine cross-plot porosity and an estimate of the lithology mix for the following given conditions:

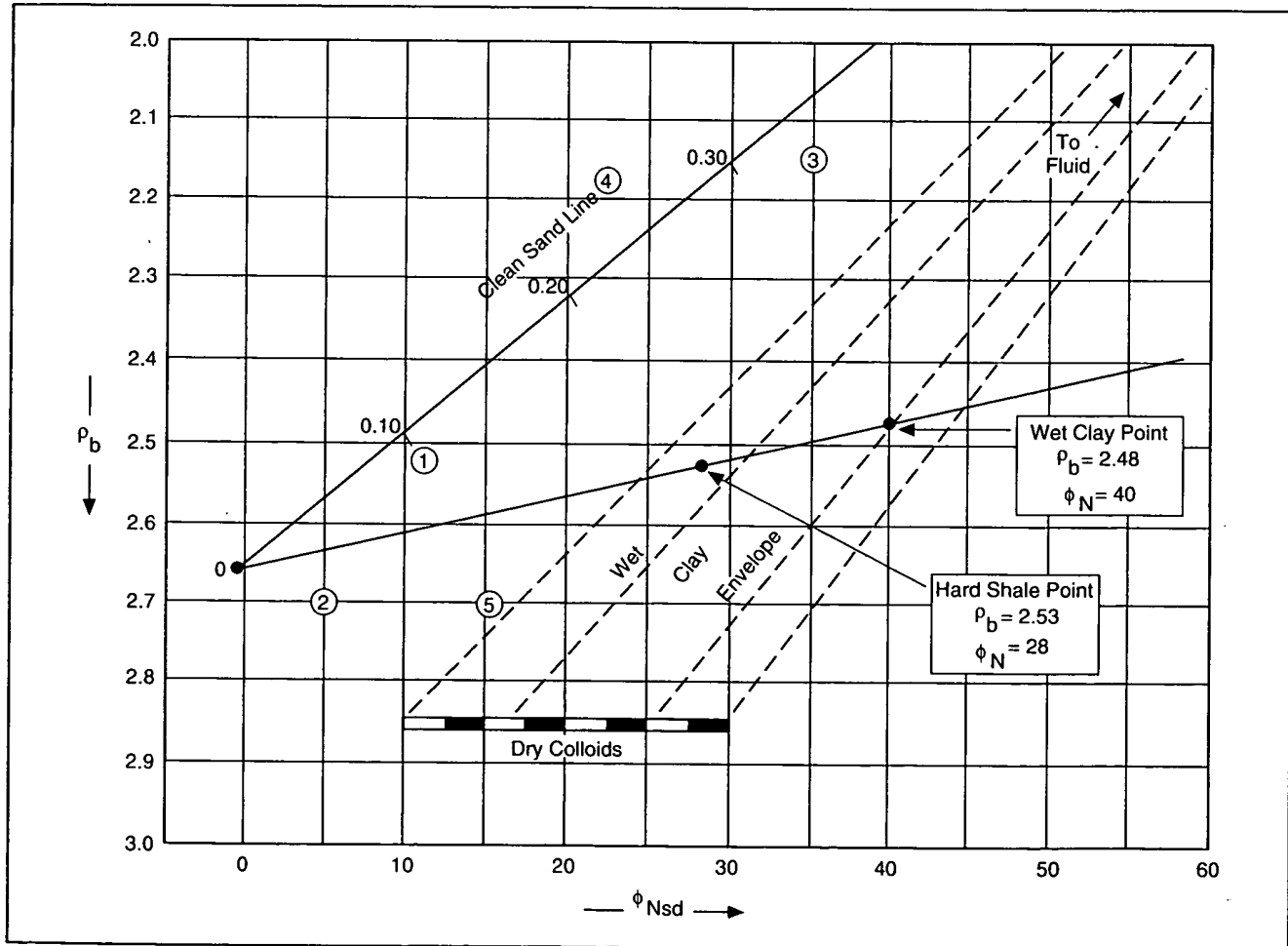
Log Values	Apparent Lithology	Lithology Porosity(%)
(1) $\rho_b = 2.52, \Delta t_{Nls} = 0.11$		
(2) $\rho_b = 2.70, \Delta t_{Nls} = 0.05$		
(3) $\rho_b = 2.15, \Delta t_{Nls} = 0.35$		
(4) $\rho_b = 2.20, \Delta t_{Nls} = 0.24$		
(5) $\rho_b = 2.60, \Delta t_{Nls} = 0.22$		



Problem 5

Given a slightly different neutron-density chart with the fluid, matrix, hard shale, and wet clay points defined, plot the five data points from Problem 4 and define them as shaly sands that have dispersed clay, laminated clay, structural clay, or clean sand.

- (1) _____
- (2) _____
- (3) _____
- (4) _____
- (5) _____



M-N CROSSPLOTS

Mineral identification from M and N data is not a 3-D crossplot technique. A crossplot is nothing more than a comparison of one type data (abscissa) to another type data (ordinate). The M-N plot actually compares a mix of acoustic and density data with a mix of density and neutron data. In M-N plots, all three sets of log data (in two forms) are used to crossplot the mixes from two differing data sets to achieve a "better idea" of the mineral mixture. Since the raw measurements from all three logs are intermixed, the *M* and *N* values are essentially independent of porosity and therefore supply important lithology-sensitive information. *M* and *N* are defined as –

$$M = \left(\frac{\Delta t_f - \Delta t}{\rho_b - \rho_f} \right) 0.01$$

and

$$N = \left(\frac{\phi_{Nf} - \phi_N}{\rho_b - \rho_f} \right)$$

For fresh-mud drilling fluid, the chart book values are $\Delta t_f \approx 189$, $\rho_f \approx 1$, and $\phi_{Nf} \approx 1$. The chart book values in salt mud are $\Delta t_f \approx 185$, $\rho_f \approx 1.1$ and $\phi_{Nf} \approx 1$. Fluid density is not a constant value, but varies somewhat with temperature, pressure, and depth, and the multiplier for the *M* solution is used for convenience to allow compatible scaling. The *M* and *N* plot is entered with calculated values, whereas the rocks/minerals indicated in specific areas or at specific points on the plot represent empirical and laboratory data (Fig. 5-18). *M* and *N* are no more than terms to represent their individual mix of log data.

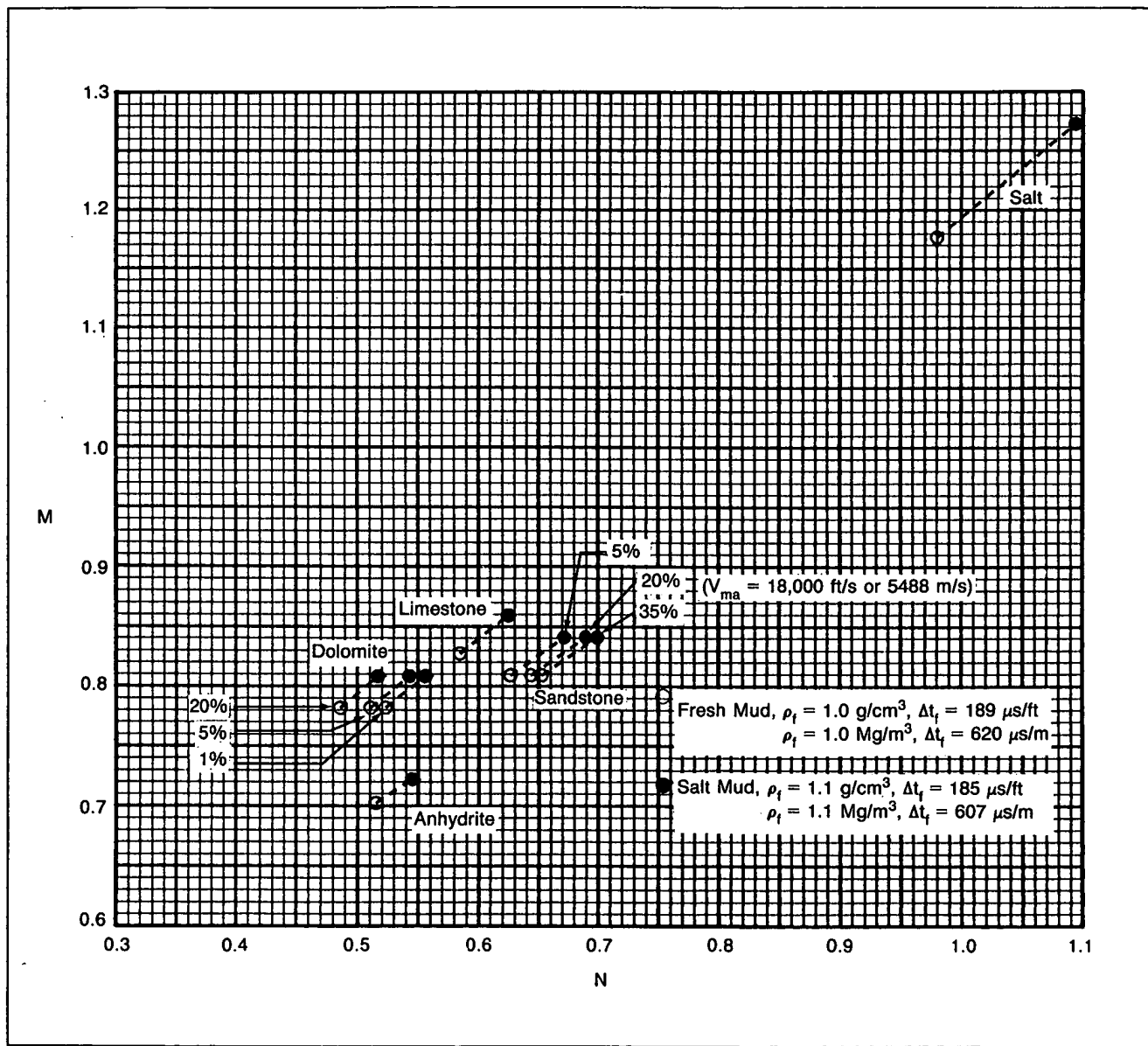


Fig. 5-18 – Mineral identification by M-N crossplot

Matrix parameters for given sedimentary rock/mineral types are seldom fixed values, and the values in Table 5-1 are approximations. In several cases, a plus or minus spread in values is given for a mineral response on certain log types. Data are presented for freshwater and saltwater muds, but applicable responses differ in oil-based muds, air-drilled holes, or mud systems such as those using KCl drilling fluids.

If a mixture of three minerals is known, log data are accurate, and a mud condition is given, the point on the plot resulting from crossplotting *M* and *N* should identify the mineral mix with reasonable accuracy. For example, if *M* = 0.76 and *N* = 0.55, the point will be within the dolomite-quartz-anhydrite triangle and will indicate an equal mixture of the three minerals. However, if the three known rock types are dolomite, quartz, and shale, a completely different interpretation will result – a slightly shaly, sandy dolomite. The crossplot does not determine the lithology mix; the analyst determines the lithology mix by relating the log responses to a known mix.

The apparent mineral mix from M-N plots can also be misleading if any of the three logging devices is affected by gas, secondary porosity, shaliness, or unfavorable borehole conditions. Admixtures of other rock types such as gypsum or salt and heavy minerals such as pyrite (FeS_2) or siderite ($FeCO_3$) can also distort M-N results. Use of M-N techniques therefore requires a comparison of all the previously described crossplots to determine if any of the logs are affected by gas, secondary porosity, salt, gypsum, or other minerals. Combining all the information available is necessary to achieve a satisfactory interpretative estimate of porosity and lithology fractions.

MINERAL IDENTIFICATION (MID) PLOT

The MID plot is another approach that essentially uses the three types of log data differently to provide more sensitivity to lithology, gas, and secondary porosity. Again, acoustic, density, and neutron data are required. Two crossplot steps are required to determine the values needed to enter the MID plot –

- Density and neutron data are plotted to determine the total apparent porosity (ϕ_a).
- Acoustic and neutron data are plotted to determine an total apparent porosity (ϕ_a).

Porosities from the two crossplot solutions virtually never agree, but each of the individually determined values is used, respectively, in the solution for apparent matrix density (ρ_{maa}) and apparent matrix transit time (Δt_{maa}) –

$$\rho_{maa} = \left(\frac{\rho_b - \phi_a \rho_f}{1 - \phi_a} \right)$$

and

$$\Delta t_{maa} = \left(\frac{\Delta t - \phi_a \Delta t_f}{1 - \phi_a} \right)$$

where

ρ_b = bulk density value from density log,

Δt = interval transit time from acoustic log,

ρ_f = density of the pore fluid,

Δt_f = transit time of the pore fluid,

and

ϕ_a = apparent total porosity determined from the two crossplots previously described

The two apparent matrix values are then used to enter the matrix identification plot (Fig. 5-19). Again, the appropriate crossplot charts for the tool types and mud salinity are necessary.

The MID plot differs from the M-N plot because of the different tool mixtures used to determine the entry values for *x* and *y* coordinates. On M-N plots, the *M* value resulted from acoustic and density data and the *N* value resulted from neutron and density data. Density and neutron measurements are used to obtain one value for entry into the MID plot, but acoustic and neutron data are used (not density and acoustic) to obtain the other entry value.

MID plot lithology definition is also hampered by the affects of gas, secondary porosity, bad hole conditions, shaliness, and the effects must be recognized by the user. Nevertheless, MID plot resolution is superior to that of the M-N plot.

Z-DENSITY DATA

P_e data improve interpretation with the density log. Deriving a porosity value from ρ_b alone requires assumptions for ρ_{ma} , a bit of guesswork that can lead to considerable error in the calculation. Photoelectric cross section is a very lithology-sensitive parameter, and it can be used to establish within reasonable tolerance whether a formation is sand, limestone, dolomite, or a mixture. Calculation of porosity from ρ_b requires a parameter for matrix density; not an absolute lithology description, but a reasonably accurate value for matrix density. Z-density data permit a dual-mineral solution to analyze the mixture of two mineral types for a more effective porosity estimate. Charts are provided for both freshwater and salt-based muds (Figs. 5-20, 5-21). The algorithms for resolving ϕ_a from ρ_b and P_e are –

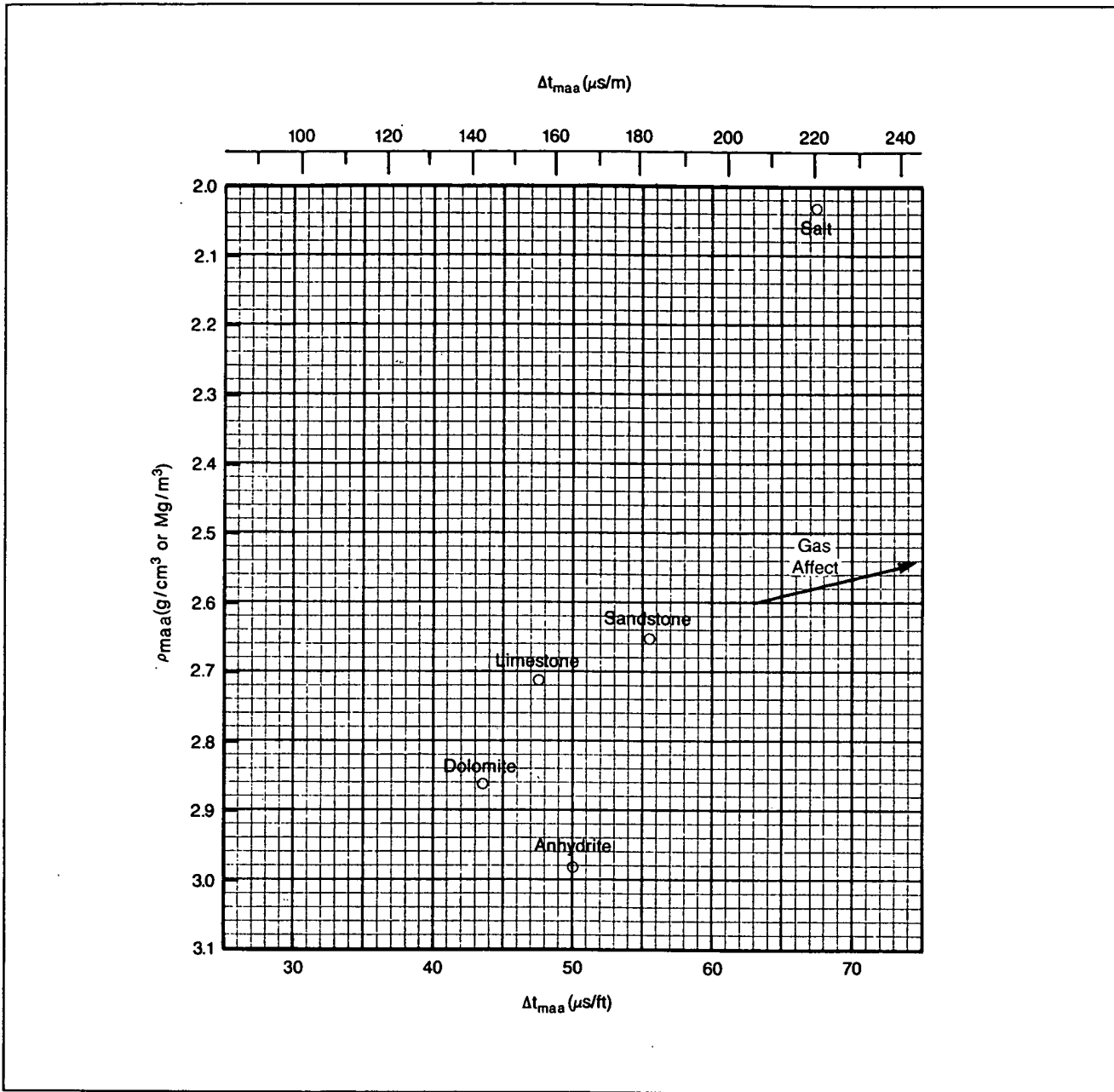


Fig. 5-19 – Mineral identification plot

$$\rho_b = \phi_a \rho_f + V_1 \rho_1 + V_2 \rho_2,$$

ρ_e = electron density index
 $(\rho_b + 0.1883)/1.0704$,

$$P_e \rho_e = \phi_a U_f + V_1 U_1 + V_2 U_2,$$

and

$$I = \phi_a + V_1 + V_2,$$

$I, 2$ = density, U values, and bulk volume values for minerals 1 and 2.

where

ρ_b = log measured bulk density (g/cm^3),

P_e = photoelectric cross section (barns/electron),

U_f = U value of fluid (charts assume 0.398),

When Z-Densilog and neutron data are used, a more accurate definition of lithology and a better estimate of porosity are made available. A direct benefit is much better distinction between oil and gas. If the predominant mineral mix is two matrices, it is a relatively simple well-site application.

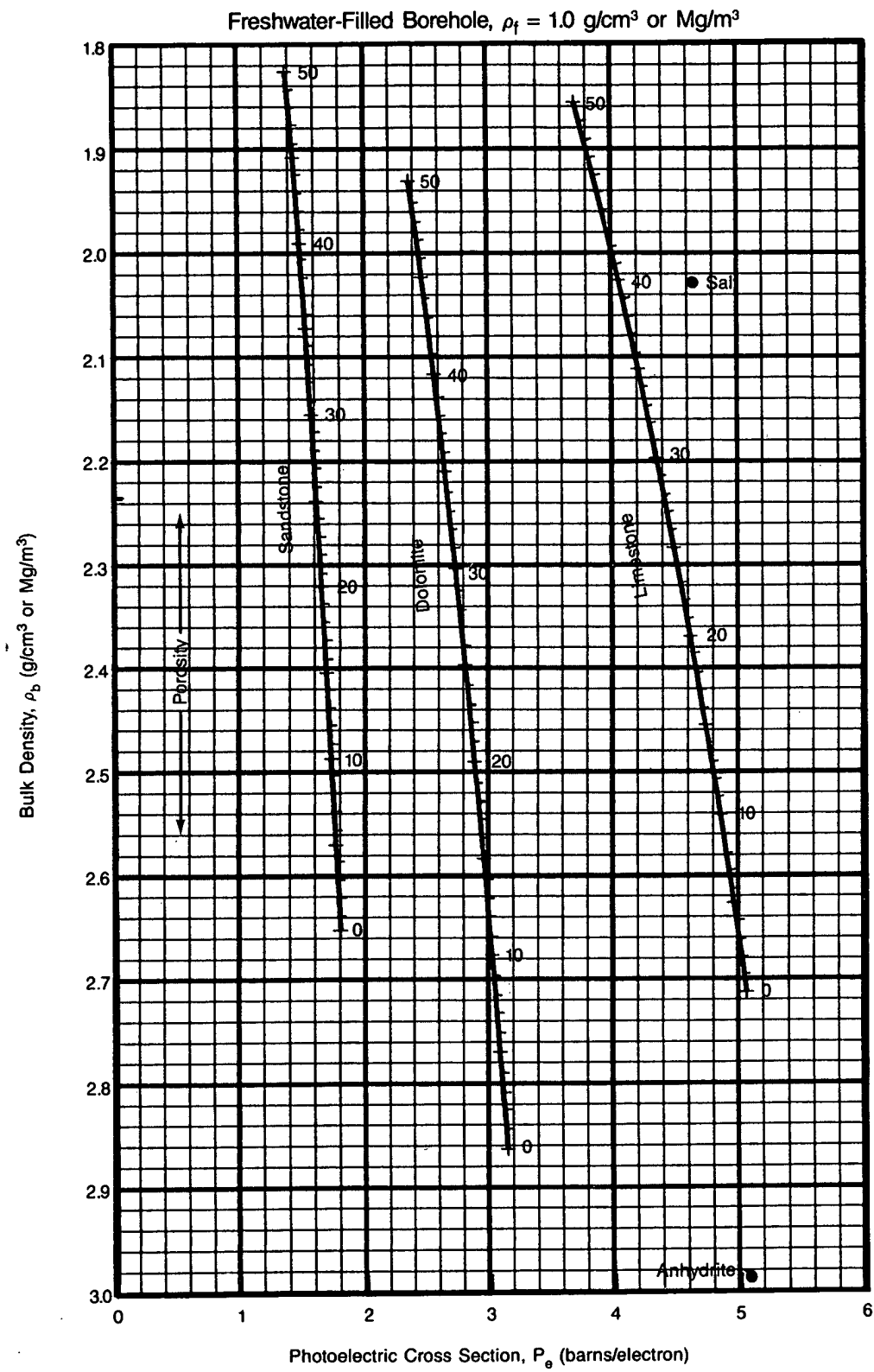


Fig. 5-20 – Porosity and lithology determination from the Compensated Z-Densilog measurement

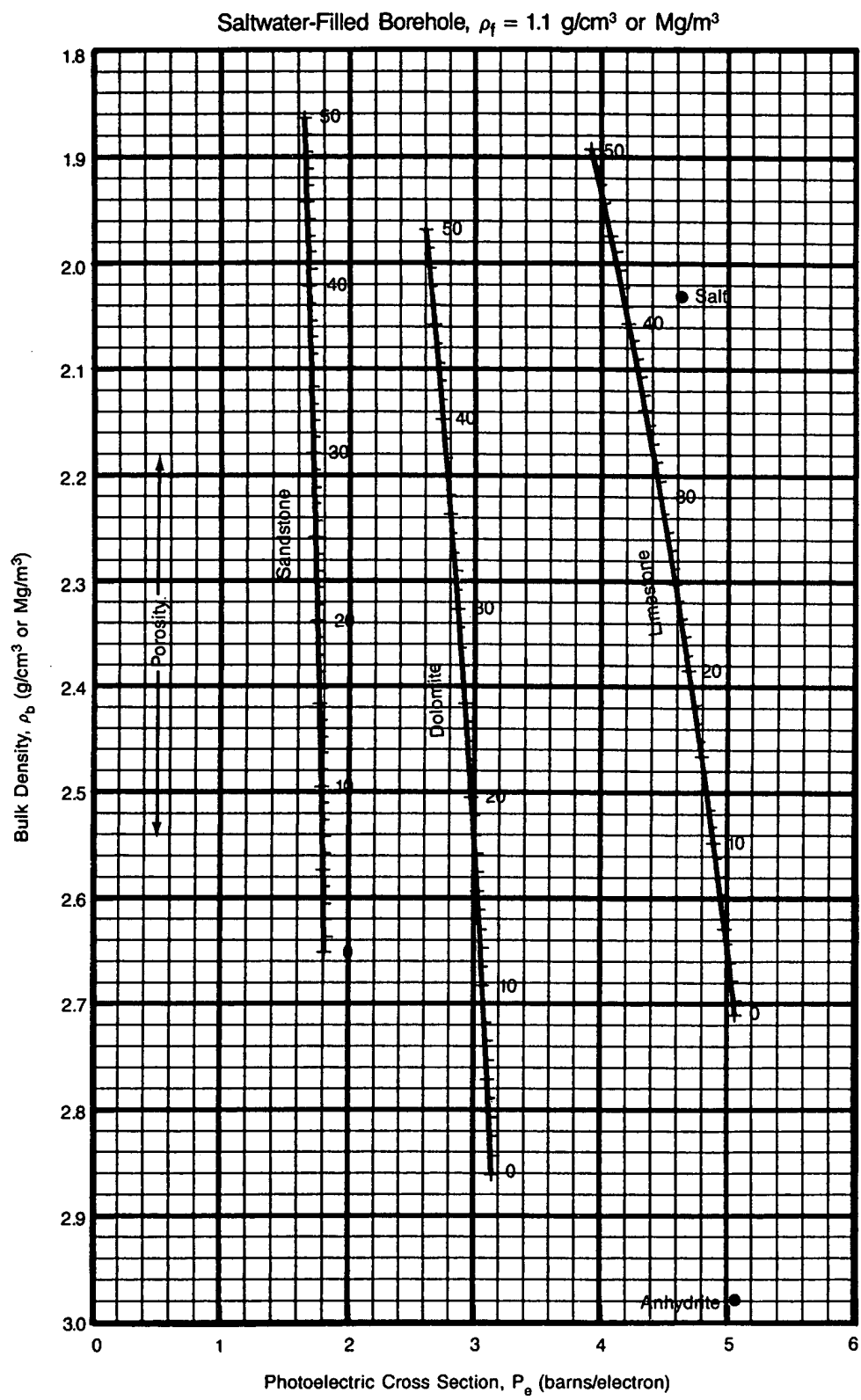


Fig. 5-21 – Porosity and lithology determination from Compensated Z-Densilog measurement

If the solution of lithology, porosity, and gas affect involves three or more minerals, more sophisticated computations and crossplot analyses are required. Computer-processing techniques are almost prerequisite if such complexity occurs. Bulk density and neutron data are crossplotted in the conventional manner to determine ϕ_a and ρ_{maa} . The apparent volumetric cross section (U_{maa}) is found by following the P_e data point vertically upward to ρ_b , then horizontally across to ϕ_a , and downward vertically to determine U_{maa} (Fig. 5-22). The volumetric term (barns/cm³) can also be calculated –

$$U_{maa} = \left(\frac{P_e \rho_e - \phi_a U_f}{1 - \phi_a} \right)$$

where

P_e = photoelectric absorption cross section,
 ρ_e = electron density ($\rho_b + 0.1883/1.0704$),
 ϕ_a = apparent total effective porosity,

and

U_f = volumetric value for the fluid.

The two porosity values derived from the two crossplots are similar if the formation is fluid filled and borehole conditions are tolerable, and the density-neutron solution is generally accepted. Gas-filled formations affect neutron logs more than density measurements; therefore, porosity from the density-neutron crossplot is somewhat pessimistic if gas is present, whereas porosity derived

from the P_e vs. ρ_b crossplot is often more reliable. P_e and U_{maa} values for several lithology and fluid types are given in Table 5-2.

TABLE 5-2
 Typical Matrix Values for Commonly Encountered Materials

	P_e	ρ_{maa}	U_{maa}	ρ_b	U_f
Dolomite	3.14	2.88	9.11	2.88	9.05
Limestone	5.08	2.71	13.78	2.71	13.78
Sandstone	1.81	2.65	4.79	2.65	4.79
Magnesite	0.83	3.00	2.50	2.98	2.47
Anhydrite	5.05	2.98	15.06	2.98	2.47
Gypsum	3.99	3.69	18.76	2.35	9.38
Halite	4.65	2.36	12.44	2.04	9.49
Sylvite	8.51	2.25	23.08	1.86	15.83
Chlorite	6.30	3.39	23.63	2.76	17.39
Illite*	3.45	2.92	10.97	2.52	8.69
Kaolinite*	1.83	2.96	6.14	2.41	4.41
Montmorillonite*	2.04	2.89	7.28	2.12	4.32
Muscovite	2.40	2.97	7.35	2.82	6.77
Biotite	6.27	3.10	19.80	2.99	18.75
Glauconite*	6.37	3.05	21.52	2.54	16.18
Coal, bituminous	0.17	1.99	0.87	1.24	0.21
Banite	267	4.09	1091	4.09	1091
Hematite	21.5	5.27	113.5	5.18	111.3
Fresh water	0.36			1.00	0.36
Salt water (330 ppk)	1.64			1.19	1.95
Oil	0.12			0.88	11

*Typical values

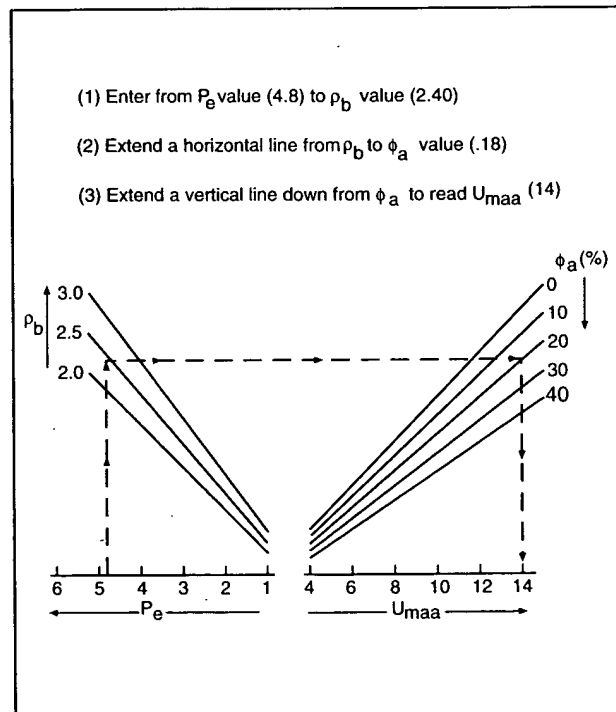


Fig. 5-22 – Chart determination of the apparent matrix volumetric cross section (U_{maa})

Complex lithology is resolved somewhat by crossplotting the U_{maa} value against the ρ_{maa} value (Fig. 5-23). The triangular points for quartz, calcite, and dolomite are configured from conventional matrix values for each mineral, and the lines connecting points along the three edges of the triangle denote the percentages of each mineral. For example, a point that falls at A is considered a mixture of 40% limestone and 60% dolomite, whereas a point that falls at B is considered a mixture of 20% sand, 20% limestone, and 60% dolomite. Triangles can also be constructed for other mineral mixes such as salt, anhydrite, and dolomite (Fig. 5-24) or salt, dolomite, and limestone (Fig. 5-25). Points for other minerals in relation to their response on P_e , ρ_b , and ϕ_N measurements can also be indicated (Fig. 5-26). However, gas affects and borehole irregularities must still be considered, and for accuracy, clays, shales, and additional rock types must be estimated by other means. Accurate solutions require a sufficient number of measurements to solve for the number of rocks and minerals present.

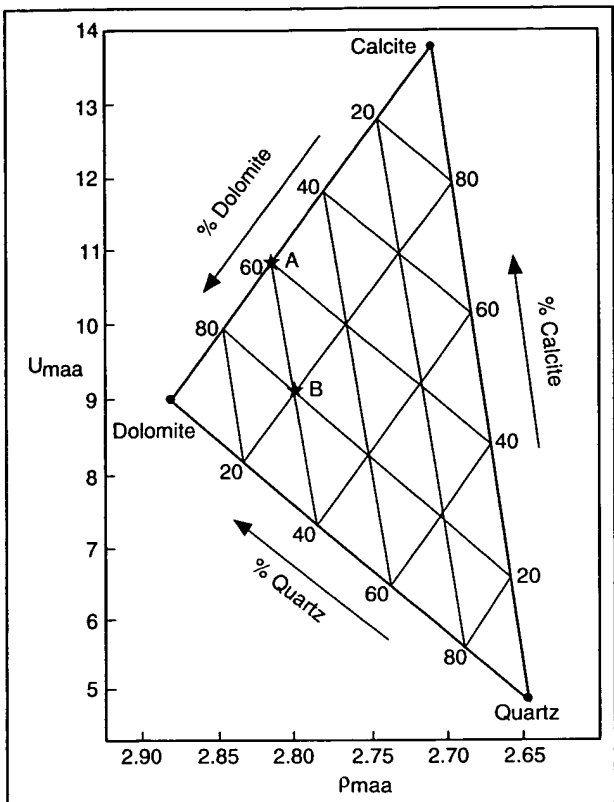


Fig. 5-23 – Complex lithology is resolved somewhat by cross-plotting the apparent matrix density vs. the apparent matrix volumetric.

Variations of lithology can lead to different triangular charts, e.g., gypsum-anhydrite-dolomite, salt-anhydrite-dolomite, or limestone-dolomite-anhydrite, etc. Some knowledge of lithology is required for input if adequate results are to be obtained.

DEFINING LITHOLOGY TRIANGLES

The concept of lithology triangles is built on the assumption that virtually all the formation is a mixture of a three-mineral group, and that points representing those three minerals on the plot will encompass any log data from that formation. Triangles representative of shale-free carbonate and anhydrite zones demonstrate the hypothesis (Fig. 5-27).

Shale is a loose geological term that is generally accepted as describing minerals or formations falling within a certain distribution of grain size and made up mostly of clastics. Ambiguity exists, but for the purposes of log analysis, carbonate reservoir rock and evaporites are generally shale free. The area marked as Shale Region on Fig. 5-28 is below the anhydrite and silica points of the M-N plot. A unique shale point is not possible because of the variable characteristics of the bound water and material form.

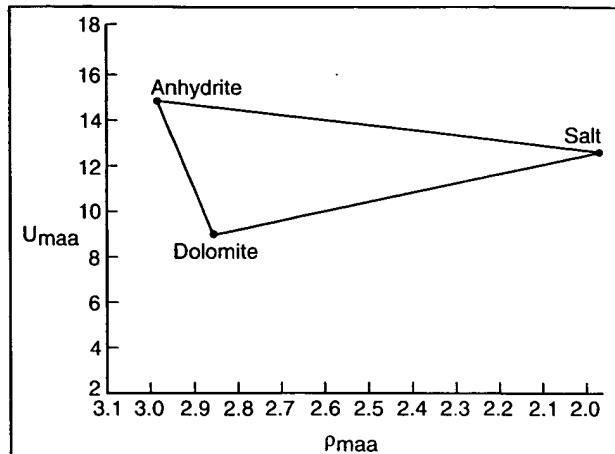


Fig. 5-24 – Triangles can be constructed for different rock types.

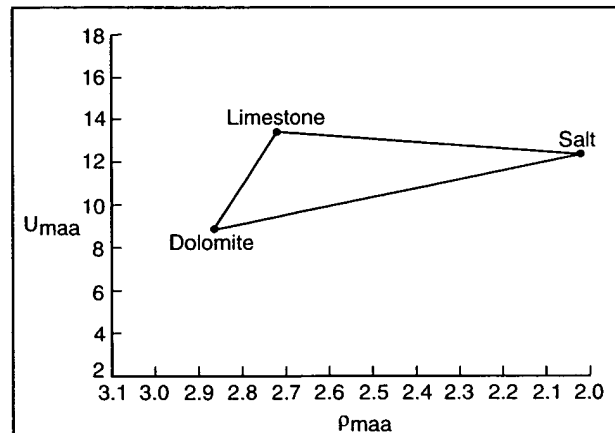


Fig. 5-25 – Another lithology triangle concept

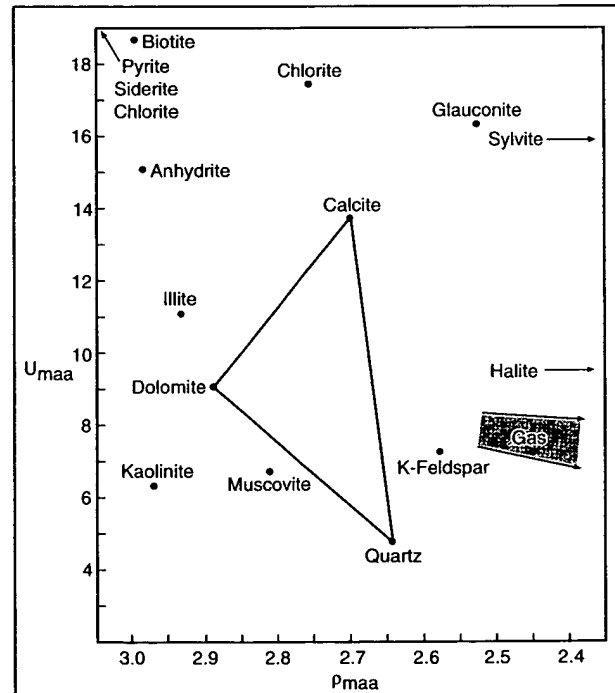


Fig. 5-26 – Points or general location of other rocks and minerals can be placed on the crossplot.

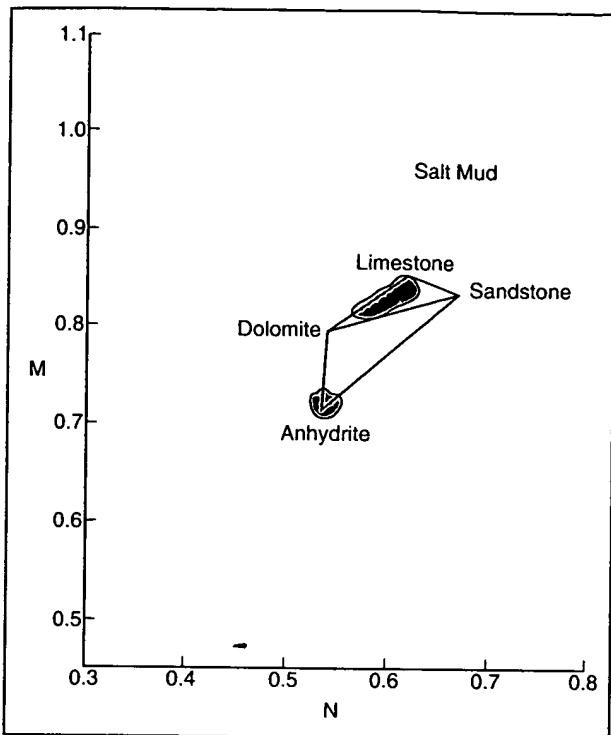


Fig. 5-27 – Limestone, dolomitic limestone, limey dolomite, and anhydrite are indicated from the location of plotted data.

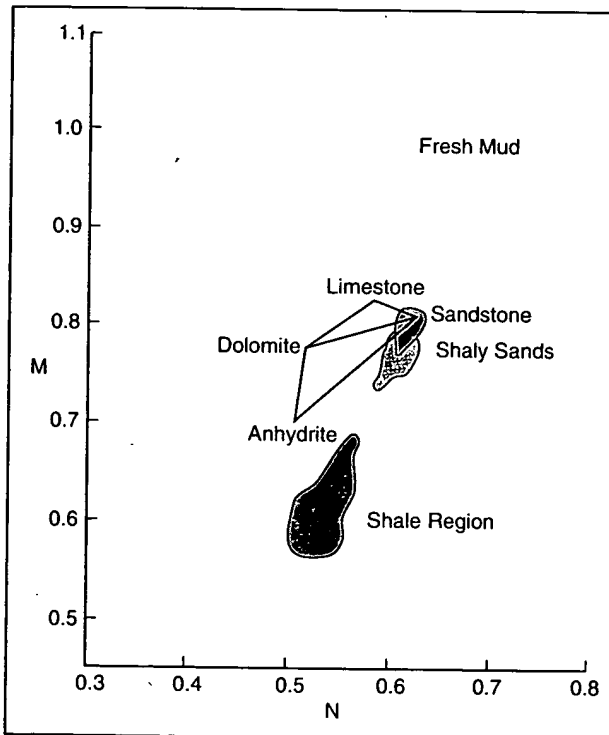


Fig. 5-28 – Shale data are identified from the general area.

Linearity on any three-way plot is also affected by the nature of the logging devices. For example, acoustic log data indicate porosity type as well as amount, and neutron measurements are distinctly nonlinear in dolomite.

No matter what vintage of density, neutron, or acoustic log, a three-way crossplot does not totally resolve the lithology dilemma.

Secondary porosity does not affect the calculation of N on an M-N crossplot, but it does affect the M value as secondary pore space increases. This is because the acoustic transit time measurement does not typically increase in the presence of vugs, fractures, or spherulitic pore space. Similar effects occur on the MID plot; ρ_{maa} is unaffected by secondary porosity, but Δt_{maa} reflects a lower value as the amount of secondary porosity increases. A general attempt to define the percentage of all possible three-mineral sets would be futile, and undoubtedly many exceptions would be noted. By careful local study, however, analysts can determine preferential mineral groupings that lead to reasonable lithology estimates. If local information is lacking, a "most likely" combination is used, and that alone is the target of chart book representations.

All three-mineral plots discussed have applications, but artificial solutions from any of them are limited to the three minerals that establish the triangle. They are not 3-D; they are 2-D plots with lines connected between the three control points that establish a linear mixture. Mathematical solutions can be used to resolve a matrix mixture, but consider that math is a nearly perfect science being applied to geology, an ambiguous and somewhat unpredictable science far removed from the disciplinary approaches of mathematics and computer science.

Numerous crossplot techniques can be used to manipulate the data. M can be plotted against GR , SP , ρ_b , ϕ_N , or Δt to verify selected control parameters. Neutron-density crossplot porosity can be compared to acoustic porosity to determine the effects of secondary pore space, shaliness, gas effects, etc. Density, neutron, and/or acoustic data can be crossplotted against GR and/or SP data to differentiate the effects of natural radiation, shaliness, borehole conditions, or lithology/porosity variances between zones when the use of only one log might cause separate depth intervals to appear similar.

PRACTICAL WORK SESSION

Apparent Lithology

Problem 1

Given the knowledge that anhydrite, salt, and dolomite are the probable rock types in particular depth intervals, enter the M-N plot (salt mud) with the following values and estimate the lithology mixture for each of the following input M and N values –

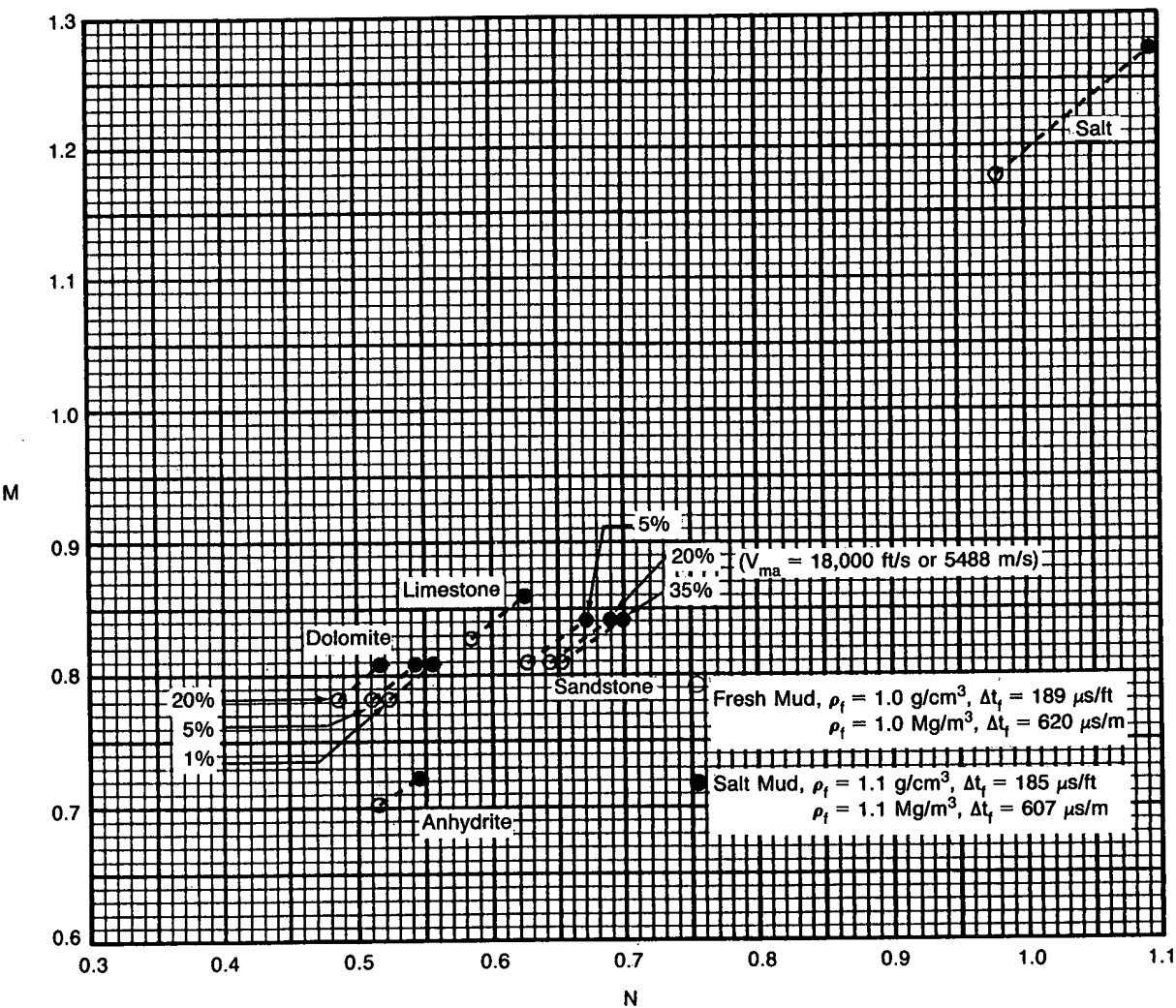
$M = 0.83, N = 0.57$ _____

$M = 0.75, N = 0.54$ _____

$M = 0.81, N = 0.57$ _____

$M = 0.72, N = 0.55$ _____

$M = 0.86, N = 0.60$ _____



Problem 2

Given a MID plot and the following input data, estimate the lithology –

Apparent Lithology

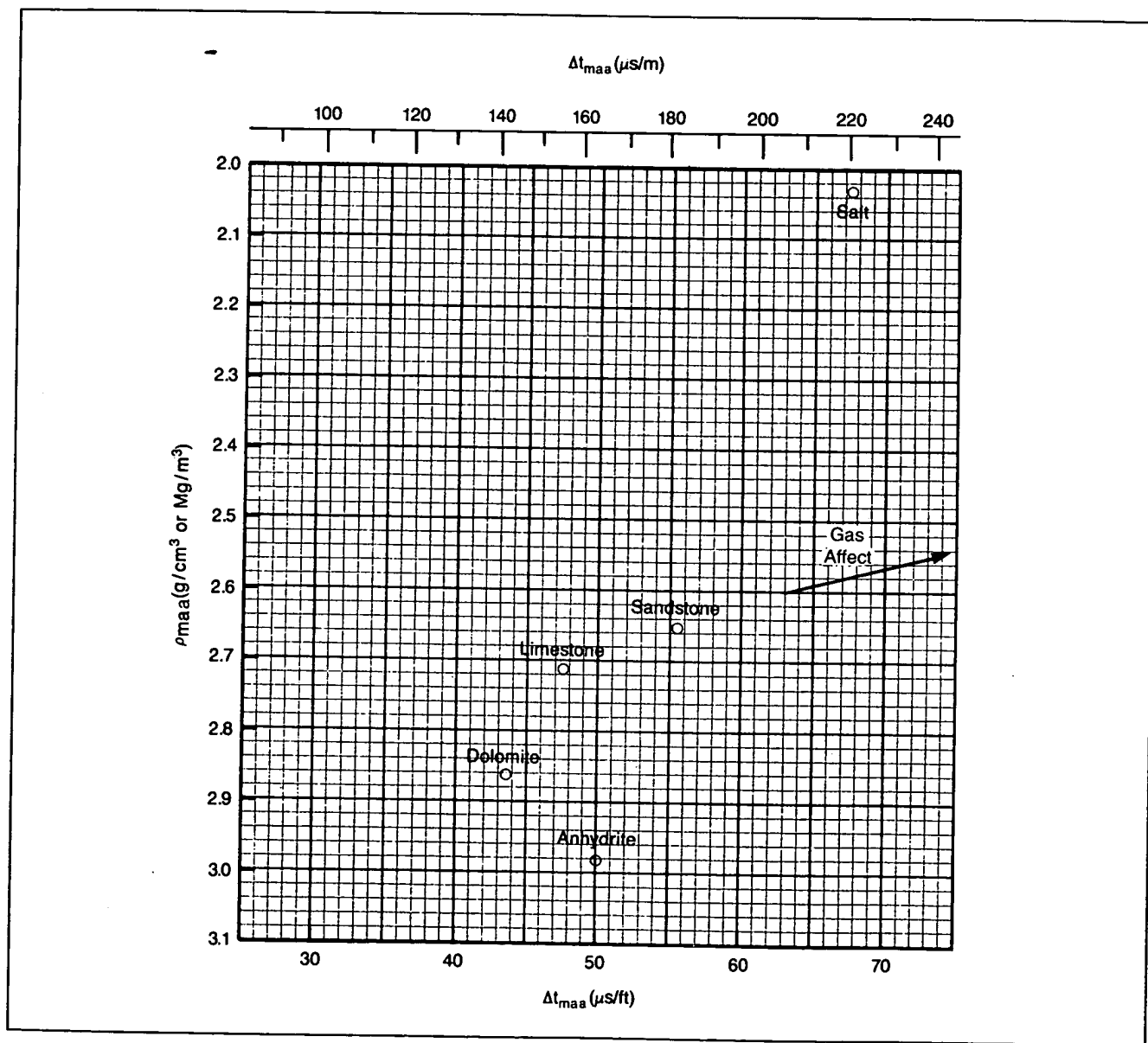
$\rho_{maa} = 2.80 \text{ g/cm}^3, \Delta t_{maa} = 48 \mu\text{sec/ft}$ _____

$\rho_{maa} = 2.77 \text{ g/cm}^3, \Delta t_{maa} = 46 \mu\text{sec/ft}$ _____

$\rho_{maa} = 2.62 \text{ g/cm}^3, \Delta t_{maa} = 59 \mu\text{sec/ft}$ _____

$\rho_{maa} = 2.94 \text{ g/cm}^3, \Delta t_{maa} = 48 \mu\text{sec/ft}$ _____

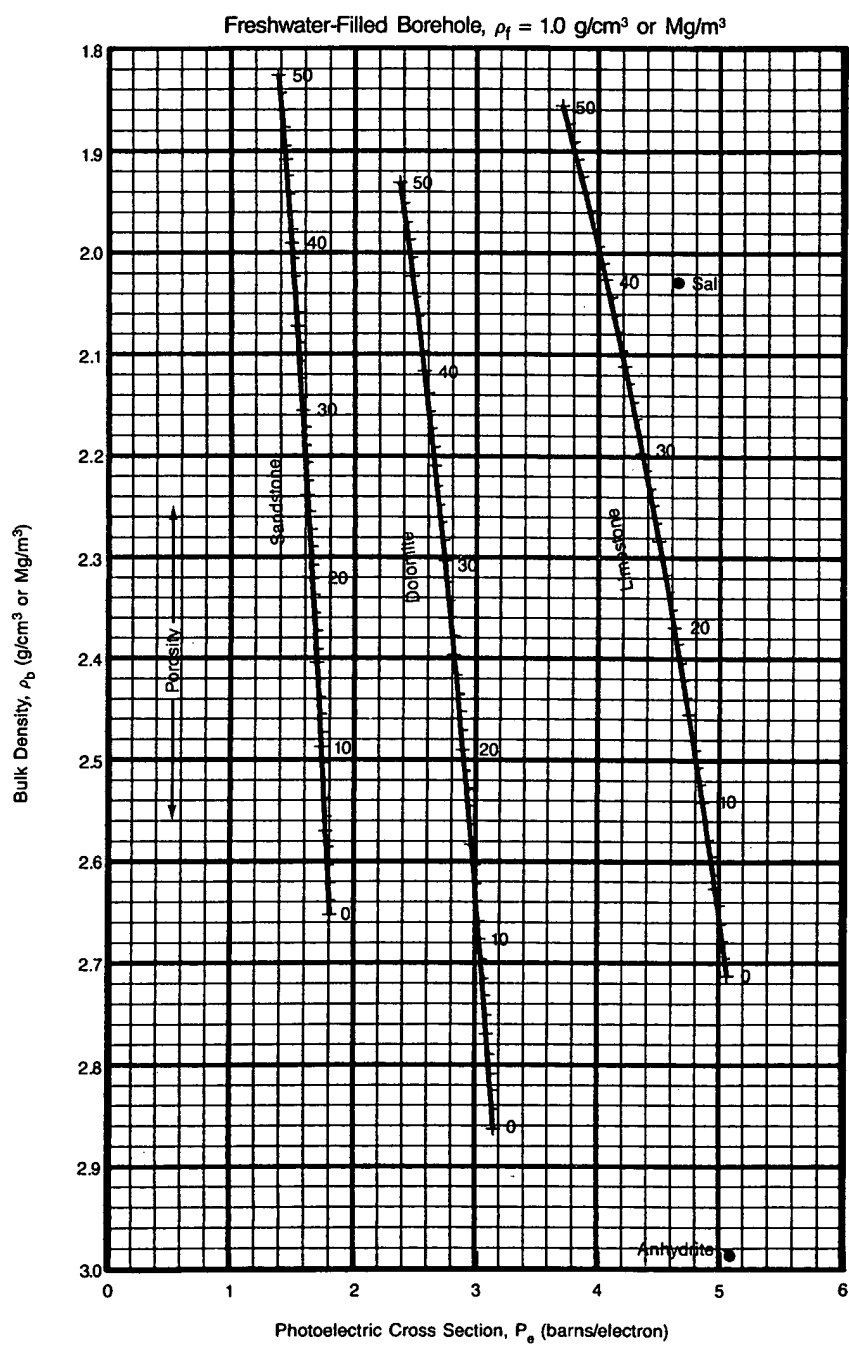
$\rho_{maa} = 2.16 \text{ g/cm}^3, \Delta t_{maa} = 65 \mu\text{sec/ft}$ _____



Problem 3

From Z-Densilog data only, determine porosity from the following measurements using the freshwater mud chart below –

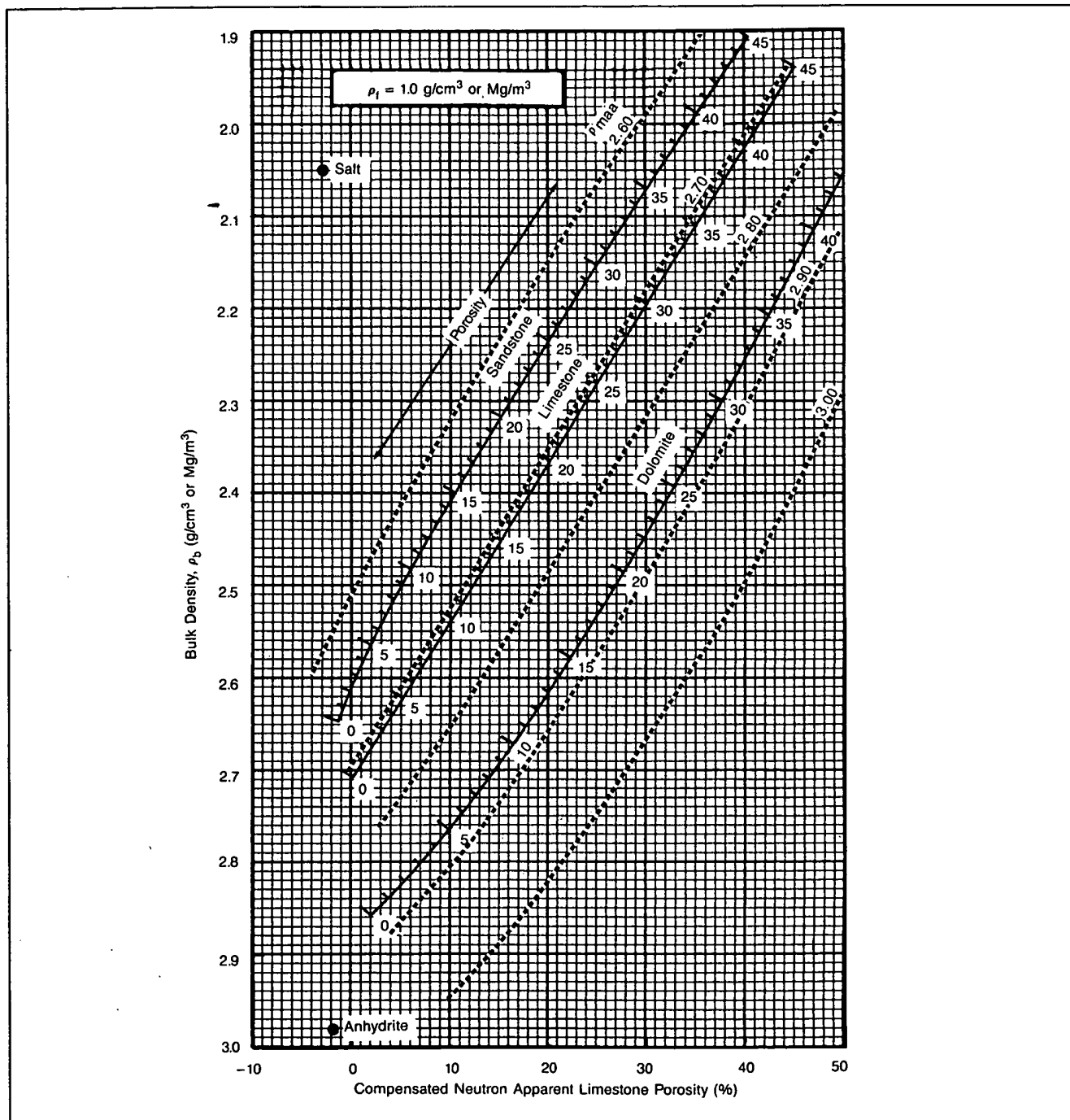
	Lithology	Porosity
$P_e = 3, \rho_b = 2.40$	_____	_____
$P_e = 1.8, \rho_b = 2.36$	_____	_____
$P_e = 4.6, \rho_b = 2.48$	_____	_____
$P_e = 5, \rho_b = 2.65$	_____	_____
$P_e = 1.8, \rho_b = 2.17$	_____	_____



Problem 4

Given the following log data, use the fresh mud density-neutron chart below to determine ρ_{maa} and effective porosity (ϕ_e). Also, indicate the apparent lithology and note by ** if gas effect occurs.

ρ_{maa}	U_{maa}	ϕ_e	Apparent Lithology
$\rho_b = 2.40, \phi_{Nls} = 0.23$	—	—	—
$\rho_b = 2.36, \phi_{Nls} = 0.15$	—	—	—
$\rho_b = 2.48, \phi_{Nls} = 0.19$	—	—	—
$\rho_b = 2.65, \phi_{Nls} = 0.06$	—	—	—
$\rho_b = 2.17, \phi_{Nls} = 0.18$	—	—	—



Problem 5

Using the ρ_{maa} and U_{maa} data from Problem 4 and the ϕ_a values determined in Problem 3, along with the given ρ_b values in both problems, determine an approximate matrix volumetric (U_{maa}) using the chart below.

U_{maa}

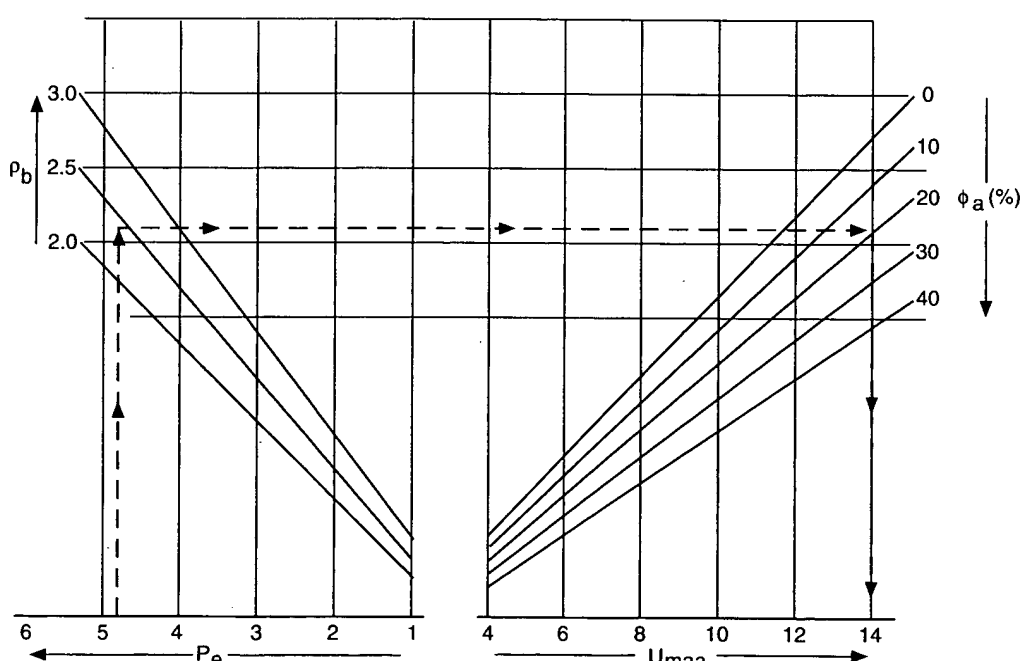
Zone 1 _____

Zone 2 _____

Zone 3 _____

Zone 4 _____

Zone 5 _____



- (1) Enter from P_e value (4.8) to ρ_b value (2.40)
- (2) Extend a horizontal line from ρ_b to ϕ_a value (.18)
- (3) Extend a vertical line down from ϕ_a to read U_{maa} (14)

Problem 6

Using the chart below and considering no shale volume, estimate the lithology by crossplotting the U_{maa} data from Problem 5 and the ρ_{maa} data from Problem 4 for each of the 5 zones.

Apparent Lithology

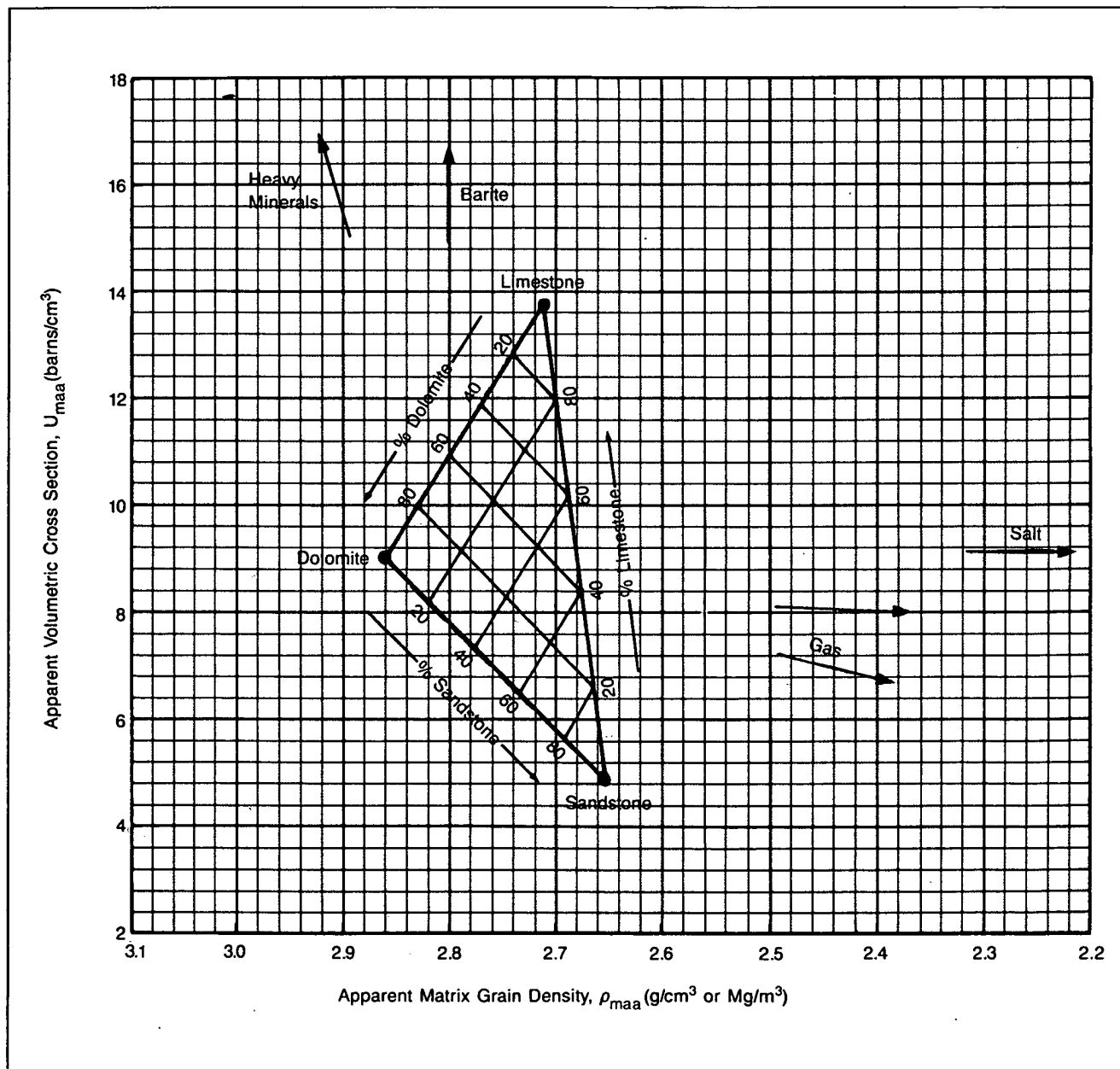
Zone 1 _____

Zone 2 _____

Zone 3 _____

Zone 4 _____

Zone 5 _____



PLOTTING DATA ON A Z-AXIS

Thus far, the discussion has been devoted to several crossplot methods that use either two or three log measurements to solve for porosity and lithology. Shale, borehole rugosity, secondary porosity, and gas influenced all the crossplots to some degree. All the plots were 2-D, and data were plotted in some form with an abscissa (x-axis) and ordinate (y-axis). The crossplot coordinates of two input data types resulted in an estimate of lithology. General areas of the plots were designated as regions where gas, shale, or hole rugosity would cause crossplotted data to fall. Computer processing of log data often presents crossplotted data for selected depth intervals by frequency of occurrence at each cell or coordinate (Fig. 5-29). The data can be overlaid with the familiar lithology lines and permit an estimate of porosity and lithology to be made (Fig. 5-30).

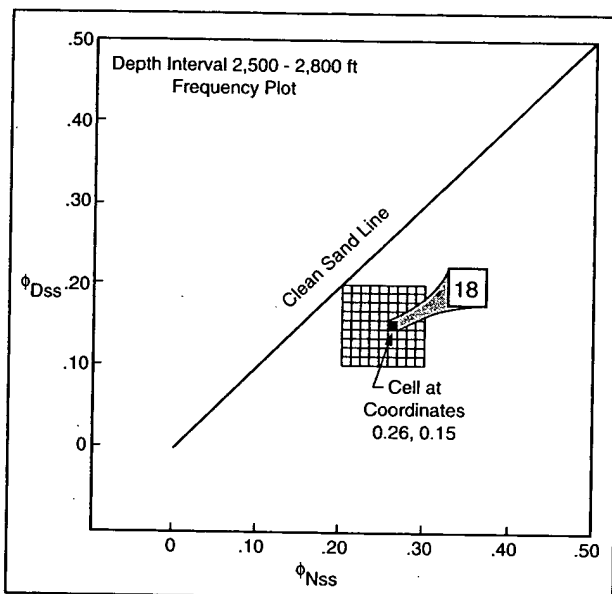


Fig. 5-29 – Eighteen data points from the selected depth interval fell in the illustrated cell.

In 1970, with the efficiency of high-speed computer processing, a new concept was introduced to crossplotting – the Z plot. Both gamma ray and SP data are influenced by shale or shaliness within an otherwise clean formation (Chapter 4). Caliper information describes changes in hole condition: Neutron measurements are often affected by gas. The z-axis concept provides a weighted average for selected third data types that are imposed as a simulation of the z-axis at any coordinate of a dual-log crossplot. If, for example, neutron and density data crossplot at the designated coordinates A (Fig. 5-31), a gamma ray z-axis can be used to determine shaliness at that depth (Fig. 5-32). Again, designated coordinates B (Fig. 5-33) could be better interpreted with caliper information

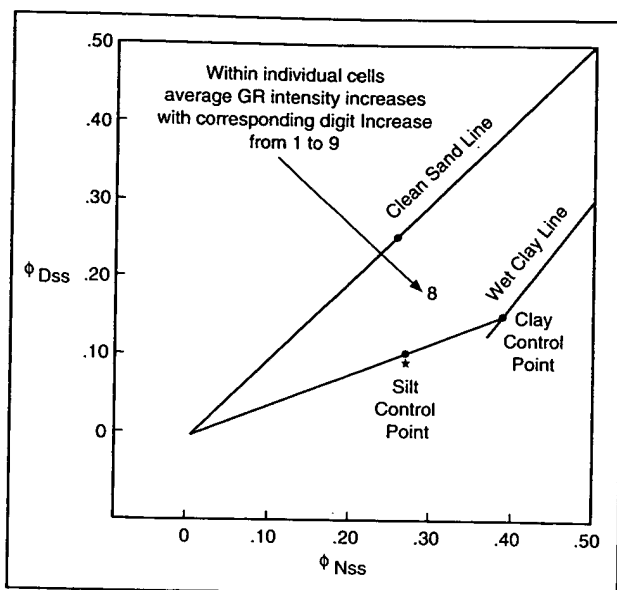


Fig. 5-30 – The eighteen data points of Fig. 5-29 appear to be representative of dirty sands or silts in the shaly sand model.

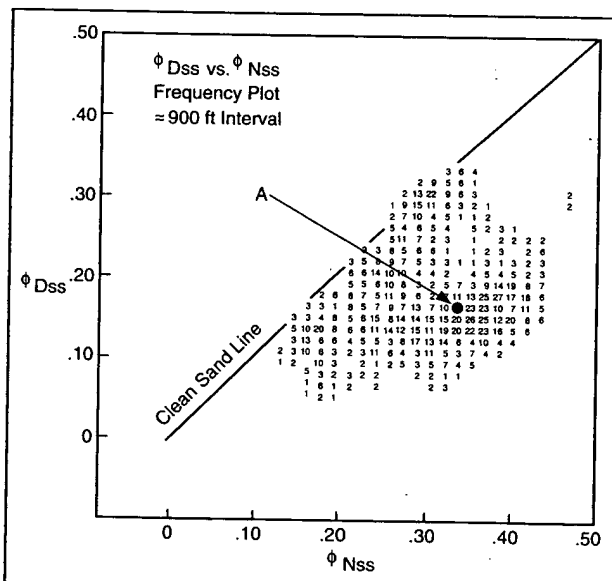


Fig. 5-31 – Frequency crossplot of density porosity vs. neutron porosity

imposed on a z-axis (Fig. 5-34). These plots were the first known log semblance to 3-D plotting, but remember that the weighted average on the z-axis for a specific cell might occur where several data points fell. Some of the depths related to those crossplotted points may have a low gamma ray count or a gauge hole, while other points that fall at the same coordinates may have higher gamma ray values or some hole rugosity.

The plot program weights the z-axis value for each cell from 1 to 9; the lower values usually represent low GR values or caliper measurements equivalent to gauge hole conditions, etc. Provision is made to allow a second z-plot to be made, dropping cells with high values; caliper

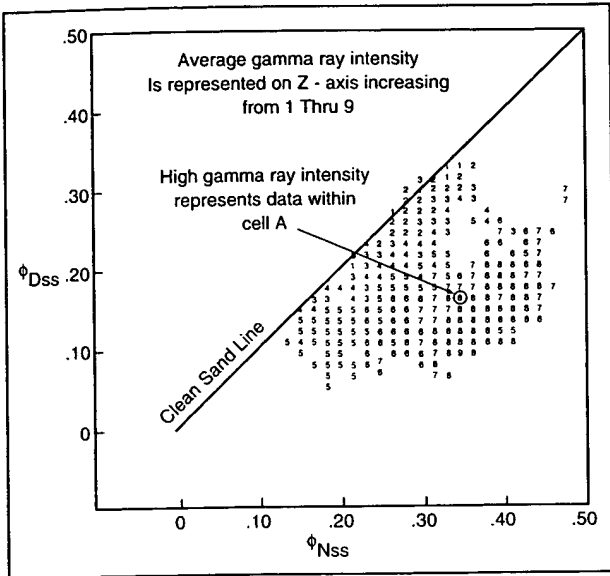


Fig. 5-32 – Crossplot of density porosity vs. neutron porosity with average gamma ray intensity shown as a z-axis representation (higher values = higher gamma ray)

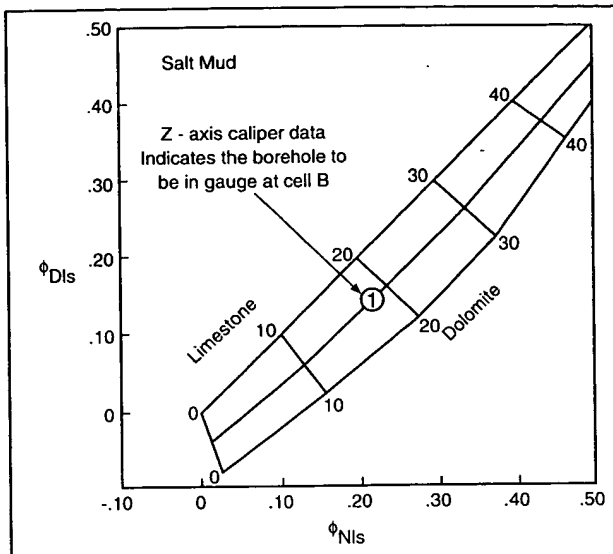


Fig. 5-34 – Low values for caliper on a z-axis indicated excellent borehole conditions.

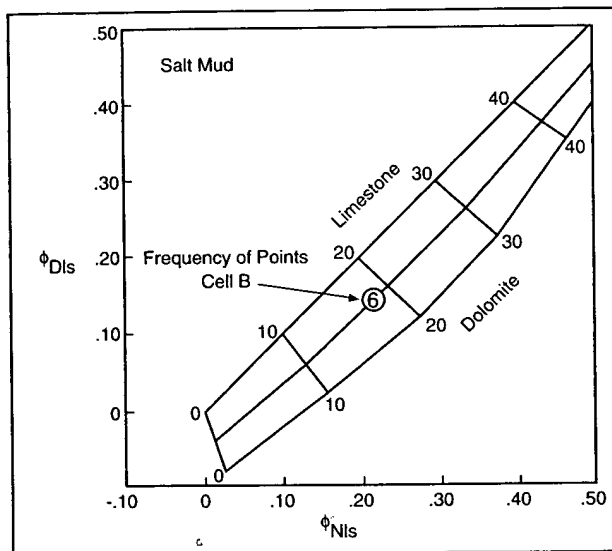


Fig. 5-33 – On the Fig. 5-32 crossplot data, Cell B would be estimated as a 50-50 mixture of dolomite and limestone having about 18% porosity.

weights 7 through 9 might be considered representative of depths that are predominantly shale as well as having rugose hole. To avoid the clutter of bad hole data, the user could plot the data again, dropping those cells with the higher z-axis caliper weights (Fig. 5-35). Other data can also be implemented on the z-axis to compare with data crossplotted from x and y coordinates.

NATURAL GAMMA RAY SPECTROSCOPY

It has been well documented that total gamma ray counts are related to the decay of the many long-lived natural radioactive nuclides. In log analysis, the most fundamen-

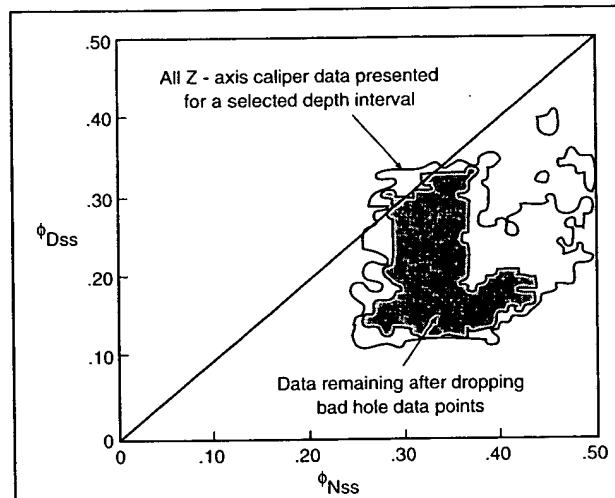


Fig. 5-35 – Comparison of z-data for all crossplotted data to z-data after dropping cells with z values > 7

tal rock constituent to identify is shale. Among several methods (GR, SP, neutron, resistivity, and various cross-plots), natural gamma ray spectroscopy provides one of the most reliable shale estimates. In the mid 1970s, Dresser Atlas introduced the Spectralog service, a tool system that analyzes the entire gamma spectrum to determine the contribution of several elements to the total response. Natural gamma rays, of particular interest to the petroleum industry, primarily result from the presence of these radioactive isotopes –

- potassium⁴⁰
- thorium²³²
- uranium²³⁸

Potassium (K^{40}) decays directly to stable argon with emission of a 1.46-MeV gamma ray. Uranium (U^{238}) and thorium (Th^{232}) decay sequentially through several daughter products until they achieve stabilization as lead isotopes. The uranium series nuclide bismuth (Bi^{214}) emits gamma rays at 1.76 MeV and the thorium series nuclide thallium 208 emits gamma rays at 2.62 MeV (Fig. 5-36). Assuming secular equilibrium, the daughter products decay at about the same rate they are produced from the parent isotope. Relative proportions in an elemental series should remain essentially constant. Gamma ray population in the specific windows of the spectrum should therefore indicate the population of the parent isotope.

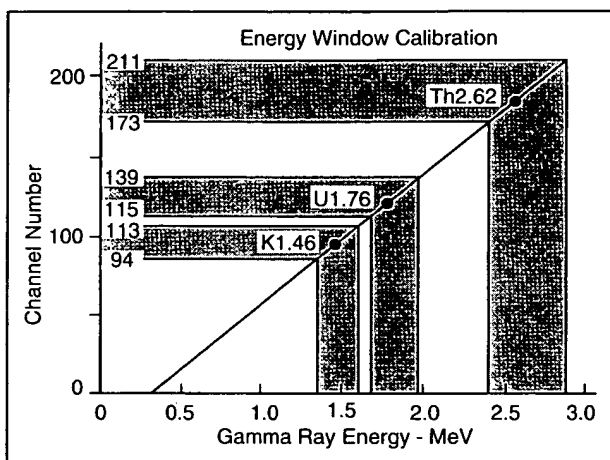


Fig. 5-36 – Energy window for Spectralog calibration

The downhole tool assembly contains a high-resolution gamma ray spectrometer that consists of a thallium-activated sodium iodide crystal optically coupled to a photomultiplier tube. The scintillation detector is housed in a vacuum-flasked pressure housing. Downhole digital electronics and a sophisticated telemetry system are used to transmit the measured data to the surface where a multichannel analyzer identifies the energy windows and corresponding peak energy values. Slow logging speeds are used to minimize statistical variations, and thorium data, located at the high-energy end of the spectrum, are scaled and recorded directly. A special stripping technique removes downscattered gamma rays of thorium from the uranium window, and downscattered gamma rays of thorium and uranium are stripped from the potassium window.

The only unstable isotope of potassium is the nuclide K^{40} ; it is also the main contributor and easily identified. Because of its abundance in nature, K is presented as a percentage; uranium and thorium are presented in parts per million (Fig. 5-37). Total gamma rays measured can be presented as counts/minute or API units. Ratio traces are optional (K/Th, Th/K or Th/U). Table 5-3 lists

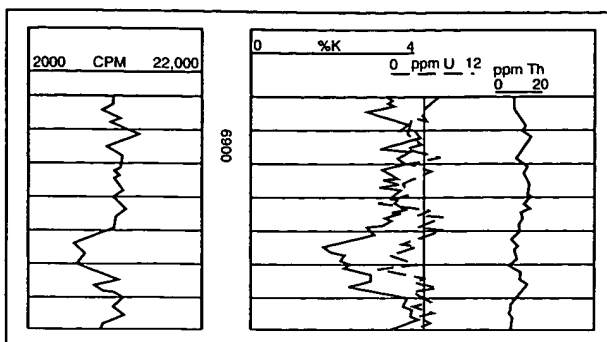


Fig. 5-37 – The common abundance of potassium with respect to thorium or uranium products forces it to have a different scale value on log presentations.

nuclides, mode of integration, and half-life of members in the uranium and thorium series. Table 5-4 shows the observed gamma ray lines of the important naturally occurring radionuclides. Table 5-5 lists common rocks and minerals and related KUTh data determined from field experience and literature search.

Clues as to clay type, presence or absence of mica or feldspar, evaporites, and/or presence of organic material can be obtained if natural gamma spectroscopy devices are used effectively. Some knowledgeable input is required, however, if the proper minerals are to be estimated. If parameters for feldspar, illite, and a second clay are input, the computer program will likely find some of each mineral in a selected depth interval. Mica could be present instead of feldspar, yet the program would identify some of the nonexistent mineral and would not find any of the available mineral. There are limits to the capabilities of artificial intelligence, and clay typing with log data is definitely a form of artificial intelligence.

Identifying the dominant clay type in the reservoir rock is an important consideration because it can affect not only estimates of reservoir productivity but also subsequent decisions about drilling fluids, completion fluids, etc.^{11,13} Different clay types as well as certain types of feldspars, micas, and evaporite admixtures tend to have preferable depositional and diagenetic environments.

The potassium, thorium, and uranium elements have certain characteristic occurrences, transport relationships, and chemical properties that provide some evidence pertaining to the depositional environment (Table 5-6). Potassium is encountered in many rocks and reservoir fluids. Within the rock matrix, K is very sensitive to erosion, weathering, and diagenetic effects. These effects can change clays that swell to mixed layered clays or to illite clays. Thorium compounds have extremely low solubility and therefore exhibit very limited mobility during weathering processes, a condition that limits them

TABLE 5-3 – Natural Gamma Ray Emitters

Uranium Series

Nuclide	Mode of Disintegration	Half Life
U1	$^{92}\text{U}^{238}$	α 4.51×10^9 yr
UX ₁	$^{90}\text{Th}^{234}$	β 24.1 d
UX ₂	$^{91}\text{Pa}^{234m}$	β, IT 1.18 min
UZ	$^{91}\text{Pa}^{234}$	β 6.66 hr
Ull	$^{92}\text{U}^{234}$	α 2.48×10^5 yr
Io	$^{90}\text{Th}^{230}$	α 8.0×10^4 yr
Ra	$^{88}\text{Ra}^{226}$	α 1620 yr
Rn	$^{86}\text{Em}^{222}$	α 3.82 d
RaA	$^{84}\text{Po}^{218}$	α, β 3.05 min
RaA'	$^{85}\text{At}^{218}$	α, β 2 sec
RaA"	$^{86}\text{Em}^{218}$	α 1.3 sec
RaB	$^{82}\text{Pb}^{214}$	β 26.8 min
RaC	$^{83}\text{Br}^{214}$	α, β 19.7 min
RaC'	$^{84}\text{Po}^{214}$	α 1.6×10^{-4} sec
RaC"	$^{81}\text{Tl}^{210}$	β 1.32 min
RaD	$^{82}\text{Pb}^{210}$	β 19.4 yr
RaE	$^{83}\text{Br}^{210}$	α, β 5.01 d
RaF	$^{84}\text{Po}^{210}$	α 138.4 d
RaE'	$^{81}\text{Tl}^{206}$	β 4.2 min
RaG	$^{82}\text{Pb}^{206}$	Stable

Thorium Series

Nuclide	Mode of Disintegration	Half Life
Th	$^{90}\text{Th}^{232}$	α 1.42×10^{10} yr
MsTh ₁	$^{88}\text{Ra}^{228}$	β 6.7 yr
MsTh ₂	$^{89}\text{Ac}^{228}$	β 6.13 hr
RdTh	$^{90}\text{Th}^{228}$	α 1.91 yr
ThX	$^{88}\text{Ra}^{224}$	α 3.64 d
Tn	$^{86}\text{Em}^{220}$	α 51.5 sec
ThA	$^{84}\text{Po}^{216}$	α 0.16 sec
ThB	$^{82}\text{Pb}^{212}$	β 10.6 hr
ThC	$^{83}\text{Br}^{212}$	α, β 60.5 min
ThC'	$^{84}\text{Po}^{212}$	α 0.30 μ sec
ThC"	$^{81}\text{Tl}^{208}$	β 3.10 min
ThD	$^{82}\text{Pb}^{208}$	Stable

TABLE 5-3 – Natural Gamma Ray Emitters
(Continued)

Material	Potassium Content by Weight (%)	
	(Average)	(Range)
Sylvite	54	
Potash	44.9	
Langbeinite	20	
Microcline	16	
Kainite	15.1	
Carnallite	14.1	
Orthoclase	14	
Polyhalite	12.9	
Muscovite	9.8	
Biotite	8.7	
Illite	5.2	3.51 – 8.31
Arkose (sandstone)	4.6	4.4 – 5.1
Synite	4.53	
Glauconite	4.5	3.2 – 5.8
Granite	4.0	2.0 – 6.0
Norite	3.3	
Granodiorite	2.90	
Shale	2.7	1.6 – 9.0
Igneous rock	2.6	
Grayrock (sandstone)	1.5	1.2 – 2.1
Diorite	1.66	
Basalt	1.3	
Sandstone	1.1	0 – 5.1
Gabbro	0.87	
Diabase	0.75	
Kaolinite	0.63	0 – 1.49
Limestone	0.27	0 – 0.71
Montmorillonite	0.22	0 – 0.60
Orthoquartzite (sandstone)	0.08	0 – 0.12
Dolomite	0.07	0.03 – 0.1
Dunite	0.04	
Sea Water	0.035	

TABLE 5-4 – Gamma Ray Lines in the Spectra of the Important, Naturally Occurring Radionuclides

Nuclide	Gamma Ray Energy MeV	Number of Photons per Disintegration in Equilibrium Mixture
$\text{Bi}^{214}(\text{RaC})$	0.609	0.47
	0.769	0.05
	1.120	0.17
	1.238	0.06
	1.379	0.05
	1.764	0.16
	2.204	0.05
$\text{Te}^{208}(\text{ThC})$	0.511	0.11
	0.533	0.28
	2.614	0.35
K^{40}	1.46	0.11

* With intensities greater than 0.05 photons per disintegration and energies greater than 100 keV.

TABLE 5-5 – Potassium (K), Uranium (U), and Thorium (Th) Distribution in Several Rock and Minerals

	K (%)	U (ppm)	Th (ppm)
Accessory Minerals			
Allanite		30 – 700	500 – 5000
Apatite		5 – 150	20 – 150
Epidote		20 – 50	50 – 500
Monazite		500 – 3000	$2,5 \times 10^4$ – 20×10^4
Sphene		100 – 700	100 – 600
Xenotime		$500 – 3,4 \times 10^4$	Low
Zircon		300 – 3000	100 – 2500
Carbonates			
Range (average)	0.0 – 2.0 (0.3)	0.1 – 9.0 (2.2)	0.1 – 7.0 (1.7)
Calcite, chalk, limestone, dolomite (all pure)	< 0.1	< 1.0	< 0.5
Dolomite, west Texas (clean)	0.1 – 0.3	1.5 – 10	< 2.0
Limestone (clean)			
Florida	< 0.4	2.0	1.5
Cretaceous Trend (Texas)	< 0.3	1.5 – 15	< 2.0
Hunton Lime (Oklahoma west Texas)	< 0.2	< 1.0	< 1.5
< 0.3	< 1.5	< 1.5	
Clay Minerals			
Bauxite		3 – 30	10 – 130
Glauconite	5.08 – 5.30		
Bentonite	< 0.5	1 – 20	6 – 50
Montmorillonite	0.16	2 – 5	14 – 24
Kaolinite	0.42	1.5 – 3	6 – 19
Illite	4.5	1.5	
Mica			
Biotite	6.7 – 8.3		< 0.01
Muscovite	7.9 – 9.8		< 0.01
Feldspars			
Plagioclase	0.54		< 0.01
Orthoclase	11.8 – 14.0		< 0.01
Microcline	10.9		< 0.01
Sandstones, range (average)	0.7 – 3.8 (1.1)	0.2 – 0.6 (0.5)	0.7 – 2.0 (1.7)
Silica, quartz, quartzite, (pure)	< 0.15	< 0.4	< 0.2
Beach sands (U.S. gulf coast)	< 1.2	0.84	2.8
Atlantic Coast (Florida, North Carolina)	0.37	3.97	11.27
Atlantic Coast (New Jersey, Massachusetts)	0.3	0.8	2.07
Shales			
"Common" Shales (range (average))	1.6 – 4.2 (2.7)	1.5 – 5.5 (3.7)	8 – 18 (12.0)
Shales (200 samples)	2.0	6.0	12.0

TABLE 5-6 – Clues Relating KUTh to Particular Depositional Environments Might be Found When KUTh Estimates are Compared to Particular Minerals¹⁴

	Chemical Properties	Transport	Occurrence
Potassium K ⁴⁰	Valence 1+ Soluble	In solution for large distances Feldspars and micaceous materials in suspension • Only a small part of original K transported arrives at the sea • K is extracted from seawater by algae	Detrital sediments • In immature sediments such as feldspars and micas • Clays in general (by absorption) • In micaceous clays structurally chemical sediments • Heaviest concentration in evaporites • In limestone originated from algae
Thorium Th ²³²	Valence 4+ Insoluble	Uniquely in suspension • Usually in the silty fraction of shale • Where heavy minerals are more abundant	Only in detrital sediments • In clay minerals by absorption • In heavy minerals (monazite, zircon, rutile) • In volcanic ashes (tuff, tuffaceous sandstone) • In residual sediments that remain after K and U are eliminated by erosion Th has never been detected in pure limestone or dolomite
Uranium U ²³⁸	By far the most soluble Valence 4+ U ⁴⁺ is soluble Valence 6+ U ⁶⁺ is soluble In the complex form UO ₂ ²⁺ depending upon the pH and eH The ion UO ²⁺ is combined with sulfates, carbonates, or organic materials UO ²⁺ is precipitated with phosphates	Post-depositional transfers are common chiefly in solution Very soluble Very mobile In suspension • Migrates easily during leaching and dissolution of carbonates Concentrates in stylolites in animals that attach to uranium	Detrital sediments • In clay minerals by absorption (high content may indicate high concentration of organic material that in turn may indicate a source bed) • In heavy minerals (zircon) • In volcanic ashes (tuff and tuffaceous sandstone) Chemical sediments • In carbonates (high in organic material) • In phosphates • In organic materials

primarily to their original environmental setting – predominantly marine. Uranium mobility and accumulation in subsurface rocks are controlled mostly by physical, chemical, biological, and hydrological factors whose interaction dictates how, what, and where uranium compounds will finally be deposited. Precipitation from subsurface waters is controlled for the most part by the Eh and pH redox potentials. These are the downward movement or infiltration of meteoric waters along with oxygen loss, bacterial action, geochemical reactions, etc. that cause Eh changes from positive (oxidizing conditions) to negative (reducing conditions).

Matrix composition can be described when two or more porosity/lithology-sensitive log measurements are available. The type and number of measurements available, as well as the complexity of the rock, are the inhibiting factors in defining complex rock mixtures. Unfortunately, radioactive elements complicate the dual-mineral protocol because concentrations of K, U, or Th occur in clean rocks that might be designated prohibitive reservoirs when observing only total natural gamma ray logs. KUTh measurements are therefore very necessary in accurate log evaluations in complex reservoirs.

SHALE, SILT, AND CLAY

Log analysts often concern themselves with shale volume (V_{sh}) more than clay type or clay volume, but clay type and volume can be very important to reservoir engineering. Remember that shale is generally considered a rock type, whereas clays are generally considered minerals. A fine and ambiguous line separates the different terms, and many technical disciplines use or abuse the terms in different ways. A rock is made up of framework grains that form a self-supporting frame at the time of deposition. The matrix can consist of various grain sizes and minerals that are interthreaded by pore tunnels (filled with fluids or gases). Matrix material is cemented by precipitation of pore fluids, and cementing can take place several times after burial (Fig. 5-38). *Diagenesis* is the term used to describe physical and chemical changes that take place after deposition, including compaction, cementation, recrystallization, and mineral replacement.

Wentworth's grain-size classification is almost universally accepted as the scale for clastic sediments. Nevertheless, layman and some of the literature generalize clays as natural, earthy, fine-grained materials that



Fig. 5-38 – Albite overgrowth on a detrital feldspar grain (SEM photo)

develop plasticity when mixed with water. Shale is also generally defined as an earthy, fine-grained ($< 62 \mu\text{m}$) sedimentary rock with a specific laminated character that includes both silt and clay-size particles. Clays, on the other hand are $< 4 \mu\text{m}$ in grain size and are generally composed of small crystalline particles that allow typing according to crystal structure.

Several specific groups of clay minerals are of interest to petroleum engineers and petroleum geologists –

- kaolinite
- smectite
- chlorite
- illite
- mixed-layer minerals

Determination of Clay Type and Amount

Log analysts generally use crossplot techniques to recognize dispersed, laminated, and structural clay. Neutron-density crossplots attempt to categorize clays as structural, dispersed, or laminated (Fig. 5-12), and empirical approximations are also used to define clay type (Fig. 5-13). Earlier in this text, methods were discussed to determine porosity and V_{sh} content with different models (dispersed clays or laminated sand-shale series). Log determination of clay type and amount is at best controversial. Comparison to SEM studies of core from the same horizon and wellbore is necessary at some point to corroborate log-derived clay analysis.

CLAY ANALYSIS USING SPECTRALOG DATA

Potassium and thorium are used in a variety of ways to determine clay type and to estimate the percentages of different clay mixtures within a reservoir rock. Although the methods provide a quantitative estimate, the results are approximations and other factors often influence the different log responses used in a crossplotting technique.

Potassium is chiefly associated with shales but is also found in evaporitic sequences and algal limestones. It is most common in arenaceous rocks composed of terrigenous sediments, usually associated with chemically unstable grains such as feldspars, micas, and alteration products including kaolinite and chlorite. Potassium is considered an element that owes its origin to erosion; it is often reworked and transported for long distances.

Thorium is associated only with detrital sediments, never with purely chemical sediments (limestone, dolomite, and aragonite). Therefore, in carbonate reservoirs, thorium becomes a very important clay indicator. It is found in mudstones where it is absorbed by clay minerals, and with heavy minerals such as zircon, monazite, and rutile, which are often abundant in the silty fractions. Thorium is also abundant in residual sediments formed from alteration of volcanic ash and is common in tuffs and tuffaceous sandstones. The nature of the thorium habitat causes its presence to be a clue to the depositional setting. Thorium is generally considered a marine element.

Uranium is found in both detrital and chemical sediments (shales, conglomerates, sandstones, and carbonates) and is also common in tuffs, tuffaceous sandstones, and phosphates. Carbonates rich in organic matter that form under reducing conditions are often very high in uranium, and they can be easily misidentified as shale from total gamma ray log data. These "radioactive carbonates" are often productive reservoirs and occur as limestone and dolomite or mixtures of the two rock types. Uranium nuclides are also absorbed by clay minerals. Associated with organic matter and uranium-bearing heavy minerals, the Spectralog uranium measurement often indicates sand and silt fractions of coastal carbonates (supratidal and intertidal environments) to be radioactive in the clastic or evaporitic admixtures. Excessively high uranium content in shales indicates source rock.

In general, subsurface precipitation of formation waters is controlled by pH and Eh potentials. As meteoric waters infiltrate downward, a combination of oxygen loss, bacterial action, and geochemical reaction within the host rock occurs and causes Eh changes from (+) oxidizing conditions to (-) reducing conditions (Fig. 5-39). Petroleum reservoirs commonly demonstrate a negative redox potential. The available uranium ions transported in

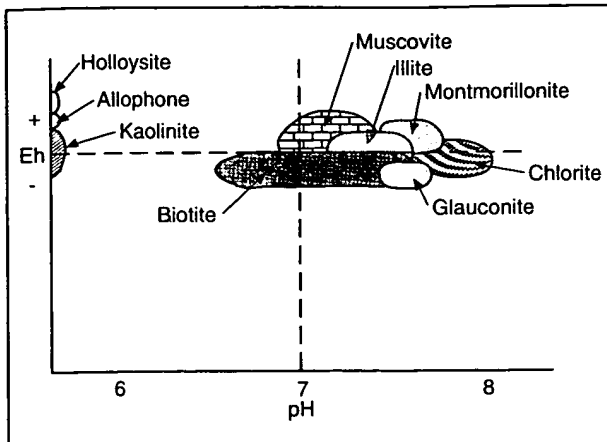


Fig. 5-39 – Generalized stability realms of clay minerals and micas

migrating subsurface waters, on exposure to organic matters, cause H_2S and SO_2 , which precipitate as UO_2 . This precipitated uranium is often concentrated in fracture and fissure systems, along fault planes, and it may migrate into any permeable clastic, carbonate, argillaceous, or igneous rock.

Spectralog data utilize three energy windows (W_1 , W_2 , W_3) to evaluate the contribution of K, U, and Th. The preceding discussion addressed the petrological, mineralogical, and environmental relationships of these three elements in nature. Minerals have characteristic concentrations of the measured spectra, which can be used to indicate the occurrence probability of certain minerals. Certain other lithological and fluid-sensitive measurements are excellent for comparison to the spectral data (P_e , neutron).

Numerous comparisons of petrophysical parameters have been published. Geologists can predict rocks that should occur in particular geological settings and, in most instances, can certify an environment by recognition of certain minerals, fossils, porosity/lithology relationships, etc. Input data of this type are not only desirable but necessary if adequate mineral analyses from log data are expected. For example, if glauconite is identified in well cuttings (information often available from mud logs, sidewall cores, or full core), it is clear evidence that a sediment was deposited in marine conditions (Table 5-7). Knowing this, it would be somewhat preposterous to consider that certain minerals of continental heritage would be present in large amounts. The comparison of spectral (KUTH) data to other log data must be viewed as a volumetric estimate at best because other minerals can exhibit similar, if not identical, log criteria fingerprints.

TABLE 5-7 – Selley's Four Generic Classifications

		Marine	Nonmarine
		Glaucite	No Glaucite
Well Winnowed	Noncarbonaceous	Barrier Bar Shoal	Marine Shelf Sands
	Carbonaceous	Turbidites Deep Sea Fans	Fluvial Lacustrine Deltaic
Poorly Winnowed	Noncarbonaceous		
	Carbonaceous		

ANALYZING COMPLEX LITHOLOGY WITH SPECTRAL GAMMA RAY, Z-DENSITY, AND NEUTRON DATA

Common sedimentary environments can be segregated into four main groups of rocks and minerals for log analysis purposes. Groupings can be made as follows –

- (1) *Detrital minerals* – These survived the vigors of erosion, transport, and reworking prior to burial.
- (2) *Secondary minerals* – These formed during the transport and weathering process; the dominant secondary minerals are clays.
- (3) *Precipitated minerals* – These formed directly from solution, either chemically or biochemically; carbonates are the dominant group of which all might be authigenic.
- (4) *Authigenic minerals* – These formed in sediments during and after deposition. Evaporation of sea water precipitates salt, whereas anhydrite is a buried evaporite that often occurs as a secondary mineral formed from primary gypsum.

For log analysis purposes, common minerals that occur in sediments are conveniently grouped into six categories –

- (1) carbonates
- (2) evaporites
- (3) silicates
- (4) clays
- (5) feldspars
- (6) micas

Spectralog, Z-Densilog, and neutron log measurements provide a plausible approach to recognition of distinct minerals from the previous categories. Spectralog measurements of K, U, and Th can be used to estimate high- and low-potassium clays and either feldspar or mica (the wrong input will give the wrong answer). Z-Densilog and neutron data are used to resolve the mixture of sand, limestone, or dolomite, or other three-mineral combinations on a three-way crossplot.

The models rely heavily on empirical observations –

- (1) Spectralog measurements (K, U, Th) are affected mostly by feldspars, micas, and the various clay minerals.
- (2) Photoelectric, density, and neutron measurements are capable of distinguishing limestone, dolomite, and silicates, and those rocks are distinguishable from the various evaporites if the rocks are clean.
- (3) Corrections to the P_e , ρ_b , and ϕ_N measurements for the influence of feldspars, micas, or clays improve the interpretative capability of differentiating carbonates, silicates, and evaporites.

Spectralog Mineral Estimates

Spectralog data are used to estimate volumetric fractions of feldspar or mica and two clay types. Glauconite or anhydrite can be substituted for the feldspar or mica parameter.

Conventional gamma ray measurements are equivalent to the following weighted sum –

$$GR = c_1 Th + c_2 U + c_3 K,$$

where the c values represent a constant. Originally, Spectralog data were used as a shale indicator. However, uranium is associated with radioactive minerals other than those found within shales (organic minerals) and is not a reliable shale indicator. As a result, it seemed sensible to compute a "uranium-free" curve by subtracting the weighted value of uranium from the total gamma ray count. A combined ThK curve is often a good shale indicator.

The uranium-free ThK curve becomes an ineffective shale indicator if potassium feldspars or micas (both high in K) are present. When this occurs, some improvement is often found by using a ThK ratio to type clays in shales or rocks expected to have high potassium concentrations.

The Th/K ratio is a function of the mineralogical composition of shale because of the ratio relation to illite percentage (Fig. 5-40); the Th/K ratio decreases as illite percentage increases. Similar relations exist between the Th/K ratio and feldspars, micas, and other clay minerals. Potassium (K) concentrations by weight were obtained from chemical analysis and used to develop a $Th(\text{ppm})$ vs. $K(\%)$ chart for spectral estimates of radioactive minerals (Fig. 5-41). Interpretation models are based on this chart or similar observations.

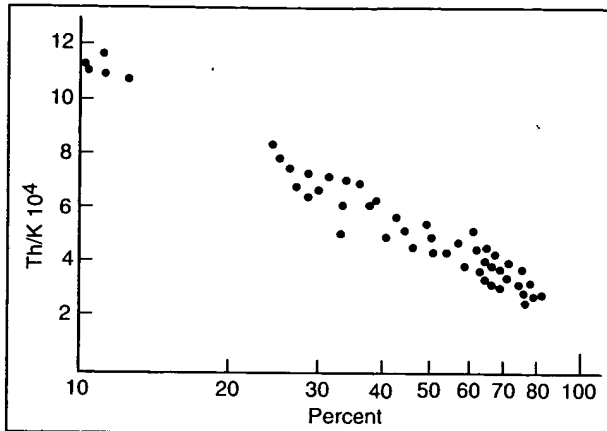


Fig. 5-40 – Correlation of illite clay percentage in shale with Th/K ratio

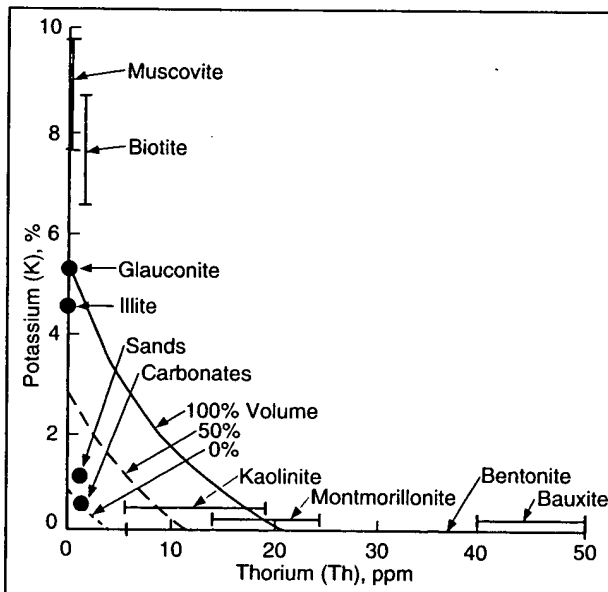


Fig. 5-41 – Typical potassium and thorium concentrations for different clay minerals and product index clay volume

X-ray diffraction data suggest most radiation originates in feldspars and clays; micas are infrequent in most sediments (the North Sea is an exception). In a specific case, natural radioactivity might be assumed to originate from

feldspar and one clay type. If a linear tool response is assumed, the weighted percentage of each of the two minerals can be estimated –

$$W_{fel} = \frac{Th/Th_{fel} - K/K_{fel}}{Th_{fel}/Th_{cl} - K_{fel}/K_{cl}},$$

and

$$W_{cl} = \frac{Th/Th_{fel} - K/K_{fel}}{Th_{cl}/Th_{fel} - K_{cl}/K_{fel}},$$

where Th_{fel} , K_{fel} , Th_{cl} and K_{cl} signify tool response in "pure feldspar" or clay, respectively. The W_{cl} equation demonstrates constant weight fractions of clay correspond to lines that parallel pure feldspar lines (Fig. 5-42). If feldspar is suspected in the rock matrix, an appropriate clay/shale indicator could be defined –

$$V_{sh} = c (Th/Th_{fel} - K/K_{fel}),$$

with c becoming a constant depending on clay type.

A more general situation might dictate that feldspar and two clay types be modeled after observing the close

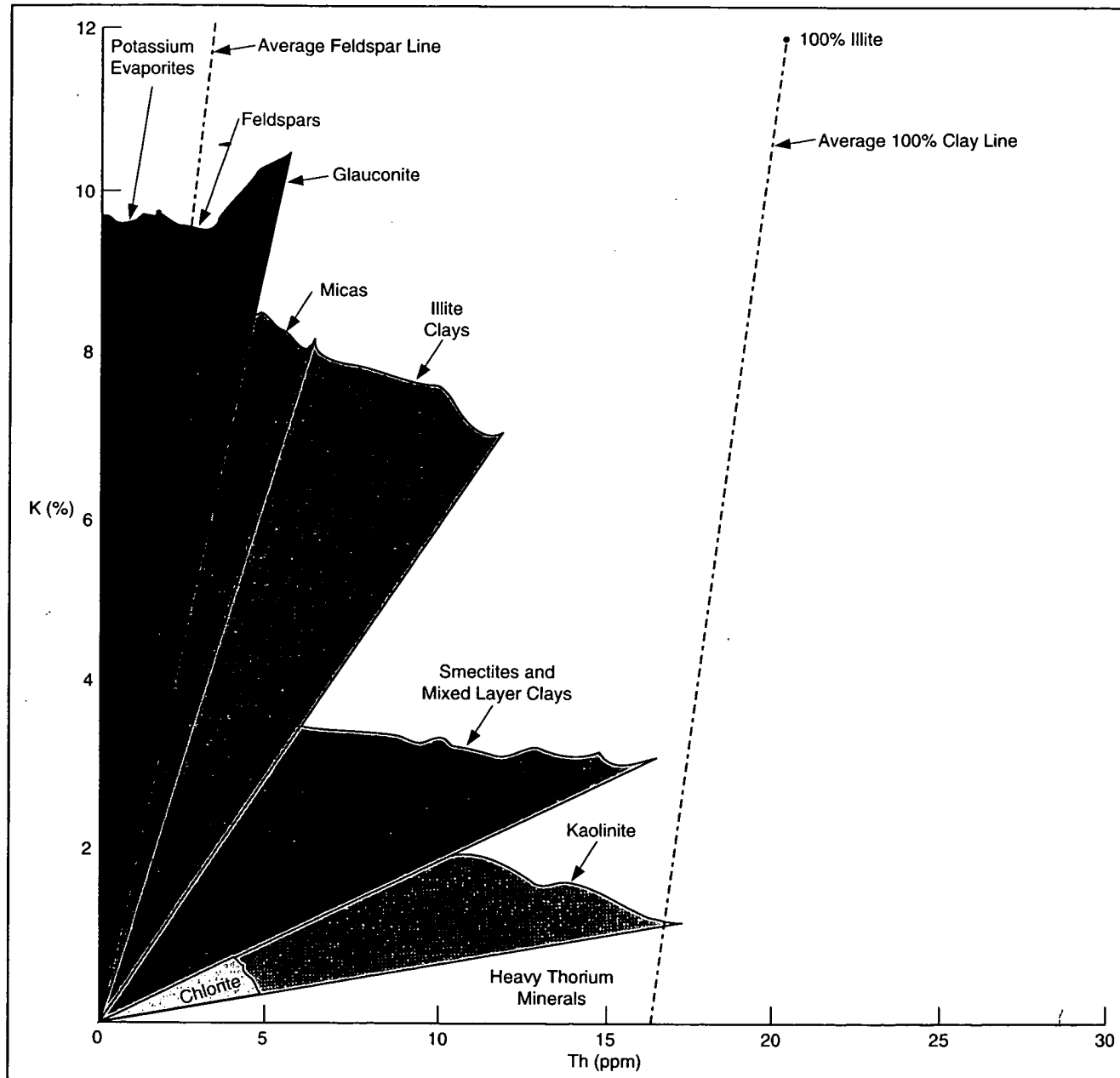


Fig. 5-42 – An interpretative model for spectral gamma ray mineral identification

proximity of the 100% points for kaolinite, chlorite, and montmorillonite (Fig. 5-43). Suggested definitions for points follow –

- (1) cl_1 , a low-potassium clay point
- (2) cl_2 , a high-potassium clay point (generally considered illite)
- (3) fel , a low-thorium, high-potassium point representing feldspar
- (4) ma , representing the clean matrix point

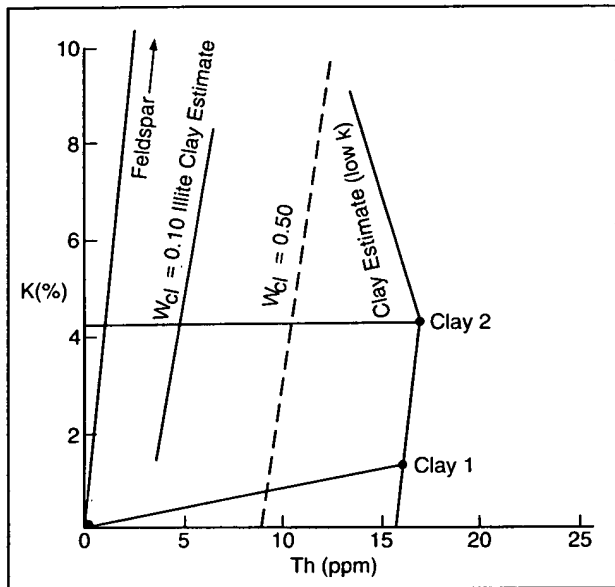


Fig. 5-43 – Modified model of feldspar and two clay types (approximations only)

A line connecting cl_1 and cl_2 is called the *clay line*, and the line from the origin through the *fel* point is called the *feldspar line*. The weighted fraction of clay (W_{cl}) is found by interpolating between the clay line and feldspar line. A different model and different lines would be constructed for clays and mica, clays and anhydrite, or glauconite and two clay types.

The proposed Spectralog interpretation model is then –

$$W_{cl} = W_{cl1} + W_{cl2}$$

$$Th = Th_{cl1}W_{cl1} + Th_{cl2}W_{cl2} + Th_{ma}W_{ma} + Th_{fel}W_{fel}$$

$$K = K_{cl1}W_{cl1} + K_{cl2}W_{cl2} + K_{ma}W_{ma} + K_{fel}W_{fel}$$

$$I = W_{cl1} + W_{cl2} + W_{ma} + W_{fel}$$

W_{cl} must be accepted as a function of Th and K . The resultant model allows mineral weight fractions to be converted to volume fractions (Fig. 5-44). These data vary with differences in natural gamma ray spectroscopy instrumentation, but the information demonstrates how Spectralog data can be used more effectively. Intelligent input controls are prerequisite to obtaining relatively accurate results; in areas where mica is common, it would be substituted for feldspar, and a slightly different model would result.

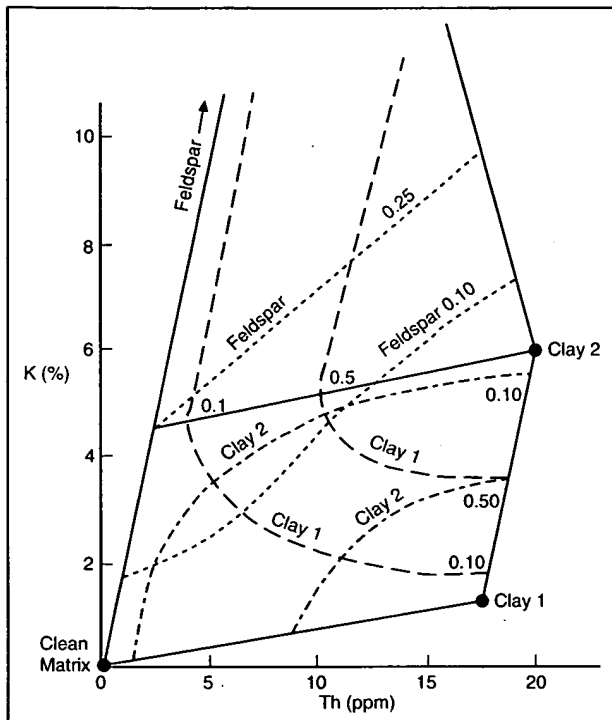


Fig. 5-44 – An empirical model to estimate proportions of feldspar and two clay types

Z-Density and Neutron Estimates of Lithology

The P_e and ρ_b measurements are sensitive to the presence of any of the six sedimentary categories described as carbonates, evaporites, silicates, clays, micas, and feldspars. Apparent total porosity (ϕ_{ta}) calculated from a neutron-density crossplot can be corrected to water-filled porosity if required. The variables ρ_{maa} and U_{maa} are used to construct the three-way crossplots scaled with the appropriate values, and the theoretical location of various minerals (based on chemical composition and calculated porosity) can be imposed on the chart (Fig. 5-26).

Information derived from the chart typically provides relatively accurate lithology analysis for clean sand and carbonate reservoirs. Nevertheless, the results can be heavily biased if feldspars, micas, or clays are present. Spectralog data analysis techniques minimize the bias

effect; ρ_{maa} and U_{maa} variables can be corrected for feldspars, micas, or clays. Clay points can be established on a model by using predicted tool responses (e.g., typical neutron clay response might be 40% porosity).

A fundamental problem with this technique, however, is that evaporite corrections must be considered for U_{maa} and ρ_{maa} values when used in the presence of feldspars, micas, and clays. A chart for silica, limestone, and dolomite with a second triangle for anhydrite, salt, and dolomite is one method used to resolve the evaporite problem. For illustrative purposes, assume the silica-limestone-dolomite triangle has been accepted as appropriate, and the input variables U_{maa} and ρ_{maa} are to be corrected for the known presence of feldspar and clay. A correction for mica proportions is required and can be resolved by –

$$\rho_{maa} - P_4\rho_4 - P_5\rho_5 = P_1\rho_1 + P_2\rho_2 + P_3\rho_3,$$

$$U_{maa} - P_4U_4 - P_5U_5 = P_1U_1 + P_2U_2 + P_3U_3,$$

$$I - P_4 - P_5 = P_1 + P_2 + P_3,$$

where

ρ_{maa} = apparent matrix density,

U_{maa} = apparent matrix volumetric cross section,

ρ numbers = densities of minerals 1 through 5,

P numbers = proportions of minerals 1 through 5,

and

U numbers = volumetric cross sections of minerals 1 through 5.

The indices numbered 1, 2, and 3 correspond to three mineral points of the triangle. The indices numbered 4 and 5 correspond respectively to the feldspar and clay corrections, while P_4 and P_5 were obtained from the Th and K spectral gamma measurements as discussed previously. It is convenient to define the matrix (Ma^{-1}) as –

$$Ma^{-1} = \begin{bmatrix} \rho_1 & \rho_2 & \rho_3 \\ U_1 & U_2 & U_3 \\ I & I & I \end{bmatrix} \quad (1)$$

The vector of the tool response (t) can be defined as –

$$t = \begin{bmatrix} \rho_{maa} \\ U_{maa} \\ I \end{bmatrix} \quad (2)$$

The vector correction to the tool response (t_c) can be defined as –

$$t_c = \begin{bmatrix} P_4\rho_4 + P_5\rho_5 \\ P_4 + P_5 \\ P_4U_4 + P_5U_5 \\ P_4 + P_5 \\ I \end{bmatrix} \quad (3)$$

The solution to the preceding system of equations (1, 2, and 3) can then be written –

$$\begin{bmatrix} P_1 \\ P_2 \\ P_3 \end{bmatrix} = M_t - (P_4 + P_5) M_{tc}$$

M_t vector represents a noncorrected three-mineral estimate of proportions. M_{tc} vector represents the correction direction, and $P_4 + P_5$ represents the amount of correction.

There should be little doubt that this method is more suited to computer processing, but it is instructional to apply the correction manually to crossplot data. The last equation demonstrates that the correction for clay should proceed along a line through both the data sample and the clay point (Fig. 5-45). Assuming the silica-limestone-dolomite model is acceptable, the minimum amount of clay possible corresponds to that amount found at the intersection of the correction line and lithology triangle at Point A (Fig. 5-46). The maximum amount possible corresponds to the intersection of the correction line and the lithology triangle at Point B (Fig. 5-46). The proportions are easily determined. The clay proportion (P_5) computed from Spectralog proportions of Th and K must be constrained by the triangular model.

All the previous equations, including constraints on clay proportion, define the basic complex lithology model for the circumstances in the above description. A check is made to test for the presence of other minerals or rocks depending on local geological conditions. In carbonate locales, the evaporite model using anhydrite, salt, and dolomite is typically used as a cross-check. The probability of each model is then computed, and final estimates of silica, limestone, dolomite, salt, and anhydrite are those obtained from the two triangular models; the silica-limestone-dolomite model having been corrected for clay and feldspar. *Weighting must be in accordance with the probability of the respective models.*

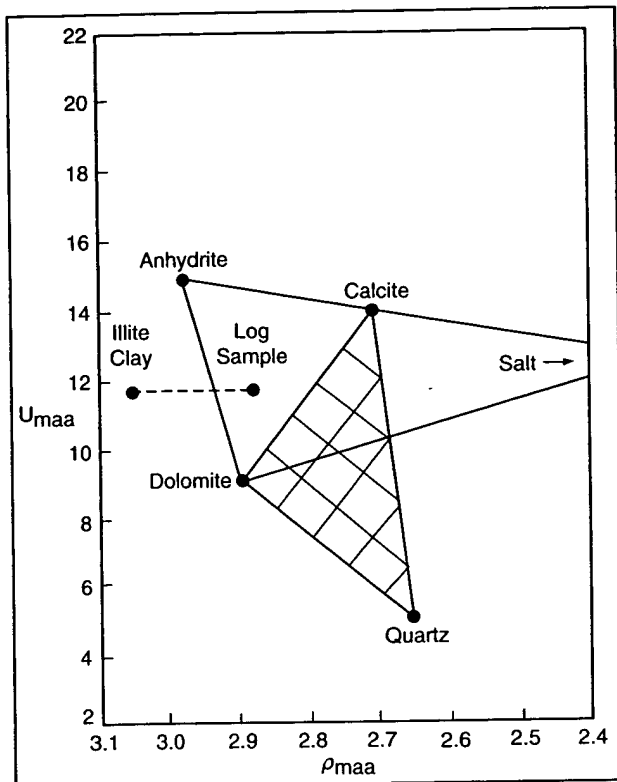


Fig. 5-45 – A line is first established through the data point and the clay point.

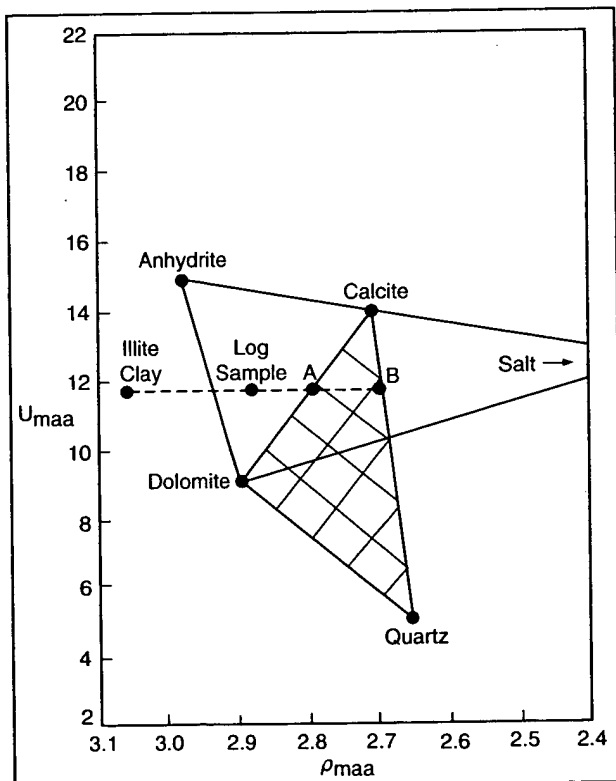


Fig. 5-46 – Minimum clay percentage should occur at point A, and maximum clay percentage should occur at point B.

A logical flow path is implemented, but detailed estimation of probabilities is beyond the scope of this text (Fig. 5-47). As an example, it can be said that the probability of anhydrite increasing occurs as a plotted data point (ρ_{maa} and U_{maa}), diverges from the silica-limestone-dolomite triangle toward the anhydrite point, and ϕ_{NLS} decreases. However, the probability is for anhydrite to decrease as clay estimates increase.

There are reasons for constructing such a complex model –

- (1) The silica-limestone-dolomite triangle frequently results in erroneous interpretation of dolomite if shales or clays are present.
- (2) Spectralog data using Th vs. K frequently leads to the misclassification of feldspar as mica, mica as feldspar, or either as a clay.

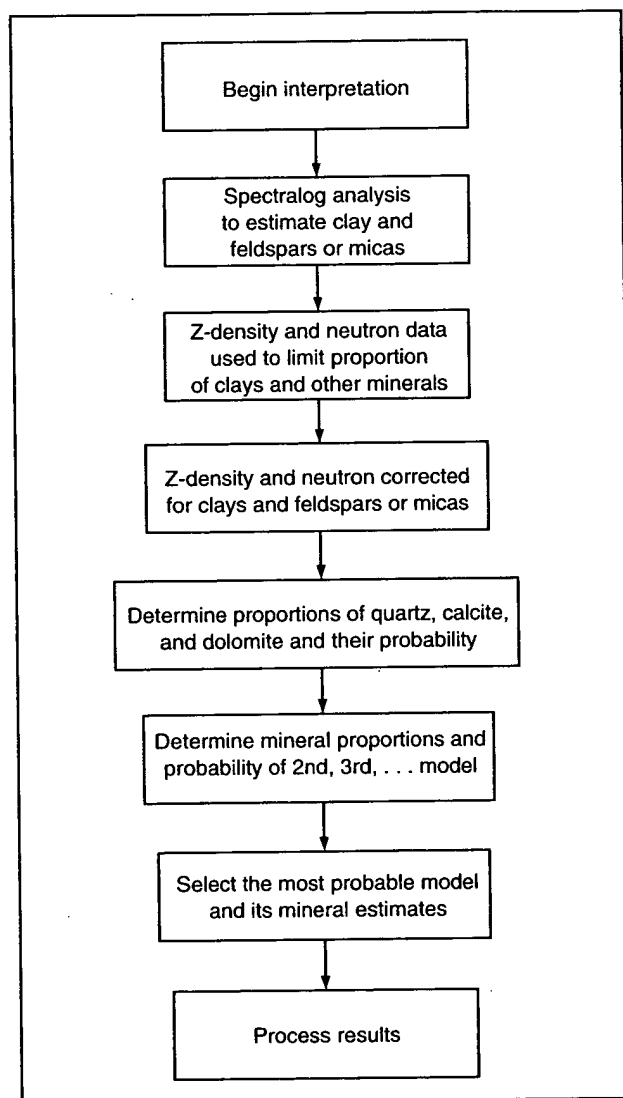


Fig. 5-47 – A logic path and procedure to resolve lithology and best estimate of porosity

- (3) The silica-limestone-dolomite triangle can miss evaporite zones, and quite often many are missed despite complex analysis routines if the depth intervals for zoning are not carefully selected (manual zoning becomes prerequisite).
- (4) There is a need for an expert system that recognizes the common sedimentary rocks and minerals.

SPECIAL CROSSPLOTS OCCASIONALLY NEEDED TO DISTINGUISH LITHOLOGY

The availability of several log measurements assists in formation evaluation, especially if computer facilities are available to manipulate the data, i.e., plotting variable against variable to find the most distinct method of segregating two minerals.

M-N products are easily accessible in computer-processed interpretations of log data if the necessary measurements are available. Earlier, it was noted that M-N crossplots are porosity-independent and, for a given mineral combination, yield a constant value. If the M-N product is plotted vs. ρ_{ma} , the four major reservoir constituents (sandstone, limestone, dolomite and anhydrite) will plot along a straight line (Fig. 5-48). By knowing ρ_{ma} , an accurate estimate of effective porosity is possible.

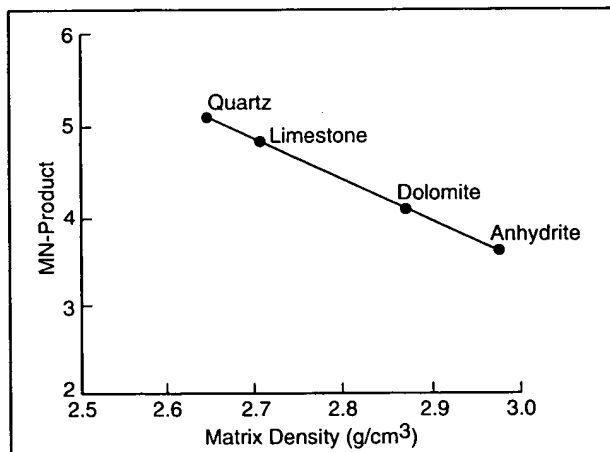


Fig. 5-48 – Plot of density data vs. the product from an M-N crossplot can help reveal lithology.

A plot of M-N vs. ρ_b also allows checking log calibration. Some restrictions exist; shale pulls data to the southwest corner of the plot, and light hydrocarbons and secondary porosity show M-N product values that are too high.

M can be plotted against ρ_b , Δt , or ϕ_N to define mineral trends including shale values, all of which are important in selecting the correct lithology model. A quality check against calibration is also afforded. Data will extend from the basic matrix material toward shale. With M on the y-axis, the shale percentage will follow a trend from the

shale point toward the clean value (Fig. 5-49). However, density and neutron data should be omitted as shale indicators when hole rugosity is a problem because both measurements are adversely affected. M vs. SP and M vs. GR often define the clean and shale extremes of SP and/or GR measurements.

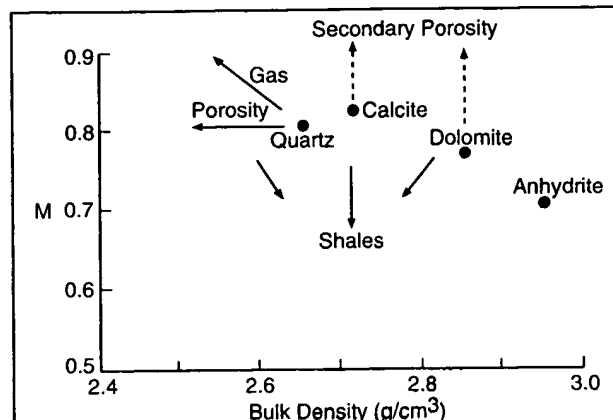


Fig. 5-49 – A plot of M vs. density data

These types of crossplots are very useful in computer log analysis and should be incorporated in the software packages of any computed log analysis program – they provide another view of the data to be analyzed.

SPECIAL CROSSPLOTS

In most geographical areas, the methods previously described provide acceptable answers. Nevertheless, the location of plotted points on conventional crossplots can be misleading for some unusual geological horizons.

Jurassic Sandstones, North Sea

Jurassic sandstones in the North Sea often contain high concentrations of micaceous minerals ($\rho_b \approx 3.1 \text{ g/cm}^3$ and $\phi_N \approx 0.3$). Density-acoustic crossplot data identify the micaceous trend (Fig. 5-50). Acoustic-neutron data also establish the mica trend (Fig. 5-51). Density-neutron data are also sensitive to the mica trend (Fig. 5-52). Similar problems occur with glauconite (Nigeria) and iron-rich minerals (North Slope of Alaska, South China Sea, etc.). As a result, local specialized crossplots are not unusual, but special-application crossplots are not meant to be used universally. Although similar applications might be needed elsewhere, the degree of implementation may vary considerably. A special factor (P) has been established for the North Sea Jurassic sands. Like M and N or MID plot data, P is essentially porosity independent. P is defined as –

$$P = \frac{100 - \phi_N}{\Delta t_f - \Delta t}$$

Mica and clay have similar affects on most log measurements, partially because both minerals are in the

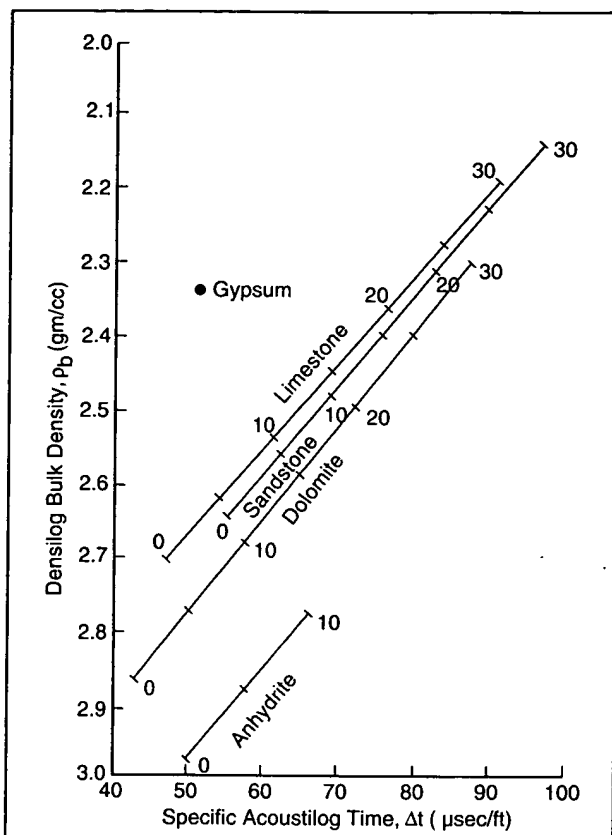


Fig. 5-50 – Typical crossplot of acoustic travel time and density

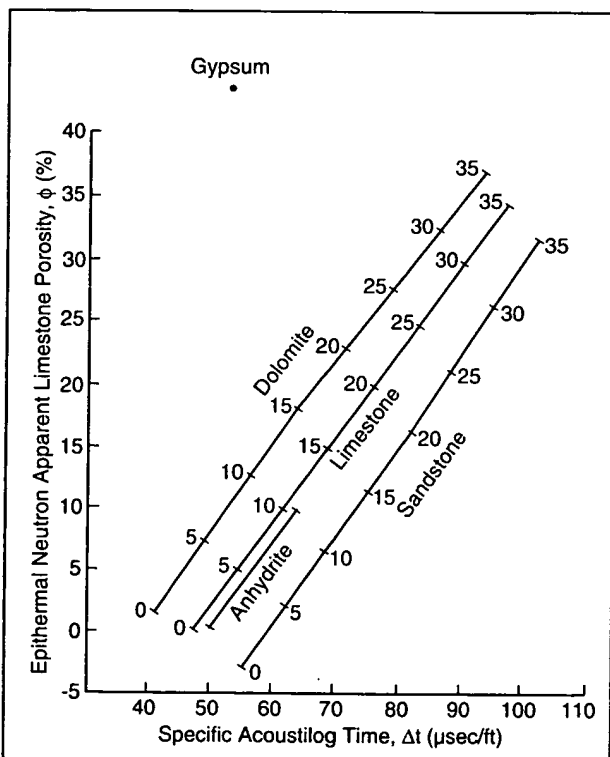


Fig. 5-51 – Typical crossplot of acoustic travel time and neutron-type data

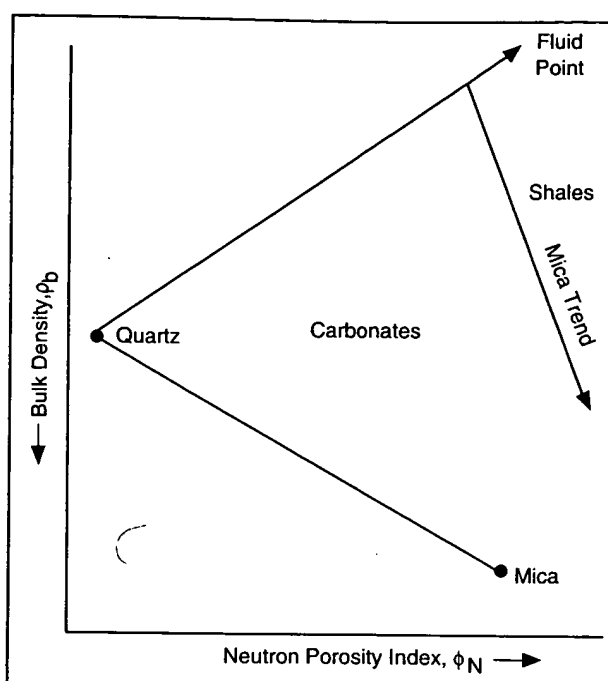


Fig. 5-52 – Density vs. neutron modelled for micaceous Jurassic sandstones of the North Sea.

form of sheet-like silicas. Both mineral types are radioactive and affect gamma ray response significantly. Shale points fall close to mica points on the density-neutron crossplot (Fig. 5-52) and fall close to water line-mica points on density-acoustic crossplots (Fig. 5-50). As a result, conventional shale/clay indicators cannot be used in the presence of mica. The range of shale values (North Sea) for density is ≈ 2.36 to 2.55 g/cm^3 , $\phi_{Nsh} \approx 35$ to 45 pu, $\Delta t_{sh} \approx 97$ to 110 $\mu\text{sec}/\text{ft}$, and $R_{sh} \approx 3$ ohm-m. A plot of the calculated P value vs. GR data expands the ability to segregate shales from micas (Fig. 5-53).

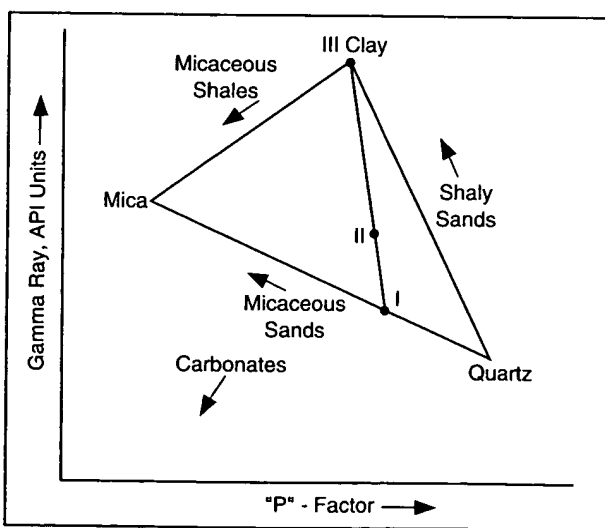


Fig. 5-53 – P factor vs. GR for quartz/mica/clay model in Jurassic sandstones, North Sea

SUMMARY AND CONCLUSIONS CONCERNING CROSSPLOT METHODS

The preceding description of crossplot methods does not encompass the entire range of data management in the literature but does provide sufficient introduction to crossplotting advantages in log analysis. Computer processing has led to an uncountable number of methods to help the analyst determine the quality and usefulness of various data types. Histograms are used in many complex computed log analysis routines. Variations of the many measurements are crossplotted against one another for specific purposes, occasionally to resolve special problems that occur locally (e.g., North Sea micas). Time and space restrict the coverage of more techniques in this introductory material, but it is sufficient to say that data management is not universally similar and instead adapts to local necessities.

PRACTICAL WORK SESSION

Problem 1

Suppose you are given log data from a formation known to be of mixed lithology (limestone, dolomite, sand, silt, clay, and some anhydrite). The data include dual laterolog-microlaterolog-GR, Z-Densilog, compensated neutron, and acoustic measurements. Which of the interpretation models would you select first?

Why? _____

What other logging service(s) might benefit the interpretative effort?

Why? _____

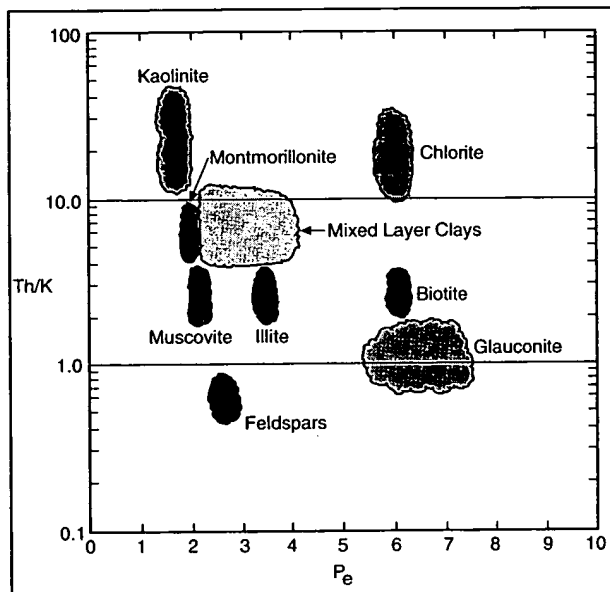
Assuming a computer analysis is to be performed, what special crossplot would you want to use?

Why? _____

Problem 2

Given the chart below (P_e vs. Th/K), plot the following values to estimate the apparent clay, mica, feldspar, etc. for each set of log data provided.

P_e	Th (ppm)	K (%)	Th/K	Estimate of Mineral(s)
6.2	6	7	—	_____
3.5	16	8	—	_____
2.5	12	<1	—	_____
6.2	20	2	—	_____
2.0	25	2	—	_____



Problem 3

Describe in your own words the attributes of crossplots.

Which crossplots are most useful for a quick manual analysis of log data?

Which crossplots are complicated enough to require computer facilities to enable the analysis of several feet (or meters) of reservoir data?
